Cellular Responses to the *Helicobacter pylori* Pore-Forming Toxin, VacA

By

Nora June Foegeding

Dissertation

Submitted to the Faculty of the

Graduate School of Vanderbilt University

in partial fulfillment of the requirements

for the degree of

DOCTOR OF PHILOSOPHY

in

Cell and Developmental Biology

May 31, 2019

Nashville, Tennessee

Approved:

Melanie D. Ohi, Ph.D.

Matthew J. Tyska, Ph.D.

Timothy L. Cover, M.D.

James R. Goldenring, M.D., Ph.D.

Jason MacGurn, Ph.D.

For Allen, Joanna, Eva, and Peggy

ACKNOWLEDGEMENTS

I wish to express my sincere appreciation to my thesis advisors, Drs. Melanie Ohi and Timothy Cover, for their mentorship, confidence, and example, all of which helped me to grow as an independent scientist. I am extremely grateful for their support.

My thanks are extended to members of the Ohi lab and the Cover lab for scientific discussions and a fun work environment. In particular, I express my sincere gratitude to Tasia Pyburn, Amanda Erwin, Rhonda Caston, Prashant Singh, and Aung Soe Lin for their research advice and friendship.

My thanks go to members of the P. Ohi lab and the Gould lab for helpful feedback during the early stages of my thesis research. Warm thanks to the members of my thesis committee, Drs. Jim Goldenring, Jason MacGurn, and Matt Tyska, for their guidance and enthusiasm. My thanks are due to the leadership and staff of the Department of Cell and Developmental Biology and the Office of Biomedical Research Education and Training for providing exceptional resources and training opportunities throughout my tenure at Vanderbilt.

My heartfelt thanks to my dear friends, Megan Dumas and Abigail Searfoss; I am exceedingly grateful for our unique companionship as colleagues and as friends.

Special thanks are due my parents, Allen and Joanna, my late mother, Peggy, and my sister, Eva, for their example and limitless wisdom; also to my cousin, Meagan, and her family, for being my home away from home. Finally, my sincere thanks are due my partner, Emma Sturgill, for her unending support and sharp advice, and for being a source of silliness and peace.

TABLE OF CONTENTS

Page

DEDICATION ii

ACKNOWLEDGEMENTS iii

LIST OF TABLES vii

LIST OF FIGURES viii

ABBREVIATIONS x

CHAPTER

I. INTRODUCTION 1

Helicobacter pylori 1
H. pylori and gastric disease 3
H. pylori colonization and virulence factors 6
Bacterial pore-forming toxins 7
Vacuolating cytotoxin A 10
VacA secretion, domain organization, and protein structure 11
VacA activities in animal models 15
VacA activities in cell culture 16
VacA cell binding, internalization, and intracellular trafficking 21
Summary 22

II. MATERIALS AND METHODS 24

Materials and chemical inhibitors 24
Cell culture 25
Purification and Alexa Fluor 488 labeling of VacA 25
Isolation of GPMVs 26
Treatment of GPMVs with VacA 26
Measurement of VacA phase partitioning 26
Stable cell line generation 27
Treatment of cells with VacA 28
Cell viability assay 29
Transfections and live-cell imaging 29
Immunostaining and fixed-cell imaging 30
Preparation of total cell lysate 30
Immunoblotting 31
Measurement of oxygen consumption rates 32
Total cell count 33
Flow cytometry 33

Targeted metabolomics....33
Statistical analysis....35

III. DETERMINANTS OF VACA LIPID RAFT PARTITIONING....36

Introduction....36
Results....38
VacA localizes to the liquid ordered phase of GPMVs....38
Acid activation is not required for VacA lipid raft association....42
Oligomerization is not required for VacA lipid raft association....46
Disruptions of the amino-terminal, pore-forming region do not abrogate VacA lipid raft association....47
The p55 domain is sufficient to target VacA to lipid rafts....49
Discussion....50

IV. INTRACELLULAR DEGRADATION OF VACA AS A DETERMINANT OF GASTRIC EPITHELIAL CELL VIABILITY....56

Introduction....56
Results....58
VacA-induced cell death is enhanced in the presence of supplemental NH_4Cl....58
NH_4Cl does not promote VacA trafficking to mitochondria....60
NH_4Cl inhibits intracellular VacA degradation....66
VacA accumulates in lysosomes and autophagosomes/autolysosomes both in the absence and presence of NH_4Cl....68
VacA degradation is independent of proteasome activity and autophagy, but dependent on lysosomal acidification....70
Discussion....74

V. VACA INTOXICATION MODULATES MITOCHONDRIAL RESPIRATION....82

Introduction....82
Results....83
VacA causes changes to mitochondrial respiration....83
Oligomerization and pore-formation are necessary for VacA to induce maximal changes to mitochondrial respiration....86
VacA does not cause changes to mitochondrial mass....88
VacA causes a reduction in glutamine and glutamic acid....88
Discussion....91

VI. CONCLUDING REMARKS 93

VacA cell surface binding and receptors 94
The target and function of the VacA pore 94
Determining the structure of VacA in a pore-forming state 96
The physiological concentration of VacA 96
Cell fate following VacA intoxication 98

REFERENCES 100

LIST OF TABLES

Table Page

3.1 Summary of raft partition coefficients across experiments 41

3.2 VacA variants and mutants used in this study 46

4.1 Summary of the Pearson correlation coefficient for MTCO2, LAMP1, and LC3 with VacA 62

5.1 List of the metabolites detected in cell lysate using targeted mass spectrometry to assess a panel of metabolites 90

LIST OF FIGURES

Figure Page

1.1 Discovery of *H. pylori* as a causative agent of gastritis. 2

1.2 Anatomy of the stomach, and progression of intestinal-type gastric adenocarcinoma 5

1.3 VacA domain organization and regions of genetic variation 12

1.4 Structural organization of VacA oligomers 15

3.1 Labeling VacA with Alexa Fluor 488 does not disrupt VacA oligomerization, internalization, or activity 39

3.2 VacA primarily localizes to the liquid ordered phase of GPMVs 40

3.3 Acid activation increases binding of VacA to membrane 44

3.4 Acid activation is not required for VacA lipid raft association 45

3.5 Oligomerization is not required for VacA lipid raft association 47

3.6 Disruptions to the VacA amino-terminal pore-forming region do not abrogate VacA lipid raft association 48

3.7 The p55 domain is sufficient for VacA partitioning into lipid rafts 50

3.8 Working model of VacA partitioning into lipid rafts 53

4.1 Loss of cell viability requires treatment with both VacA and supplemental NH_4Cl 59

4.2 Treatment with NH_4Cl does not promote VacA trafficking to mitochondria 61

4.3 Analysis of VacA localization with mitochondria in living cells in the presence of NH_4Cl 63

4.4 Analysis of VacA localization with mitochondria in living cells in the absence of NH_4Cl 64

4.5 Analysis of VacA localization with early and late endosomes in living cells 65

4.6 NH_4Cl inhibits intracellular VacA degradation 67

4.7 NH_4Cl inhibits VacA degradation in HeLa cells 68

4.8 VacA accumulates in lysosomes and autophagosomes/autolysosomes in both the absence and presence of NH_4Cl 69

4.9 MG132 does not inhibit VacA degradation 71

4.10 VacA degradation is independent of autophagy 72

4.11 VacA degradation is dependent on lysosome acidification.....74

4.12 Proposed model for the cellular response to VacA.....79

5.1 VacA causes changes to mitochondrial respiration in both AGS and AZ521 cells.....84

5.2 Assessment of total cell count accuracy 85

5.3 Oligomerization and pore-formation are necessary for VacA to induce maximal changes to mitochondrial respiration.....87

5.4 VacA does not cause changes to mitochondrial mass 88

5.5 VacA causes a reduction in glutamine and glutamic acid.....89

6.1 The ability of VacA to associate with cells is influenced by the extracellular pH 98

LIST OF ABBREVIATIONS

3-MA	3-methyladenine
ATP	Adenosine triphosphate
BabA	Blood group antigen-binding adhesion
β-ME	β-mercaptoethanol
BSA	Bovine serum albumin
CagA	Cytotoxin-associated antigen A
CCD	Charge-coupled device
CDC	Cholesterol-dependent cytolysin
DIC	Differential interference microscopy
DMSO	Dimethyl sulfoxide
DRM	Detergent-resistant membrane
DTT	Dithiothreitol
EDTA	Ethylenediaminetetraacetic acid
EE	Early endosome
EGFR	Epidermal growth factor receptor
EM	Electron microscopy
FCCP	Trifluoromethoxy carbonylcyanide phenylhydrazone
FCS	Fetal calf serum
GEEC	GPI-AP enriched early endosomal compartment
GPI-AP	Glycosylphosphatidyl inositol anchored protein
GPMV	Giant plasma membrane vesicle
HEPES	4-(2-hydroxyethyl)-1-piperazineethanesulfonic acid

LE	Late endosome
LLO	Listeriolysin O
LPS	Lipopolysaccharide
LRP1	Low-density lipoprotein receptor-related protein-1
LUT	Lookup table
MALT	Mucosa-associated lymphoid tissue
MRSA	Methicillin resistant *Staphylococcus aureus*
MTG	MitoTracker green
NEM	*N*-ethyl maleimide
OCR	Oxygen consumption rate
PAGE	Polyacrylamide gel electrophoresis
PCC	Pearson correlation coefficient
PBS	Phosphate buffered saline
PFT	Pore forming toxin
RPTP	Receptor protein tyrosine phosphatase
RT	Room temperature
SD	Standard deviation
SDS	Sodium dodecyl sulfate
T4SS	Type IV secretion system
TCA	Tricarboxylic acid
VacA	Vacuolating cytotoxin A

CHAPTER I

INTRODUCTION

A portion of this chapter was previously published as:

Foegeding NJ, Caston RR, McClain MS, Ohi MD, and Cover TL. (2016) An Overview of Helicobacter pylori VacA Toxin Biology. *Toxins* 8,173

HELICOBACTER PYLORI

Chronic gastritis and stomach ulcers were for a long time believed to be caused by elevated levels of acid in the stomach as a result of stress, smoking, or genetics (1). It was not until the 1980s, when Drs. Robin Warren and Barry Marshall published two seminal articles in the *Lancet* describing the isolation of a new bacterial species associated with chronic gastritis and peptic ulcer disease (2, 3), that the idea that gastric ailments could be caused by a bacterial infection began to take hold. Yet, many physicians and scientists remained unconvinced; the stomach was considered to be too harsh of an environment to be colonized by microorganisms (4). Frustrated by the skeptics, and by the lack of an animal model required to prove causation, Marshall drank a culture of *Helicobacter pylori* and developed gastritis within two weeks (Figure 1.1) (5). For their discovery of *H. pylori* and its role in gastric disease, Warren and Marshall were awarded the 2005 Nobel Prize in Physiology or Medicine.

Figure 1.1 Discovery of *H. pylori* as a causative agent of gastritis. (A) A comic depicting Dr. Barry Marshall drinking a culture of *H. pylori* in order to fulfill Koch's postulates. Adapted from (1). **(B)** Spiral bacilli observed in a gastric biopsy specimen collected from Marshall 10 days post ingestion of *H. pylori*. Adapted from (5).

H. pylori and gastric disease

H. pylori is a spiral shaped, Gram-negative, microaerophilic bacterium that colonizes the human stomach (3). Infection with *H. pylori* causes chronic inflammation of the gastric mucosa (gastritis), and although most individuals infected with *H. pylori* never develop severe disease, infection with *H. pylori* can cause peptic ulcer disease and gastric cancer (6).

More than 50% of the world's population is chronically infected with *H. pylori.* Therefore, even though < 2% of *H. pylori* infections progress to cancer, because the prevalence of *H. pylori* infection is high, stomach cancer is a common malignancy. In 2012, stomach cancer was the 6th most common cancer and the 3rd most common cause of cancer related death worldwide (7). Approximately 89% of non-cardia gastric cancer cases (representing ~ 78% of all gastric cancer cases) are attributable to chronic *H. pylori* infection, making infection with *H. pylori* the leading cause of stomach cancer (8, 9). As such, *H. pylori* is classified by the World Health Organization as a Group 1 carcinogen (9).

Prevalence of *H. pylori* infection varies widely between regions and countries (10). In general, *H. pylori* infection is more prevalent in developing countries than in industrialized countries. In the United States, Canada, Australia, New Zealand, and parts of Europe, less than 40% of the population is infected with *H. pylori*. In Mexico, China, Japan, and India, between 50 – 69% of the population is infected with *H. pylori.* In Russia and parts of South America and Africa, more than 70% of the population is infected with *H. pylori.* Infection usually occurs during childhood and, when left untreated, persists throughout the lifetime of the host (11, 12). Transmission of *H. pylori*

remains poorly understood; the most likely route of transmission is considered to be person-to-person contact (11, 12).

The factors that determine whether an *H. pylori* infection remains asymptomatic or progresses into peptic ulcer disease or gastric cancer are not completely understood. However, it is clear that disease progression can be influenced by strain specific *H. pylori* virulence factors, host genetics, and diet (11, 12). For example, individuals infected with strains of *H. pylori* that produce CagA, toxic forms of VacA, or BabA (three *H. pylori* virulence factors) are at an increased risk of developing severe gastric disease (13, 14). Similarly, infected individuals harboring polymorphisms in the promoter region of the cytokine IL-1β associated with elevated *IL-1β* expression are at an increased risk of developing severe *H. pylori*-mediated disease (15). Additionally, excessive dietary salt intake and decreased dietary iron intake are associated with an increased risk of gastric cancer (16-18), and it has been suggested that a diet low in fruits and vegetables may influence disease pathogenesis (19).

The clinical course of *H. pylori* infection correlates with the location of gastritis (20). Patients with gastritis in the gastric antrum, the most common form of *H. pylori* gastritis, are predisposed to duodenal ulcers (Figure 1.2 A). Patients with gastritis in the gastric body (also called the corpus) are predisposed to gastric ulcers and gastric cancer (Figure 1.2 A). Two subtypes of gastric cancer exist: *diffuse-type gastric adenocarcinoma* and *intestinal-type gastric adenocarcinoma* (11). Diffuse-type usually occurs at a younger age and is less well defined. Intestinal-type usually occurs at advanced ages and progresses through a well-defined series of stages (Figure 1.2 B) (11, 19). During the development of intestinal-type gastric adenocarcinoma, chronic

superficial gastritis transitions into *atrophic gastritis,* characterized by the loss of gastric glandular cells, which then leads to *intestinal metaplasia*, or the encroachment of intestinal-type epithelial cells into the normal gastric mucosa. This is followed by *dysplasia*, which is characterized by cells of an abnormal type within a tissue, and finally *adenocarcinoma,* or the presence of fully transformed malignant tissue. *H. pylori* infection also significantly increases the risk of developing gastric MALT (mucosa-associated lymphoid tissue) lymphoma (21).

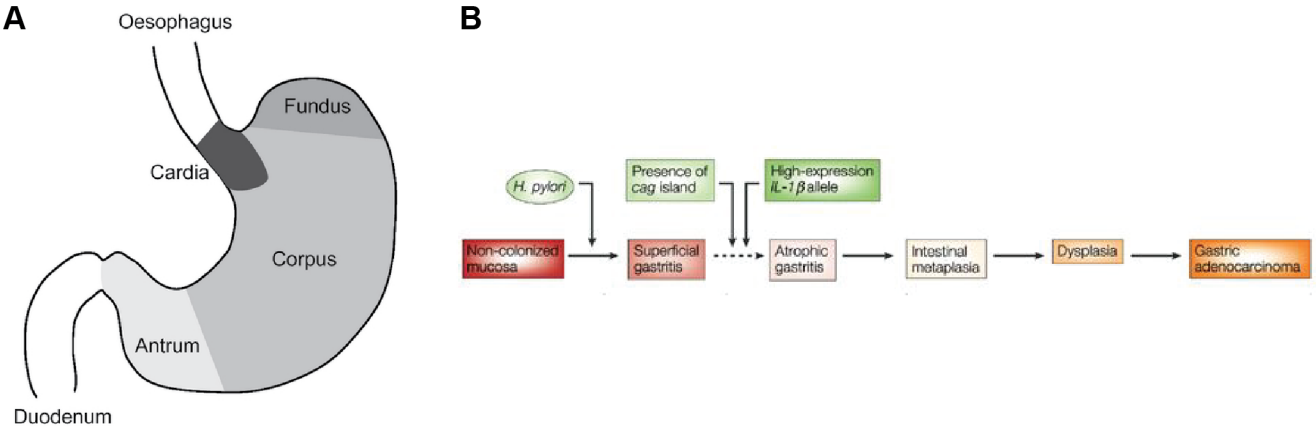

Figure 1.2 Anatomy of the stomach, and progression of intestinal-type gastric adenocarcinoma. (A) Schematic illustration of the human stomach. Most diseases associated with *H. pylori* occur in the antrum, corpus, or duodenum. Adapted from (4). **(B)** Intestinal-type gastric adenocarcinoma involves a transition of superficial gastritis to atrophic gastritis, followed by intestinal metaplasia, dysplasia, and gastric adenocarcinoma. Several factors, like the presence of the *cag* island (which encodes cagA and a type IV secretion system) within the *H. pylori*-infecting strain, or host polymorphisms associated with high expression of the cytokine IL-1β, contribute to the development of gastric adenocarcinoma. Adapted from (11).

Early detection and eradiation of *H. pylori* infection can successfully prevent peptic ulcer disease and gastric cancer (20). Infection with *H. pylori* is most commonly treated with triple therapy regimens consisting of two antimicrobial agents and one acid

suppressor. Acid suppression enhances the effectiveness of certain antimicrobial agents. Treatment regimens are ~80% effective in clearing *H. pylori* infection, with antibiotic resistance and patient noncompliance being the two main reasons for treatment failure. As a result of growing antibiotic resistance, alternative strategies are being investigated to treat *H. pylori* infection and prevent disease.

H. pylori colonization and virulence factors

The human stomach poses a challenging environment for bacteria to colonize, largely due to its acidic pH and presence of proteolytic enzymes (22). Secretion of hydrochloric acid (HCl) from specialized gastric cells helps to maintain the lumen of the stomach at a pH of < 4. Gastric epithelial cells are protected from the harsh luminal pH by a thick layer of bicarbonate-rich mucus coating at the apical cell surface (23). Bicarbonate ions within the barrier neutralize acid, and as a result, the mucus layer provides a neutral pH barrier between the stomach lumen and the epithelial cells.

Several features permit *H. pylori* to evade gastric juice and establish colonization. *H. pylori* are highly motile, having a spiral shape and several flagella emanating from one end (24). This enables *H. pylori* to move towards, and burrow through, the neutral mucus layer. *H. pylori* can be found either adherent to epithelial cells or free swimming in the mucus layer, within 25 μm from the surface of the epithelium (25). *H. pylori* also utilize chemotaxis to move directionally, away from the acidic lumen of the stomach and towards the neutral epithelium (25, 26). As another tool, *H. pylori* generates urease, which converts urea into the weak base ammonia, a process that protects *H. pylori* from gastric acidity (27).

H. pylori produces several strain-specific virulence factors. Three virulence factors in particular, CagA, VacA, and BabA, are associated with an increased risk of developing severe *H. pylori*-mediated disease (11). CagA and BabA are briefly introduced here, and VacA, a pore-forming toxin, is discussed in detail in a section to follow. CagA (cytotoxin associated gene A) is a 120 – 145 kDa effector protein that is translocated into the cytosol of host cells by a type IV secretion system (T4SS) (28). Once inside the host cell, CagA localizes to the inner leaflet of the plasma membrane, where it is phosphorylated, and induces changes in cell signaling and host cell morphology. The *cagA* gene and all the genes required to build the T4SS are encoded on a 40 kb region of the *H. pylori* genome referred to as the *cag* pathogenicity island (*cag* PAI). Roughly 60% of *H. pylori* isolated from infected individuals in Western countries are *cagA*-positive; however, in East Asia, almost 100% of isolates are *cagA*-positive (11, 28). BabA (blood group antigen-binding adhesion) is an *H. pylori* outer membrane protein that binds Lewis b (Le^b) antigens expressed on gastric epithelial cells (11). BabA expression is proposed to influence adhesion of *H. pylori* to the gastric epithelium (29).

BACTERIAL PORE-FORMING TOXINS

Pore-forming toxins (PFTs) are the most common type of bacterial toxin, as 25 – 30% of all cytotoxic bacterial proteins are PFTs (30). PFTs function by forming channels in host cell membrane, including both the plasma membrane and the membrane of intracellular organelles. Disruption of membrane permeability by bacterial PFTs can elicit a wide range of outcomes, including the death of target cells (31), intracellular

delivery of bacterial factors (32), release of nutrients from target cells (33), and escape of intracellular bacteria from host-cell vacuoles (34).

Intact cellular membrane is critical to maintaining cellular homeostasis as a membrane functions to enclose specific biological material and separate it from other biological material (35). As a barrier, cellular membrane is permeable to certain molecules and impermeable to others. In this way, two environments separated by membrane can regulate and maintain different molecular compositions. Small, nonpolar molecules readily associate with the hydrophobic interior of the lipid bilayer and therefore freely diffuse across cellular membrane. Large, polar molecules and ions readily associate with water and therefore do not freely diffuse across cellular membrane. In order to take in nutrients, release unwanted intracellular material, and regulate ion composition, cells have evolved ways to regulate the transport of molecules across membrane. Transporters and channels, two types of membrane proteins, directly shuttle small, polar molecules and ions across membrane, while mechanisms of endocytosis and exocytosis regulate the exchange of large macromolecules across membrane.

In general, PFTs are secreted from bacteria as water-soluble monomers that form a channel by oligomerizing and inserting into target membrane. The oligomer stoichiometry and, in turn, pore diameter vary greatly among PFTs. For example, the *Aeromonas hydrophila* PFT aerolysin is a heptamer with a pore diameter of ~1.7 nm (36), while a family of PFTs termed cholesterol-dependent cytolysins (CDCs) form large oligomers made up of 30 – 50 monomers with pore diameters between 25 – 35 nm (37, 38). PFTs are classified as α- or β-PFTs depending on whether the secondary structural

features of the membrane-spanning pore are α-helices or β-barrels (37).

Although all PFTs disrupt membrane permeability, the molecules to which a membrane becomes permeable vary depending on the properties of the PFT pore (39). As a result, PFTs can cause a range of cellular disruptions and host responses. Decades of research has helped to elucidate the molecular mechanisms of certain PFTs, as well as the array of host pathways and immune responses PFT exposure can trigger (37, 39-41). In order to introduce the pleiotropic effects of PFTs, two extensively studied PFTs are briefly reviewed in the paragraphs to follow.

One of the first bacterial toxins to be identified as a PFT was *Staphyloccus aureus* alpha-toxin (also called alpha-haemolysin) (42). *S. aureus* is a leading cause of skin infections, endocarditis, osteomyelitis, and bacteremia, and infections caused by methicillin resistant *Staphylococcus aureus* (MRSA) are increasingly difficult to treat. Alpha-toxin is a major *S. aureus* virulence factor, being associated with skin necrosis and lethal infection (43). Alpha-toxin is a β-PFT that forms heptameric oligomers with pore diameters of 2-3 nm. Alpha-toxin targets multiple cell types, including keratinocytes, endothelial cells, red blood cells, pneumocytes, and immune cells. Depending on the toxin concentration to which the cell is exposed, alpha-toxin can cause membrane barrier disruption, activation of signaling pathways, apoptosis, cell lysis, or several other effects. Therefore, the role of alpha-toxin in the pathogenesis of *S. aureus* disease is complex and not clearly defined.

Listeria monocytogenes is the causative agent of listeriosis, a disease that primarily affects pregnant women, newborns, and immunocompromised individuals, and can cause gastroenteritis or more serious outcomes, such as infections of the brain

(meningitis) or mother-to-fetus infections (44). Infection with *L. monocytogenes* occurs upon ingestion of contaminated food. As an intracellular pathogen, *L. monocytogenes* resides in vacuoles, but the bacterium must escape the vacuole in order to replicate in the host cell cytosol. The release of *L. monocytogenes* from the vacuole has been shown to depend on pore-formation by the *L. monocytogenes* PFT, listeriolysin O (LLO). LLO is a member of the CDC family of β-PFTs and forms large oligomers made up of ≥ 30 monomers, with pore diameters ranging between 25 – 35 nm (38). In addition to its role in facilitating vacuole escape, LLO has been shown to activate signaling pathways, cause ion flux across host cell plasma membrane, induce mitochondrial fragmentation, modulate immune activity, and more, suggesting LLO may play multiple roles in promoting bacterial virulence (44).

As these examples demonstrate, a single PFT can elicit complex cellular responses in multiple cell types, making its precise contribution to bacterial pathogenesis difficult to establish.

VACUOLATING CYTOTOXIN A

Vacuolating cytotoxin A (VacA) was discovered in 1988, when it was reported that *H. pylori* broth culture filtrates contained a protein that caused cellular vacuolization (45). VacA is a pore-forming toxin, and many of its effects on target cells are attributed to the formation of membrane channels at the cell surface or at intracellular sites (46). The most extensively studied VacA activity is its ability to induce cellular vacuolation, but VacA has been found to elicit a wide range of responses from several cell types. Although many bacterial toxins enter host cells and cause cellular alterations by

exerting an enzymatic activity, VacA has no known enzymatic activity.

VacA secretion, domain organization, and protein structure

The *vacA* gene encodes a 140 kDa precursor protein which undergoes cleavage at the amino- and carboxy-terminals during secretion to yield an 88 kDa mature VacA toxin (47-50). The VacA precursor protein is comprised of an N-terminal signal sequence (3 kDa), the mature VacA toxin (88 kDa), a peptide of unknown function (12 kDa), and a C-terminal domain (35 kDa) predicted to be an autotransporter β-barrel (Figure 1.3 A) (47-49, 51-53). For VacA to be secreted from *H. pylori* into the extracellular environment, it must cross both the inner and outer membranes of the cell envelope. The Sec-pathway is proposed to export VacA across the inner membrane, cleaving the N-terminal signal sequence in the process (47, 52). The C-terminal autotransporter domain is proposed to insert into the outer membrane, forming a channel that exports the mature VacA toxin into the extracellular environment (54).

The amino acid sequence of the mature VacA protein is not closely related to sequences of any other known bacterial toxin. The 88 kDa secreted VacA protein can undergo limited proteolysis in the presence of trypsin or during prolonged storage to yield 33 kDa and 55 kDa fragments (48, 55). These are considered to be two domains of VacA (p33 and p55) (Figure 1.3 B). Mixtures of recombinant p33 and p55 proteins can reconstitute a functionally active form of VacA (56, 57). The p55 domain has a predominantly right-handed β-helical structure (58), which is a feature shared by the passenger domains of several proteins secreted by an autotransporter mechanism in other Gram-negative bacterial species (59). The p33 also has a predominantly right-

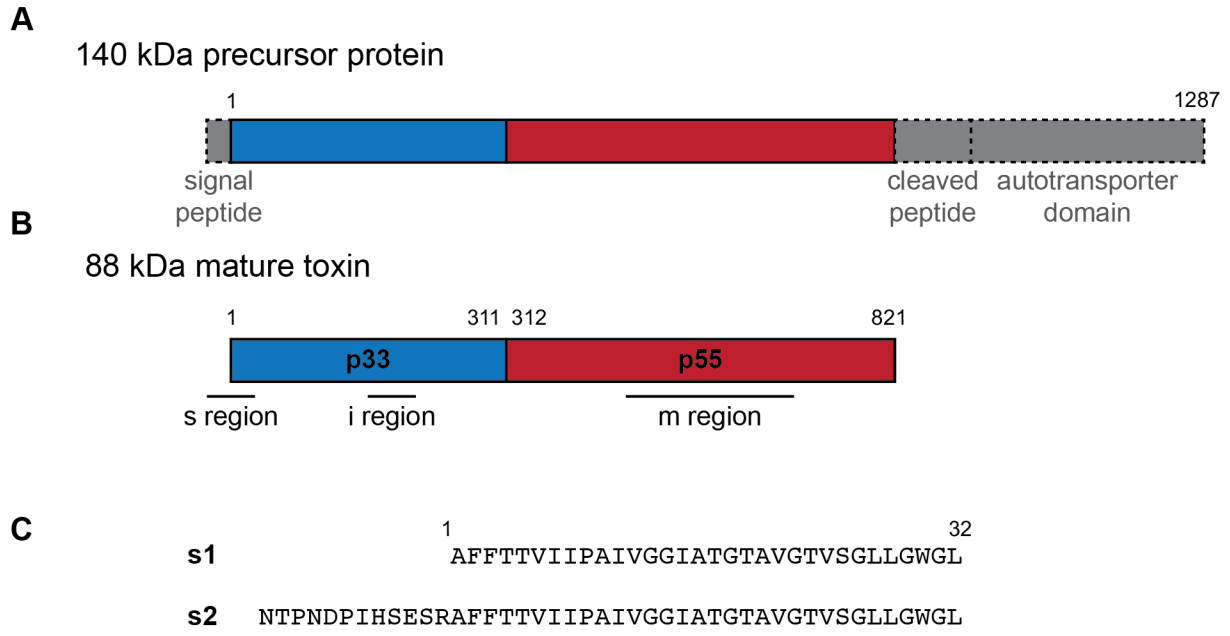

Figure 1.3 VacA domain organization and regions of genetic variation. (A) VacA is translated as a 140 kDa precursor protein (1287 amino acids). The signal peptide, a 12 kDa peptide of unknown function, and the autotransporter domain (grey regions) are cleaved to yield the mature toxin (blue and red regions). The autotransporter domain is proposed to insert into the outer membrane of *H. pylori* and form a channel through which VacA is secreted. **(B)** The 88 kDa mature toxin (821 amino acids) secreted into the extracellular space has two domains, p33 (blue) and p55 (red). There is a high level of sequence variation between *vacA* alleles found in different *H. pylori* strains. The three main regions of sequence variation (s-, i-, and m-region) are shown. **(C)** Representative signal peptides from type s1 and s2 VacA proteins. The s-region contains a hydrophobic stretch of 32 amino acids important for channel formation. Compared to s1-type VacA, s2-type VacA proteins contain a 12-amino-acid hydrophilic extension that disrupts channel formation.

handed β-helical structure with two short α-helices at residues 30-37 and 68-74 (60, 61). No high-resolution structural data are available for residues 1-26 in the p33 domain, residues 300-334 between the p33 and p55 domains, or residues 812-821 at the C-terminus of the p55 domain, suggesting these regions are highly flexible (60, 61). Residues within both the p33 and p55 domains are involved in protomer-protomer interactions to facilitate oligomerization (60, 61).

Both p33 and p55 are required for efficient binding of the toxin to the plasma membrane (56). The p33 domain is required for insertion of VacA into membranes to form anion-selective channels (62, 63). When expressed intracellularly, the minimal VacA region required for cell vacuolation encompasses residues 1-422, which includes the entire p33 domain plus 111 amino acids from the amino-terminal portion of the p55 domain (64-66).

The N-terminus of the p33 domain contains a sequence of 32 uncharged amino acids, corresponding to the only predicted hydrophobic segment within VacA long enough to span a membrane (62, 63, 67). Deletion of this region results in a VacA mutant lacking vacuolating activity and defective in membrane channel formation in planar lipid bilayers (62). The amino-terminal hydrophobic region of VacA includes three tandem GXXXG transmembrane association motifs (defined by glycine residues at positions 14, 18, 22, and 26) (63, 67, 68). Mutagenesis of amino acids within this region, including glycine residues at positions 14 and 18 or a proline residue at position 9, abolishes VacA channel formation and vacuolating activity (63, 69, 70).

Every strain of *H. pylori* contains the *vacA* gene, however only 50% of *H. pylori* strains produce active VacA toxin (45, 47, 71). Lack of active VacA production may be due to variation in VacA transcription efficiency (72), variation in the level of VacA protein secretion (51), or *vacA* sequence variation (73). Indeed, there is a high level of sequence variation between *vacA* alleles found in different strains of *H. pylori,* and certain VacA variants have been shown to be more active than others (73). There are three main regions of sequence variation; the signal sequence region (s-region), the intermediate region (i-region), and the middle region (m-region) (Figure 1.3 B) (73, 74).

The s-region corresponds to the amino-terminal signal sequence and the amino-terminus of the mature toxin. Compared to s1-type VacA, s2-type VacA has a 12-amino-acid hydrophilic extension that impairs pore formation and inhibits vacuolation (Figure 1.3 C) (73, 75). The i-region is located within the p33 domain and is not well characterized, however i1-type VacA has been shown to be more active than i2-type VacA (74, 76). The m-region corresponds to a stretch of ~250 – 300 amino acids in the p55 domain with only 55 – 60% sequence similarity (73, 77). Variation within the m-region has been linked to cell type specificity and may also influence channel activity (78, 79). Multiple combinations of s-, i-, and m- regions can occur, and strains containing s1, i1, or m1 forms of *vacA* are associated with a higher risk of gastric cancer or peptic ulcer disease compared to strains containing s2, i2, or m2, forms of *vacA* (73, 74).

VacA oligomerizes in solution to form an assortment of flower- or snowflake-shaped structures (Figure 1.4) (80). These include double-layered structures (dodecamers and tetradecamers) as well as single layered structures (mainly hexamers and heptamers, but occasionally higher order forms). Several lines of evidence indicate that oligomerization is required for VacA activity (62, 81). Membrane-bound VacA organizes into hexameric oligomers, therefore membrane channels formed by VacA are proposed to be hexamers (82). It is thought that double-layered structures are favorable formations of VacA in solution, as this organization would bury hydrophobic membrane binding sites.

Exposure of VacA oligomers to acidic pH or alkaline pH results in the disassembly of VacA oligomers into monomers (83, 84). When added to cultured cells, preparations

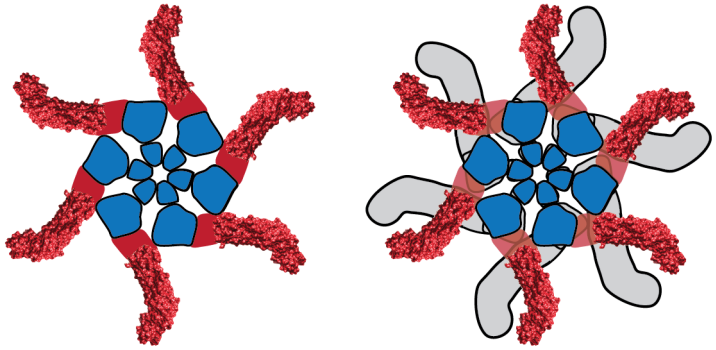

Figure 1.4 Structural organization of VacA oligomers. A hexamer (left) and dodecamer (right) are shown. Within each p88 protomer, p33 and p55 domains are shown in blue and red, respectively. A crystal structure has been solved for a portion of p55 (85), corresponding to peripheral elements of the oligomer (80). Single-layered hexamers are proposed to be structurally similar to membrane channels formed by VacA (82).

of VacA exposed to low pH or high pH have greatly increased cytotoxic activity compared to preparations of oligomeric VacA (86, 87). Therefore, it is thought that VacA first interacts with the plasma membrane of host cells as a monomer, where it oligomerizes and inserts to form a functional membrane channel.

VacA activities in animal models

The precise role of VacA in *H. pylori* infection and disease is not well understood, however *in vitro* studies suggest a few potential roles. It has been shown that wild type *H. pylori* strains can colonize mice more efficiently than Δ*vacA* strains (88-90) and can outcompete Δ*vacA* strains (89), indicating that VacA may function to promote *H. pylori* colonization of the stomach. However, VacA is not essential for colonization, as *H. pylori* Δ*vacA* strains successfully colonize mice, gerbils and gnotobiotic piglets (89, 91-93). Other studies suggest VacA contributes to the development of stomach ulcers. In mice studies, oral treatment with purified VacA or

with culture extracts from *H. pylori vacA*+ strains is reported to cause immune cell infiltration, damage to gastric cells, and ulceration (48, 94-96). Gastric damage and inflammation is reported to be more severe when *H. pylori* strains encode s1/i1 compared to s2/i2 *vacA* alleles (97). Additionally, in a study involving infection of gerbils with *H. pylori*, gastric ulceration occurred less commonly in gerbils infected with a *ΔvacA* strain compared to gerbils infected with a wild type strain (93). Finally, two studies report VacA has immunomodulatory activities in mice, suggesting VacA may facilitate immune tolerance to *H. pylori* infection (88, 98).

VacA activities in cell culture

Endosomal alterations. The most extensively studied activity of VacA is its ability to cause vacuolation of cultured cells. Most studies of this phenomenon and other VacA activities have been conducted with the most active form of VacA (type s1i1m1). Vacuolation can be observed within a few hours after addition of VacA to cells and is enhanced by the presence of weak bases (99). The membranes of VacA-induced vacuoles contain markers typically found in membranes of late endosomes (LEs) and lysosomes (100, 101), which suggests that the vacuoles arise from late endosomal/lysosomal compartments. The current model for VacA-induced vacuolation (46, 102) proposes that the secreted monomeric form of VacA binds to the plasma membrane. Upon binding, VacA monomers form oligomers which are endocytosed and trafficked to LEs, where they form anion-selective channels in the LE membrane (103-107). Transit of chloride ions through VacA channels in the LE membrane leads to an increase in intraluminal chloride concentration, which in turn triggers the enhancement

of V-ATPase proton pumping activity and a decrease in intraluminal pH (108, 109). Membrane-permeant weak bases diffuse into LEs, where they are protonated in the acidic environment and trapped. As a result, LEs undergo osmotic swelling, resulting in cell vacuolation (110). In addition to causing cell vacuolation, VacA causes a variety of functional alterations related to disruption of proper endocytic compartment trafficking. These include inhibition of intracellular degradation of epidermal growth factors (111), inhibition of procathepsin D maturation (111), perturbation of transferrin recycling (112), and in immune cells, inhibition of antigen presentation (113).

Mitochondrial alterations. Treatment of cells with VacA results in an assortment of mitochondrial alterations, including reduction of mitochondrial transmembrane potential (114-116), release of cytochrome *c* (116-118), activation of Bax and Bak (116, 119), and mitochondrial fragmentation (119). After entry into host cells, it has been shown that VacA can localize to mitochondria (115, 117, 119, 120), leading to the hypothesis that the toxin acts directly on mitochondria. In support of this model, VacA has been shown to cause a reduction in the transmembrane potential of isolated mitochondria (115), and there is evidence that VacA is imported into the inner mitochondrial membrane (IMM) (121, 122). The ability of VacA to induce mitochondrial dysfunction is dependent on VacA channel activity (115, 118, 119). Thus, one model proposes that VacA is imported into mitochondria and induces mitochondrial transmembrane potential reduction, perhaps by pore formation. This depolarization stimulates an initial release of cytochrome *c*, the activation of Bax/Bak, and the subsequent Bax/Bak-dependent release of cytochrome *c*. Another hypothesis is that VacA-induced mitochondrial dysfunction is due to indirect actions of VacA. For example, VacA may act indirectly by

activating pro-apoptotic factors to trigger mitochondrial-dependent apoptosis (116).

Epithelial barrier alterations. When added to cultured epithelial cells, VacA causes increased plasma membrane permeability, resulting in efflux of several anions, including chloride, urea, and bicarbonate, into the extracellular space (123, 124). VacA-induced permeabilization of cells is attributed to the formation of VacA channels in the plasma membrane (107). In addition to causing increased permeability of the plasma membrane, VacA causes increased paracellular permeability of polarized monolayers (125-127). The mechanism by which VacA causes increased paracellular permeability is not well understood.

Altered cell signaling. Several cellular alterations can be detected very rapidly after exposure of cells to VacA, and are likely due to the binding of VacA to the surface of host cells. In both gastric epithelial cells (128, 129) and T cells (130), VacA activates p38, a mitogen-activated protein (MAP) kinase. VacA-induced activation of the p38 signaling pathway leads to induction of cyclooxygenase 2 (COX-2) expression, which results in enhanced prostaglandin E2 production (129). VacA-induced activation of the p38 signaling pathway has also been shown to lead to the activation of activating transcription factor 2 (ATF-2) (128). VacA can also activate other MAP kinases, including ERK1/2 (128). In addition to activating MAP kinases, VacA can activate a signaling pathway that activates G protein-coupled receptor kinase interactor (Git1) (94), a signaling pathway that leads to the upregulation of vascular endothelial growth factor (VEGF) (131), and the β-catenin signaling pathway (132). The VacA cell surface receptors required for activating most of these pathways have not been characterized, but RPTP-β is reported to be the VacA receptor required for activation of Git1 (94) and

epidermal growth factor receptor is reported to be responsible for upregulation of VEGF (131).

Autophagy. When added to cultured gastric epithelial cells, VacA induces autophagy, the regulated degradation and recycling of cellular components in the cytoplasm. VacA is necessary and sufficient for *H. pylori*-induced autophagy (133). Similar to VacA-induced vacuole formation, VacA-induced autophagy is dependent on the capacity of VacA to form membrane channels, but the autophagosomes formed in response to VacA are proposed to be distinct from the more abundant and larger intracellular vacuoles that form in response to VacA-induced vacuolation (133). Although the mechanisms by which VacA induces autophagy are not fully understood, VacA-induced autophagy has been shown to depend on binding of VacA to low-density lipoprotein receptor-related protein 1 (LRP1) (134). Inhibition of autophagy leads to increased stability of intracellular VacA and increased cell vacuolation (133). One hypothesis is that the induction of autophagy upon exposure to VacA is a response initiated by the host cell to degrade VacA and prevent additional toxin-induced cell damage. Although acute exposure of host cells to VacA induces autophagy, prolonged exposure of host cells to VacA has been shown to disrupt autophagy and promote *H. pylori* infection (135, 136).

Cell death. VacA can induce cell death when cells are exposed to high concentrations of the toxin for extended periods of time (137, 138). AZ-521 cells (which are of duodenal origin) are particularly susceptible to VacA-induced cell death (139, 140). VacA-induced cell death is preceded by an assortment of mitochondrial alterations (116, 118, 119, 141), which suggests that these alterations are mechanistically

important in the process of VacA-induced cell death. VacA reduces the expression of pro-survival factors (142) and causes ER stress (143), which could also contribute to VacA-induced cell death. VacA can cause cell death by both apoptosis and necrosis (139).

Effects on immune cells and parietal cells. VacA can alter the function of many types of immune cells, including lymphocytes, macrophages, eosinophils (144, 145), mast cells (146, 147), and dendritic cells (88, 148). VacA inhibits activation and proliferation of T cells and B cells (130, 149-151), and can interfere with antigen presentation in B cells (113). In macrophages, VacA contributes to the formation of large vesicles termed megasomes, and impairs the maturation and function of vesicular compartments (152, 153). VacA alters various signal transduction pathways in macrophages (154, 155), and can cause macrophage apoptosis (156). These VacA-induced effects may function to impair the ability of macrophages to engulf *H. pylori.* In addition to immunosuppressive effects, VacA stimulates the expression of the proinflammatory enzyme COX-2 in macrophages and neutrophils (130).

Two studies reported that VacA inhibits gastric acid secretion from parietal cells (157, 158). In one study, exposure of parietal cells to VacA resulted in permeabilization of the plasma membrane and calcium influx that ultimately caused the disruption of actin arrangement in apical microvilli and an inhibition of acid secretion (158). At present, it is not known whether this effect of VacA on parietal cells contributes to a reduction in gastric acid secretion that is sometimes observed in the course of *H. pylori* infection.

VacA binding, internalization, and intracellular trafficking

Cell surface binding and receptors. Various studies have reached differing conclusions about whether VacA binding to cells is saturable (159-161) or nonsaturable (87, 162, 163). Therefore, it is unclear whether VacA binds to a single abundant, low-affinity receptor or to multiple cell surface components. Multiple putative VacA receptors on the surface of epithelial cells have been reported, including both protein and lipid receptors. These include receptor protein tyrosine phosphatases (RPTP) α and β (84, 94, 164, 165), low-density lipoprotein receptor-related protein 1 (LRP1) (134), epidermal growth factor receptor (EGFR) (166), heparan sulphate (167), sphingomyelin (168, 169), glycosphingolipids (170), and phospholipids (171). Although several putative receptors for VacA have been identified on epithelial cells, β2 integrin subunit (CD18) is the only VacA receptor that has been identified on T cells (172).

VacA binding to RPTP-β triggers alterations in cell signaling that ultimately lead to gastric tissue damage (94). Correspondingly, oral administration of VacA to wild-type mice results in gastric damage, whereas RPTP-β knockout mice are resistant to VacA-induced gastric damage (94). RPTP-β is not the sole receptor for VacA, as VacA is still internalized into the epithelial cells in RPTP-β knockout mice (94). VacA binding to LRP1 is important for VacA-induced autophagy and apoptosis (134).

Pore formation at the cell surface. After binding to the cell surface, VacA increases plasma membrane permeability and causes membrane depolarization (63, 107). These alterations are attributed to insertion of VacA into the plasma membrane and formation of anion-selective membrane channels (103-107).

VacA internalization and intracellular trafficking. Upon binding to the cell surface,

VacA is internalized by a clathrin-independent, Cdc42 dependent, and Rac1 dependent route that requires actin polymerization (173-175). Within 10 minutes after internalization, VacA is found in glycosylphosphatidyl-inositol anchored protein (GPI-AP)-enriched early endosomal compartments (GEECs), within 30 minutes in early endosomes (EEs), and within 2 hours in LEs (175).

Several studies have provided evidence that the intracellular localization of VacA is not limited to endosomal compartments. As one example, VacA has been detected in association with mitochondria in host cells (115, 141). The mechanisms by which VacA traffics to mitochondria are not well understood. One model proposes that a subset of VacA-containing endosomes co-localize with mitochondria, and that VacA is transferred directly from endosomes to mitochondria (141). Another model proposes that VacA is released into the cytosol and is imported into mitochondria via mitochondrial import proteins (121, 122). Although VacA gains access to the cytosol if expressed or microinjected inside host cells (64, 117), it is not known whether VacA added externally to cells can ultimately gain access to the cytosol (either by directly crossing the plasma membrane or by release from endosomes). It has been suggested that VacA may travel retrograde through the Golgi and endoplasmic reticulum (ER) (176), but this has not been investigated in detail. Further studies are needed to better understand VacA trafficking within host cells.

Summary

VacA is a pore-forming toxin that enhances *H. pylori* colonization of the stomach and contributes to the pathogenesis of *H. pylori*-mediated disease. VacA can elicit a

range of cellular responses from diverse cell types, yet it is currently unclear which of these *in vitro* responses are most relevant to VacA activity *in vivo*. We sought to gain a deeper understanding of 1) what structural features target VacA to host cells (Chapter III), 2) what the localization and fate of VacA is inside host cells (Chapter IV), and 3) what happens to cells following VacA intoxication (Chapter IV and V). Altogether, the work presented here addresses cellular responses to VacA; from contact at the cell surface, to intracellular localization, to changes in cellular homeostasis.

CHAPTER II

MATERIALS AND METHODS

Materials and chemical inhibitors

DiI-C12 was purchased from Life Technology. Dithiothreitol (DTT) was purchased from Research Products International. Formaldehyde and *N*-ethyl maleimide (NEM) were purchased from Fisher Scientific. Crystal violet (0.5% final concentration) was purchased from Sigma. Ammonium chloride (NH_4Cl; 5 mM or 25 mM final concentrations) and chloroquine (CQ; 100 μM final concentration) were purchased from Sigma and were prepared in culture media from a water-based stock solution. High levels of NH_4Cl can cause cell death, however minimal reductions in cell viability are observed in the presence of 5 mM NH_4Cl (177, 178). MG132 (5 μM final concentration) was purchased from Calbiochem and bafilomycin A1 (Baf A1; 10 nM final concentration) was purchased from Sigma. MG132 and BafA1 were prepared in culture media from a dimethyl sulfoxide (DMSO)-based stock solution. 3-methyladenine (3-MA; 10 mM final concentration) was purchased from Sigma was prepared in culture media from a water-based stock solution made immediately before each experiment. Control cells were mock treated with either water or DMSO as appropriate.

Cell culture

HeLa and AGS cells were purchased from ATCC. AGS cells were verified by ATCC to be an exact match of the ATCC human cell line CRL-1739. HeLa “Kyoto” cells were a gift from Ryoma Ohi. HeLa ATG16L1 KO and parental cells were purchased from Edigene (Beijing, China; Cat. no. CL0031242024A). HeLa cells, HeLa “Kyoto” cells, HeLa ATG16L1 KO and parental cells were cultured in DMEM supplemented with 10% FCS, penicillin, and streptomycin. AGS cells were cultured in RPMI 1640 supplemented with 10% FBS, 10 mM HEPES, penicillin, and streptomycin.

Purification and Alexa Fluor 488 labeling of VacA

All VacA variants and mutants used in this study were derived from WT VacA from *H. pylori* strain 60190 (a type s1m1 form of the protein). Untagged WT VacA, VacA Δ6-27, and VacA s2m1 were purified from *H. pylori* broth culture supernatants by gel filtration as previously described (62, 75, 83, 87). Strep-tagged WT VacA (with a Strep-tag II at position 808) and Strep-tagged VacA Δ346-7 (with a Strep-tag II at position 312) were purified using Strep-Tactin resin (IBA) as previously described (179). VacA p55 was purified from *E. coli* as a recombinant protein, as previously described (58). Details on the mutants used are provided in Table 3.2.

Purified VacA proteins were labeled using the Alexa Fluor 488 Microscale Protein Labeling Kit (Molecular Probes) or the Alexa Fluor 488 Antibody Labeling Kit (Thermo Fisher Scientific), both of which utilize an Alexa 488 tetrafluorophenyl (TFP) ester that reacts with primary amines. Labeled VacA was flash frozen in liquid nitrogen in single use aliquots and stored at -80°C.

Isolation of GPMVs

GPMVs were isolated using both DTT and NEM methods (180). GPMV buffer (2 mM $CaCl_2$, 10 mM HEPES, 0.15 M NaCl, pH 7.5) was supplemented with either 25 mM formaldehyde and 2 mM DTT or 2 mM NEM to make active buffers. Cells were seeded at around 60-70% confluency a day prior to GPMV isolation. The cells were washed twice with PBS then incubated in the respective, active GPMV buffer for 1-2 hours. GPMVs were isolated by decanting the solution. Prior to incubation with VacA, GPMVs were labeled with DiI-C12 (0.5 μg/mL final concentration), a marker for disordered phase (181, 182).

Treatment of GPMVs with VacA

Unless stated otherwise, purified VacA preparations were acid-activated before addition to GPMVs. Acid-activation of purified VacA was accomplished by dropwise addition of 0.1 M – 0.5 M HCl until the pH was reduced to ~4.0 (83, 86, 87). Acid-activated, Alexa Fluor labeled-VacA was then added to GPMVs at a final concentration of 5 μg/mL.

Measurement of VacA phase partitioning

All imaging was performed within 2 hours of incubation with VacA. Individual GPMVs were imaged using Zeiss LSM 510 confocal microscope using a 40X 1.3 NA oil objective. GPMVs were allowed to settle on the slide. Only GPMVs that were phase separated, exhibited a detectable signal in the DiI-C12 channel and had no visible vesiculation were selected for imaging. The fluorophores were excited using the 488 nm

line of a 40 mW Argon laser (VacA) and 543 nm line of a HeNe laser (DiI-C12). The confocal pinhole was set at 5 airy units for all experiments for both wavelengths. A single Z-plane image of individual GPMVs was collected at 10X optical zoom for quantifying raft localization. Imaging was performed at 2-10°C using a Peltier stage cooler (Physitemp Instruments), a temperature at which the GPMVs exhibited clear phase partitioning even in the absence of VacA binding (183). Partitioning of VacA was quantified as previously described (181) and is elaborated in Figure 3.3. Briefly, a linescan was drawn across the GPMV to determine the fluorescence intensity of VacA in both the ordered and the disordered phase. A moving average of 3 pixels was used to smooth the data and the fluorescence intensity of VacA at the ordered (I_{raft}) and disordered ($I_{non\text{-}raft}$) phase was determined. The raft partitioning coefficient (P_{raft}) was calculated as $P_{raft} = I_{raft}/(I_{raft} + I_{non\text{-}raft})$. In all merged images, the disordered phase marked with DiI-C12 is displayed in red and 488-VacA is marked in green. In the text, P_{raft} values are reported as mean ± standard error. Table 3.1 summarizes P_{raft} values measured in all the experiments.

Stable cell line generation

Non-targeting scramble control shRNA and ATG5 shRNA (Sigma) expressed from the pLKO.1 vector (Addgene) were used to create stable ATG5 KD cell lines using lentiviral transduction. Lentivirus particles containing the shRNA sequences were generated as previously described (184). For lentivirus transduction, AGS cells were grown to 70% confluency, media was supplemented with 10 µg/mL polybrene (Millipore Sigma), and cells were infected with lentivirus for 24 hr. After infection, cells were

allowed to recover for 24 hr. Cells were then cultured in media supplemented with 4 μg/mL puromycin to select for stable integration. After selection, AGS scramble and ATG5 KD cells line were cultured in media containing 2 μg/mL puromycin. The cell line created from shRNA clone TRCN0000151963 is referred to as ATG5 KD1 cell line. The cell line created from shRNA clone TRCN0000330392 is referred to as ATG5 KD2 cell line.

Treatment of cells with VacA

For all experiments involving VacA treatment of intact cells, VacA was acid-activated before use by adding 200 mM HCl drop wise until the pH was reduced to ~4.0 (83, 86, 87). For cell viability assays in Figure 4.1, cells were treated with 5 μg/mL (55 nM) or 20 μg/mL (222 nM) of VacA once a day for five days. For VacA trafficking studies or for analysis of VacA levels by Western blot, cells were treated with a pulse of 5 μg/mL VacA for either 1 hr at 4°C or 5 min at 37°C. In general, the treatment method of 1 hr at 4°C was used for experiments involving Western blots, in order to ensure sufficient binding of VacA to cells important for the subsequent detection of protein, and for experiments involving a 0 min time point, in order to ensure endocytosis is inhibited. Alternatively, for time course experiments requiring addition of VacA to cells in a multi-well plate at multiple time points, cells were pulsed with VacA for 5 min at 37°C in order to avoid the repeated exposure of cells to 4°C temperatures. Then medium overlying cells, containing unbound VacA, was removed, cells were washed with PBS, warm culture media was added, and cells were incubated at 37°C for the indicated times in the presence of respective inhibitors or mock treatments. Transmitted light images were

acquired with an EVOS FL digital inverted microscope (AMG) to assess for vacuolation.

Cell viability assay

Cell viability was quantified using the ATPlite 1step Luminescence Assay (Perkin Elmer) according to the manufacturer's instructions. Cells were seeded in 96-well flat bottom black polystyrene plates (Corning). Luminescence was measured with a Synergy HT microplate reader (BioTek).

Transfections and live-cell imaging

Plasmid transfections were performed using Lipofectamine 2000 (Invitrogen) according to manufacturer's instructions. The following amounts of plasmid DNA were transfected into cells for all experiments: 1 μg/mL Mito-RFP, mCherry-Rab5a, and mCherry-Rab7.

For live-cell imaging of VacA trafficking, transfected cells were seeded on glass-bottom poly-D-lysine coated dishes (MatTek) ~24 hr post-transfection and treated with VacA ~24 hr post-seeding. Cells were imaged in the presence of CO_2 at 37°C in movie media (Leibovitz's L-15 Medium without phenol red, 10% FCS, penicillin, streptomycin, 7 mM HEPES, pH 7.7) using a 60x 1.4 NA objective (Olympus) on a DeltaVision Elite imaging system (GE Healthcare) equipped with a Cool SnapHQ2 CCD camera (Roper). Optical sections were collected at 200 nm intervals and deconvolved in SoftWorx (GE Healthcare). Movies and images were prepared for publication using ImageJ.

Immunostaining and fixed-cell imaging

Cells were fixed with 4% paraformaldehyde (Electron Microscopy Sciences and Alfa Aesar) for 15 min at 37°C. The following primary antibodies were used in this study: and anti-MTC02 at 1:200 (Abcam), anti-LAMP1 at 1:100 (Cell Signaling Technology), and anti-LC3 at 1:200 (Medical and Biological Laboratories). Cells were incubated with primary antibodies for 1 hr 45 min. Secondary antibodies conjugated to Alexa 488 or Alexa 647 (Invitrogen) were used at 1:1000 for 45 min. DNA was counterstained with 5 μg/mL Hoechst 33342. Stained cells were mounted with Prolong Gold (Invitrogen) and imaged using a 60X 1.4 NA or a 100x 1.4 NA objective (Olympus) on the aforementioned DeltaVision Elite system. Either single optical slices or z-sections spaced 200 nm apart were acquired and deconvolved in SoftWorx (GE Healthcare), unless noted otherwise. Images were prepared for publication using ImageJ. To determine the Pearson correlation coefficient (PCC), single z-slice images were collected using the 100x 1.4 NA objective and the PCCs were determined in ImageJ from non-deconvolved images using the Intensity Correlation Analysis plugin (185). Nuclei were excluded from the colocalization analysis. The number of experimental replicates and the number of cells measured are listed in Table 4.1. To quantify fluorescence intensities, z-sections were collected using the 60X 1.4 NA objective and ImageJ was used to create maximum intensity z-projections and measure the integrated densities of individual cells.

Preparation of total cell lysate

To analyze VacA protein levels in treated cells, trypsinized VacA-treated cells were

pelleted, washed with PBS, resuspended in ice-cold NP40 lysis buffer (10 mM sodium phosphate, pH 7.2, 150 mM NaCl, 2 mM EDTA, 1% NP40) with protease inhibitors, and incubated for 15 min on ice. Total cell lysate was clarified by spinning at max speed (16,000 rcf) for 15 min at 4°C. Extracts were transferred to new microcentrifuge tubes on ice and protein concentration was determined using a Bradford assay (Bio-Rad). To store samples, protein extracts were mixed with 4X LDS Sample Buffer (Invitrogen) with supplemental BME (Sigma), boiled for 5 min, and frozen at -20°C.

Immunoblotting

Equivalent amounts (20-60 µg) of protein extracts were resolved on 4-12% Bis-Tris SDS-PAGE gels (Life Technologies) and transferred onto PVDF (EMD-Millipore) or nitrocellulose membrane (PerkinElmer). Immunoblots were blocked with 50% (v/v) Odyssey Blocking Buffer diluted in PBS or 2% milk diluted in TBST for 1 hr at RT and then probed with primary antibody overnight at 4°C or 1 hr at room temperature. The following primary antibodies were used in this work: anti-VacA (51, 186) (1:5000 or 1:10,000), anti-DM1α (1:5000) (Sigma-Aldrich), anti-ubiquitin (Life Sensors), anti-ATG5 (1:1000) (Abcam), anti-ATG16L1 (1:5000) (Abcam), and anti-GAPDH (1:1000) (Abcam). For fluorescence detection, secondary antibodies conjugated to Alexa Fluor 700 (Invitrogen) or Alexa Fluor 800 (LI-COR Biosciences) were used at 1:5000 for 45 min at room temperature and bound antibodies were detected using an Odyssey CLx imaging system (LI-COR Biosciences). For chemiluminescence detection, secondary antibodies conjugated to horseradish peroxidase (HRP) (Promega) were used at 1:10,000 for 1 hr at room temperature and bound antibodies were detected by x-ray film. ImageJ was

used to quantify signal intensity.

Measurement of oxygen consumption rates

Experiments were performed using the Cell Mito Stress Test kit (Agilent; Cat. no. 103015-100) according to the manufacturer's instructions and carried out using an Agilent Seahorse XFe96 Analyzer (Agilent) at the Vanderbilt High-Throughput Screening Facility. One day prior to the assay, AGS and/or AZ521 cells were seeded (20,000 cells per well) in an XF Cell Culture Microplate (Agilent) and placed in a tissue culture incubator at 37°C, and a Utility Plate (Agilent) was hydrated with tissue culture grade water at 37°C in a non-CO_2 incubator. On the day of the assay, spent culture medium was replaced with fresh medium, cells were treated either with acid-activated VacA (see figure legend for final concentration) or with acidified buffer and placed in a tissue culture incubator at 37°C for 4 hr. Immediately prior to completing the assay, spent medium was removed, cells were washed once with 200 µL Seahorse XF RPMI Medium, pH 7.4 (Agilent; Cat. no. 103576-100) supplemented with 2 mM L-glutamine and 11 mM glucose (hereon referred to as Agilent Complete Medium) pre-warmed to 37°C, medium was replaced with 180 µL Agilent Complete Medium, and cells were placed in a non-CO2 incubator at 37°C for 1 hr. Also immediately prior to completing the assay, water was removed from the Utility Plate and replaced with 200 µL of pre-warmed, 37°C XF Calibrant (Agilent) and placed in a non-CO_2 incubator for 45 min to 1 hr. Stock compounds were prepared and loaded into Sensor Cartridge (Agilent) ports according to the manufacturer's instructions, maintaining a final well concentration of 1 µM oligomycin, 0.25 µM FCCP, and 0.5 µM rotenone/antimycin A across all

experiments. Basal respiration, maximal respiration, and spare respiratory capacity were calculated according to the manufacturer's instructions.

Total cell count

Immediately following completion of the Cell Mito Stress Test on the Seahorse XFe96 Analyzer, cells were incubated with 4 μM Hoechst 33342 for 20 min at 37°C to stain nuclei. Images were acquired using a 4x objective with an ImageXpress Micro XL at the Vanderbilt High-Throughput Screening Facility and cell nuclei were quantified using MetaXpress Software.

Flow cytometry

Mitochondrial mass was measured by flow cytometry (3-laser BD LSRII) and data were analyzed using FlowJo software (FlowJo, LLC), both available at the Vanderbilt Flow Cytometry Shared Resource. To stain mitochondria, cells were incubated for 25 min with 200 nM MitoTracker Green (MTG) (Thermo Fisher Scientific) according to the manufacturer's instructions. Cells were then washed 3x with PBS, trypsinized, resuspended in phenol red-free RPMI 1640 medium, and immediately analyzed by flow cytometry.

Targeted metabolomics

AGS cells were treated for 4 hr with acid-activated VacA (20 μg/mL) or acidified buffer. Confluent cells from three T75 flasks were harvested per condition. Briefly, cells were placed on ice, culture medium was removed, and cells were washed 3x with ice-

cold 0.9% saline solution. Cells were lysed on ice in 1.5 mL 80% mass spec grade methanol (20% mass spec grade water), then scraped using cell scrapers and transferred to tubes on ice. Scraped and collected cells were exposed to three cycles of freeze thawing using liquid nitrogen and a 37°C water bath. Lysate was cleared by centrifugation at 16,000 g for 20 min at 4°C.

Analysis of metabolites were performed at the Vanderbilt University Mass Spectrometry Research Center using an Acquity UPLC system (Waters, Milford, MA) interfaced with a TSQ Quantum triple-stage quadrupole mass spectrometer (Thermo Scientific), using heated electrospray ionization operating in multiple reaction monitoring (MRM) mode. To 100 µl of each cell lysate sample, 10 µL of a methanol solution was added that contains stable isotope-labeled internal standards: tyrosine-d_2 and lactate-d_3 (Cambridge Isotope Lab, Tewksbury, MA). After centrifuging at 10,000 g for 10 minutes, 90 µL supernatant was transferred and injected into UPLC. Chromatographic separation was performed with a Zic-cHILIC column, 3 µm, 150 x 2.1 mm (Merck SeQuant, Darmstadt, Germany) at a flowrate of 300 µL/min. The mobile phases were A) 15 mM ammonium acetate with 0.2% acetic acid in water/acetonitrile (90:10, v/v), and B) 15 mM ammonium acetate with 0.2% acetic acid in acetonitrile/water/methanol (90:5:5, v/v). The gradient was as follows: 0 min, 85%B, 2 min, 85%B, 5 min, 30%B, 9 min, 30%B, 11 min, 85%B, 20 min, 85%B. Spray voltage was set to 5 kV and the capillary and vaporizer temperatures were 300°C and 185°C; with sheath gas, and auxiliary gas set to 50 and 5 psi, respectively. The skimmer offset was set to -10 V and the collision pressure was 1.5 mTorr.

Statistical analysis

GraphPad Prism 5 was used to generate all graphs and perform statistical analysis. Differences between two groups were assessed by a t test. Differences between multiple groups were assessed by an ANOVA followed by the Dunnett's Multiple Comparison Test.

CHAPTER III

DETERMINANTS OF VACA LIPID RAFT PARTITIONING

A modified version was previously published as:

Raghunathan K*, Foegeding NJ*, Campbell AM, Cover TL, Ohi MD, Kenworthy AK. (2018) Determinants of Raft Partitioning of the Helicobacter pylori Pore-Forming Toxin VacA. *Infection and Immunity* 86:e00872-17
*co-first authors

INTRODUCTION

A number of bacterial toxins bind to lipid raft microdomains in cell membranes (reviewed in (187). Lipid rafts are membrane microdomains enriched in cholesterol, glycosylphosphatidylinositol anchored proteins (GPI-APs), and sphingolipids (188, 189). For oligomeric toxins, lipid rafts are advantageous targets as they concentrate receptors (190, 191). Indeed, VacA is an example of an oligomeric toxin that is proposed to associate with lipid rafts (168, 169, 173, 174, 186, 192-194). In support of this hypothesis, VacA was shown to co-migrate with detergent-resistant membrane (DRM) domains (168, 174, 186). Furthermore, depleting cholesterol and GPI-AP in cell membranes inhibits VacA-induced vacuolation and, to varying degrees, VacA cell binding and internalization (186, 194, 195). These observations suggest that intact lipid rafts are required for VacA toxicity. Multiple putative VacA receptors on the surfaces of

cells have been identified (196) and VacA can also bind lipid bilayers directly (82, 192). Thus, partitioning of VacA into rafts could potentially occur immediately upon or shortly after it associates with cell membranes. Consistent with the latter possibility, the toxin has been postulated to undergo receptor-mediated translocation into rafts (193). However, the mechanisms responsible for targeting VacA to lipid rafts have not been fully defined.

An ongoing challenge in studying the association of proteins with raft-like domains in cells is the small size and dynamic nature of these domains in live cells (197). In recent years, giant plasma membrane vesicles (GPMVs) have emerged as a tractable model system with which to study raft targeting mechanisms (198-201). Derived from the plasma membrane of adherent cells, GPMVs represent an attractive system that combine the experimental simplicity of working with *in vitro* model membranes while retaining the compositional complexity of plasma membranes (202, 203). These blebs are distinct from apoptotic blebs, have a composition similar to that of intact plasma membranes (204), and are devoid of cytoskeleton (205). Importantly, GPMVs have been shown to phase separate into coexisting liquid phases akin to model membranes, without the need to disrupt membrane organization with harsh detergents and/or globally altering cell membrane lipid composition (202-204). The two liquid phases seen in GPMVs, ordered and disordered, are thought to correspond to lipid raft and non-raft regions in cellular plasma membrane, respectively (200). These domains reach much larger sizes than are seen in cell membranes, presumably as the result of eliminating cytoskeletal barriers that limit the size of rafts in intact cells (206). Furthermore, it has been shown that biochemically-defined raft associated proteins partition into the liquid

ordered region while non-raft associated proteins partition into the liquid disordered region (207). These features have made GPMVs an ideal model system to understand mechanisms underlying raft association and formation as well as to probe potential biological functions of lipid rafts (181, 182, 208-217). In the current study, we use GPMVs to characterize the phase preference of VacA and dissect the structural features of VacA that dictate its affinity for raft domains.

RESULTS

VacA localizes to the liquid ordered phase of GPMVs

VacA has been previously been shown to bind to lipid rafts in cell membranes, based on experiments using biochemical approaches (168, 174, 186, 194). Therefore, we first set out to test whether the protein localizes to the ordered phase in GPMVs. To address this question, we generated GPMVs from HeLa cells, a cell line commonly used to study VacA trafficking (174, 218). At room temperature, GPMVs derived from HeLa cells form coexisting raft and nonraft phases that can be readily visualized by fluorescence microscopy (219). These GPMVs can be used to directly measure the degree of raft association of a given protein by comparing their localization to that of a marker of the ordered or disordered phase (200).

To examine the phase preference of VacA in GPMVs, we first labeled VacA with Alexa Fluor 488. Control experiments verified that Alexa 488-labeled VacA was able to oligomerize, enter cells, and induce vacuolation (Figure 3.1). GPMVs were isolated from HeLa cells and labeled with DiI-C12 (1,1'-didodecyl-3,3,3',3'-tetramethylindocarbocyanine perchlorate), a dye that marks the disordered phase. The

GPMVs were then incubated with 5 μg/ml of Alexa Fluor 488-labeled VacA and imaged within 2 hr of incubation. All imaging was performed at temperatures at which a large fraction of HeLa cell-derived GPMVs are known to exhibit phase separation (183).

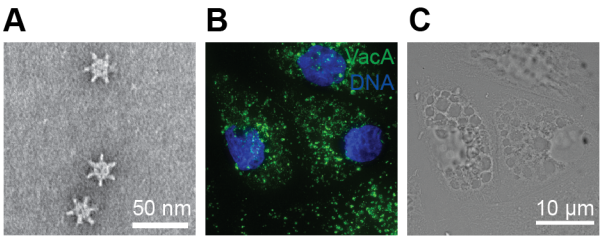

Figure 3.1 Labeling VacA with Alexa Fluor 488 does not disrupt VacA oligomerization, internalization, or activity. (A) Negative stain image of 488-VacA. **(B)** AGS cells were treated with 5 μg/mL of acid-activated 488-VacA (green) for 24 hr in the presence of 5 mM NH_4Cl. DNA, blue. **(C)** A corresponding transmitted light micrograph was taken to assess for vacuolation.

We found that in the majority of GPMVs, Alexa Fluor 488-VacA was primarily excluded from the phase labeled by DiI-C12, indicating that VacA associates with the liquid ordered phase of GPMVs (Figure 3.2 A). This result was verified across several independent experiments in which we quantified the phase preference of VacA in multiple GPMVs by measuring the fluorescence intensity *I* of VacA in the liquid ordered phase (I_{raft}) and the liquid disordered phase ($I_{non\text{-}raft}$). The raft partition coefficient *P* was then calculated as $P_{raft} = I_{raft}/(I_{raft} + I_{non\text{-}raft})$ (200). A P_{raft} of between 0 and 0.5 corresponds to a nonraft-preferring protein, whereas P_{raft} between 0.5 and 1.0 corresponds to a raft-preferring protein (181). In GPMVs derived from HeLa cells, the P_{raft} for VacA ranged from 0.47 to 0.82, with a mean raft partitioning coefficient (± standard error of the mean [SEM]) of 0.67 (± 0.01) (Table 3.1). These results indicate that in a majority of GPMVs, VacA shows significant localization to raft domains.

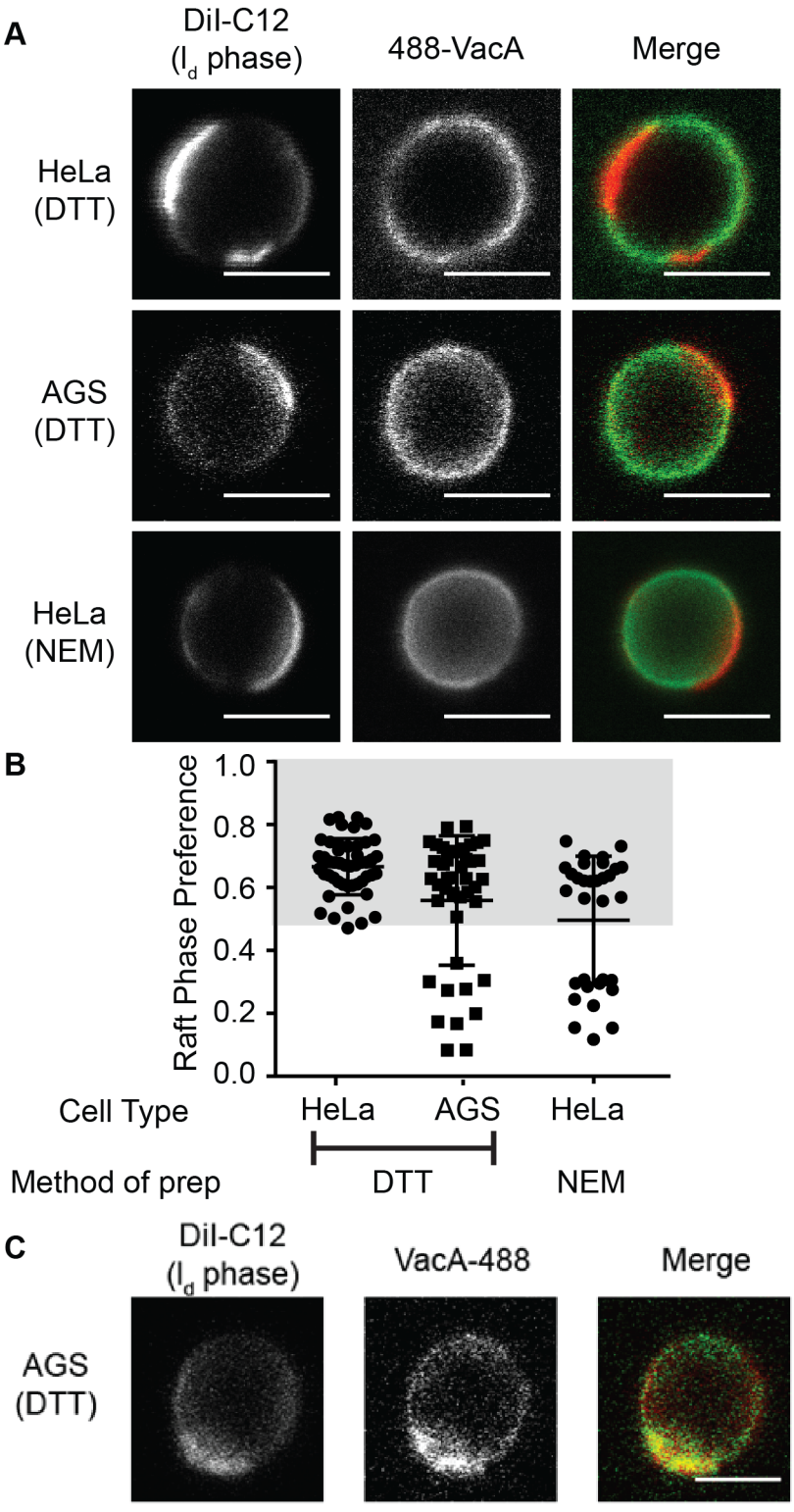

Figure 3.2 VacA primarily localizes to the liquid ordered phase of GPMVs. (A) Representative images of GPMVs isolated from HeLa and AGS cells using the DTT method as well as from HeLa cells using the NEM method. GPMVs were incubated with DiI-C12 (red) and acid-activated 488-VacA (green) and imaged within 2 hr at 2°C (HeLa

cells with the NEM method), 5°C (AGS cells with the DTT method), or 10°C (HeLa cells with the DTT method). The temperature differences in imaging relate to the differences in transition temperature between the different samples. Dil-C12 marks the disordered phase (l_d). Scale bar, 5 μm. **(B)** Quantification of the phase preference of VacA for each condition represented in panel A. Each data point represents a raft partitioning coefficient measured from a single GPMV. VacA preferentially partitioned into the ordered phase (gray-shaded area) in the majority but not all of the GPMVs across the conditions tested. Nonshaded area represents the liquid disordered phase. Bars and whiskers represent mean values ± standard deviations (SD). **(C)** Representative image of a GPMV isolated from AGS cells using the DTT method in which VacA partitioned into the disordered phase. Around 20% of the GPMVs exhibited this behavior. GPMVs were incubated with Dil-D12 (red) and acid-activated 488-VacA (green) and imaged within 2 hr. Dil-C12 marks the disordered phase. Scale bar, 5 μm

Table 3.1 Summary of raft partition coefficients across experiments.

Figure Number	Condition/ form of VacA studied	Raft partition coefficient (Mean ± SEM)	Number of independent experiments	Total number of GPMVs analyzed for each condition
Figure 3.2	HeLa-DTT	0.67 ± 0.01	3	48
	AGS-DTT	0.56 ± 0.03	2	42
	HeLa-NEM	0.55 ± 0.02	2	29
Figure 3.4	Activated WT	0.67 ± 0.01	2	48
	Non-Activated WT	0.60 ± 0.01	2	43
Figure 3.5	Δ346-7	0.61 ± 0.02	3	80
Figure 3.6	Δ6-27	0.54 ± 0.02	2	50
	s2m1	0.61 ± 0.01	2	47
Figure 3.7	p55	0.55 ± 0.01	2	29

To test the generality of this finding, we explored whether VacA associates with the liquid ordered phase of GPMVs isolated from a different cell type. For this, we used AGS cells, a gastric cancer cell line that has been used extensively in studies of *H. pylori*-host cell interactions (138, 174, 193). Consistent with its phase preference in GPMVs isolated from HeLa cells, VacA also localized to the liquid ordered phase of GPMVs isolated from AGS cells (Figure 3.2 A), with a mean raft partitioning coefficient

of 0.56 (± 0.03). Interestingly, in GPMVs isolated from AGS cells, we observed a biphasic behavior of VacA raft partitioning: in ~20% of the GPMVs, VacA was localized to the disordered phase (Figure 3.2 B and C). Therefore, despite VacA being a raft-preferring toxin, our data suggest that VacA has the potential to bind to the nonraft phase.

To ensure that VacA's preference for the liquid ordered phase of GPMVs was not an artifact of the way the GPMVs were prepared, we determined the phase preference of VacA in GPMVs isolated using the *N*-ethyl maleimide (NEM) method (180). This alternate method of GPMV preparation, unlike the most commonly used dithiothreitol (DTT) method, avoids the nonspecific cross-linking of proteins (180, 200, 220). It also preserves protein palmitoylation, which is disrupted by the DTT method (212). Using NEM, we found that VacA also localized to the liquid ordered phase of the majority of GPMVs (Figure 3.2 A and B), with a mean raft partitioning coefficient of 0.55 (± 0.02). Once again, there was a small subset of GPMVs where VacA bound to the disordered phase. Nevertheless, irrespective of the method of GPMV preparation, in the majority of the GPMVs, VacA behaves as a raft-associated toxin.

Having established that VacA associates preferentially with raft domains, we next investigated which regions of VacA are required for its raft partitioning. For consistency, all subsequent studies were performed with GPMVs derived from HeLa cells using the DTT method.

Acid activation is not required for VacA lipid raft association

In solution at neutral pH, VacA can assemble into large, double-layered oligomeric

complexes, in which the hydrophobic membrane-binding interfaces are partially occluded (80, 82). Acid activation triggers the disassembly of inactive VacA oligomers into monomers and enhances VacA cell binding and activity (83, 87, 103). It was previously reported that acid activation, in addition to enhancing VacA cell binding and activity, is required for VacA association with DRMs, suggesting that acid activation is required for VacA to bind lipid rafts (186). To test this hypothesis, we asked whether nonactivated VacA is able to localize to the liquid ordered phase of GPMVs. For these experiments, we incubated GPMVs with Alexa Fluor 488-VacA that was not acid activated.

Compared to fluorescence signals in GPMVs labeled with identical amounts of acid-activated VacA, increased fluorescence in the medium surrounding the GPMVs and decreased VacA fluorescence were observed for GPMVs labeled with nonactivated VacA (Figure 3.3). These findings suggest that binding of nonactivated VacA to GPMVs is decreased compared to the binding of acid-activated VacA. However, independent of its membrane affinity, nonactivated VacA still partitioned to the liquid ordered phase similarly to acid-activated VacA, with a mean raft partitioning coefficient of 0.60 (± 0.01) (Figure 3.4).

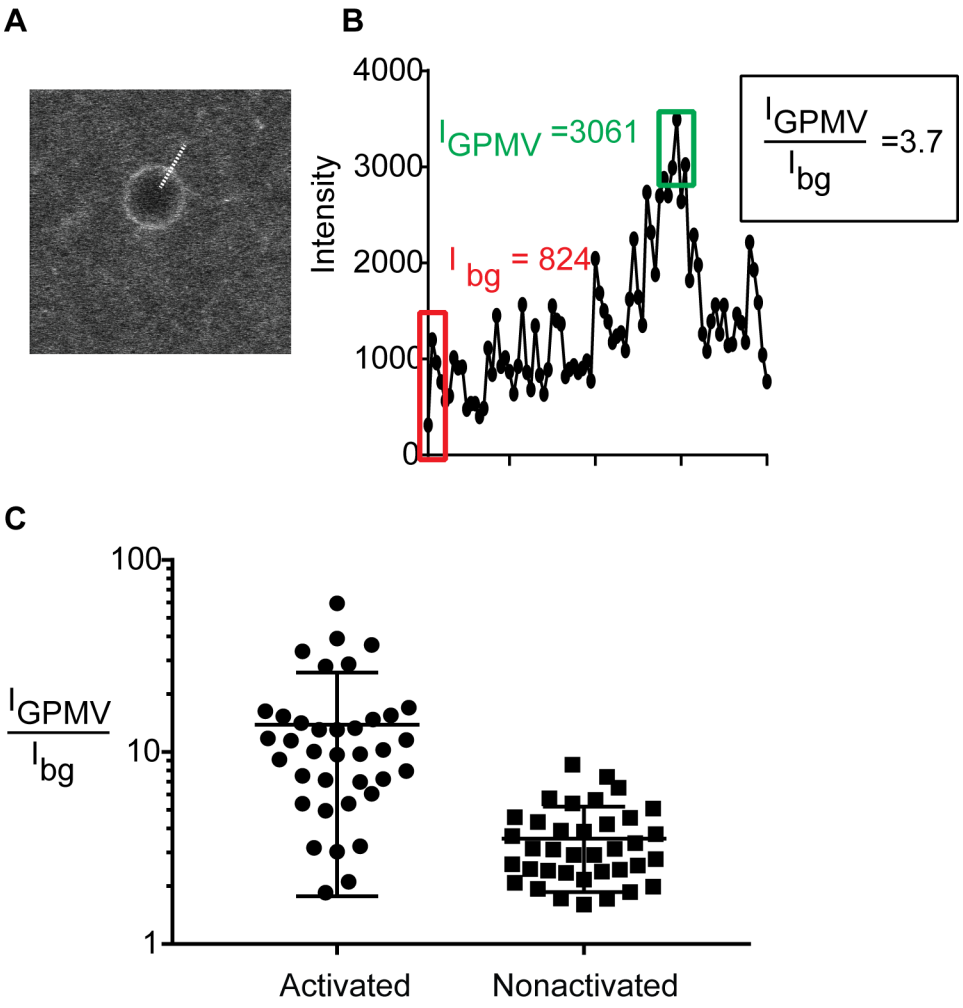

Figure 3.3 Acid activation increases binding of VacA to membrane. (A) Representative GPMV image with a typical line scan. **(B)** Line scan of intensity. The average of the first three pixels of the line scan as highlighted in the red box is used as the intensity of the background I_{bg} and the average of the pixel intensity as highlighted by the green box is used as the intensity of the GPMV, I_{gpmv}. The ratio of the two values (I_{gpmv}/ I_{bg}) was quantified as the relative binding of VacA to the GPMV. **(C)** Relative binding of VacA to GPMVs under acid activated and nonactivated conditions.

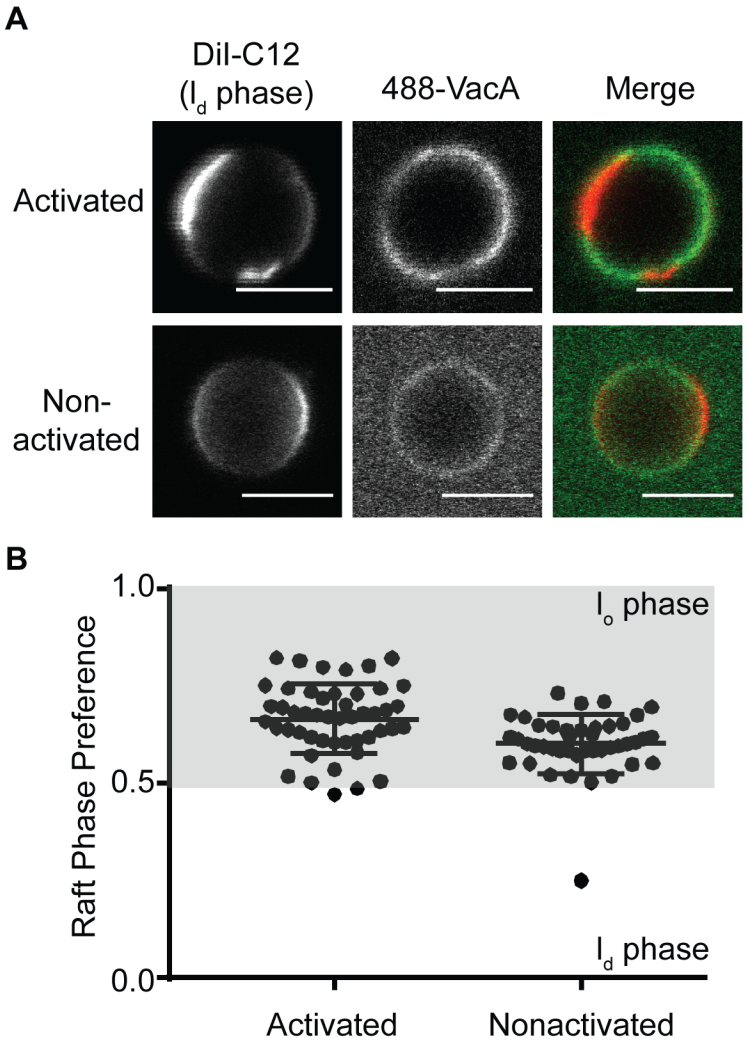

Figure 3.4 Acid activation is not required for VacA lipid raft association. (A) Representative images of GPMVs, isolated from HeLa cells using the DTT method, after incubation with either acid-activated (top) or nonactivated (bottom) Alexa Fluor 488-VacA. Note that the extent of binding of nonactivated VacA to GPMVs was markedly lower than that of acid-activated VacA and the VacA signal in the medium surrounding the GPMVs was higher for nonactivated VacA compared to acid-activated VacA. Scale bar, 5 μm. **(B)** Quantification of the phase preferences of activated and nonactivated VacA. Each data point corresponds to a raft partitioning coefficient measured from a single GPMV. Bars and whiskers represent mean values ± SD. I_o, liquid ordered phase (gray-shaded area); I_d, liquid disordered phase (nonshaded area).

Oligomerization is not required for VacA lipid raft association

Oligomerization has been shown to drive raft association of other bacterial toxins (181, 191, 221). Therefore, we next tested whether this is also the case for VacA by using a nonoligomerizing mutant, VacA Δ346-7, which lacks aspartic acid 346 and glycine 347 (Table 3.2). VacA Δ346-7 cannot oligomerize in solution or on membranes (82, 179, 222), but it is able to bind membranes (82). Surprisingly, the binding behavior of VacA Δ346-7 was very similar to what was observed for wild-type VacA. A majority of VacA Δ346-7 localized to the liquid ordered phase (Figure 3.5), with a mean raft partitioning coefficient of 0.61 (± 0.02). In ~ 20% of GPMVs, VacA Δ346-7 partitioned into the nonraft phase. Thus, oligomerization is not essential for the targeting of VacA to lipid rafts.

Table 3.2 VacA variants and mutants used in this study.

Variant	Oligomerizes	Forms Pores	Vacuolates Cells	References
s1m1 (WT)	✓	✓	✓	52,71,79,102
Δ346-7	×	×	×	80,178
Δ6-27	✓	Inefficiently	×	61,73
s2m1	✓	Inefficiently	×	73,221
p55	×[a]	×	×	57,58,59,61

[a] Although the p55 domain does not oligomerize into flower-shaped hexamers, it is purified as a dimer.

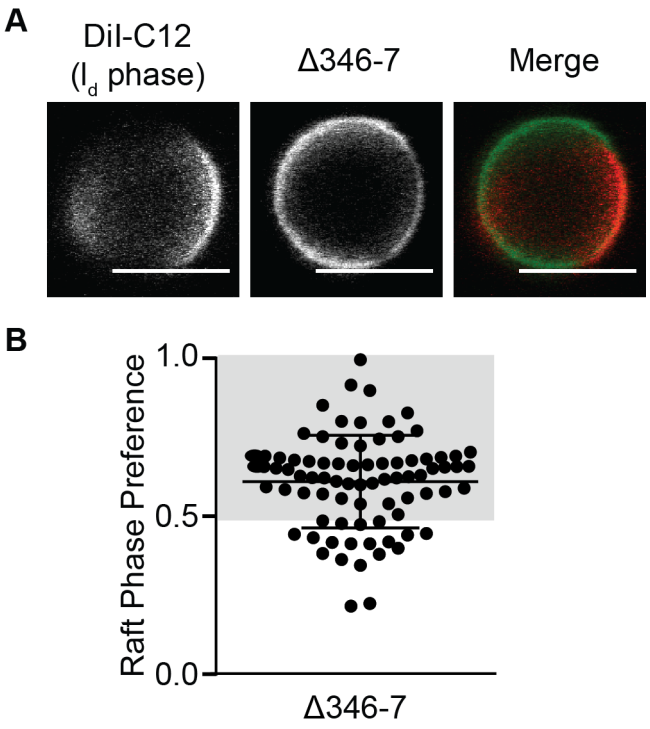

Figure 3.5 Oligomerization is not required for VacA lipid raft association. (A) A representative image of GPMVs incubated with Alexa Fluor 488-VacA Δ346-7 demonstrates that the nonoligomerizing mutant localizes to the ordered phase. Scale bar, 5 μm. l_d, liquid disordered phase. **(B)** Quantification of the phase preference of VacA Δ346-7. Each data point corresponds to a raft partitioning coefficient measured from a single GPMV. Bars and whiskers represent mean values ± SD. Gray-shaded area represents the liquid ordered phase, and nonshaded area represents the liquid disordered phase.

Disruptions of the amino-terminal, pore-forming region do not abrogate VacA lipid raft association

We next asked whether sequences contributing to VacA's ability to form pores also influence its raft binding preference. Regions of the p33 domain of VacA have been proposed to insert into the lipid bilayer to form a membrane channel (82). For instance, the amino-terminal portion of the p33 domain (residues 1 to 32) contains three tandem GXXXG transmembrane dimerization motifs (62, 63, 67). To test the importance of these repeats for raft association, we examined the phase preference of VacA Δ6-27, a

mutant lacking these three GXXXG motifs due to a deletion of a strongly hydrophobic 22-amino-acid stretch in the amino terminus (62). For comparison, we also examined VacA s2m1, a variant of VacA that contains 12 additional residues at the N-terminus that are known to disrupt pore formation (75). Both VacA Δ6-27 and VacA s2m1 can assemble into oligomeric structures, but they exhibit reduced channel activity and fail to induce cellular vacuolation (Table 3.2) (62, 75, 80, 223). When incubated with GPMVs, VacA Δ6-27 and VacA s2m1 predominantly partitioned into the liquid ordered phase (Figure 3.6), with mean partition coefficients of 0.54 (± 0.02) and 0.61 (± 0.01), respectively. Similarly to wild-type VacA and VacA Δ346-7, in a small proportion of

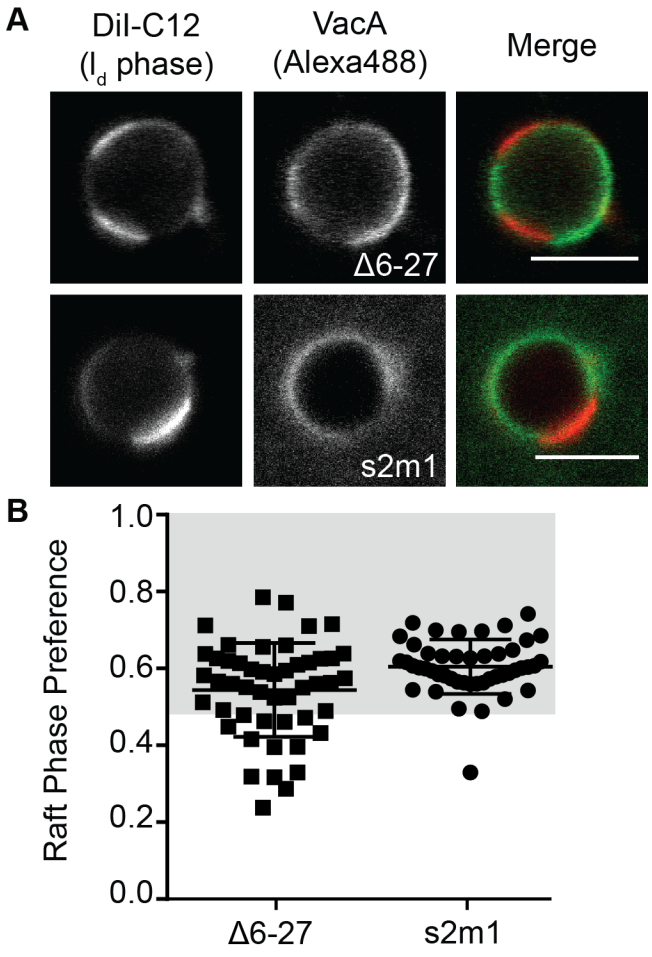

Figure 3.6 Disruptions to the VacA amino-terminal pore-forming region do not abrogate VacA lipid raft association. (A) Representative images of GPMVs after incubation with either acid-activated Alexa Fluor 488-VacA Δ6-27 (top) or acid-activated Alexa Fluor 488-VacA s2m1 (bottom). Scale bar, 5 μm. l_d, liquid disordered phase. **(B)** Quantification of the phase preference of VacA Δ6-27 and VacA s2m1. Each data point corresponds to a raft partitioning coefficient measured from a single GPMV. Bars and whiskers represent mean values ± SD. Gray-shaded area represents the liquid ordered phase, and nonshaded area represent the liquid disordered phase.

GPMVs, VacA Δ6-27 partitioned into the nonraft phase. These data show that alterations of the amino-terminal, pore-forming region of VacA do not abrogate its lipid raft association and suggest that VacA need not be able to form a functional pore in order to associate with lipid rafts.

The p55 domain is sufficient to target VacA to lipid rafts

Since none of the tested mutants with mutations in the p33 region disrupted VacA raft partitioning in GPMVs, we hypothesized that the p55 domain may be sufficient to target VacA to lipid rafts. The isolated p55 domain is known to bind membranes, but it is unable to assemble into large oligomeric structures (Table 3.2) (56, 58, 63). To test our hypothesis, we incubated recombinant p55 with GPMVs and measured its phase preference. We found that indeed, the p55 domain alone bound to GPMVs, where it localized to the liquid ordered phase (Figure 3.7 A and B) with an average raft partitioning coefficient of 0.55 (± 0.01). Thus, the p55 domain is sufficient to target VacA to lipid rafts.

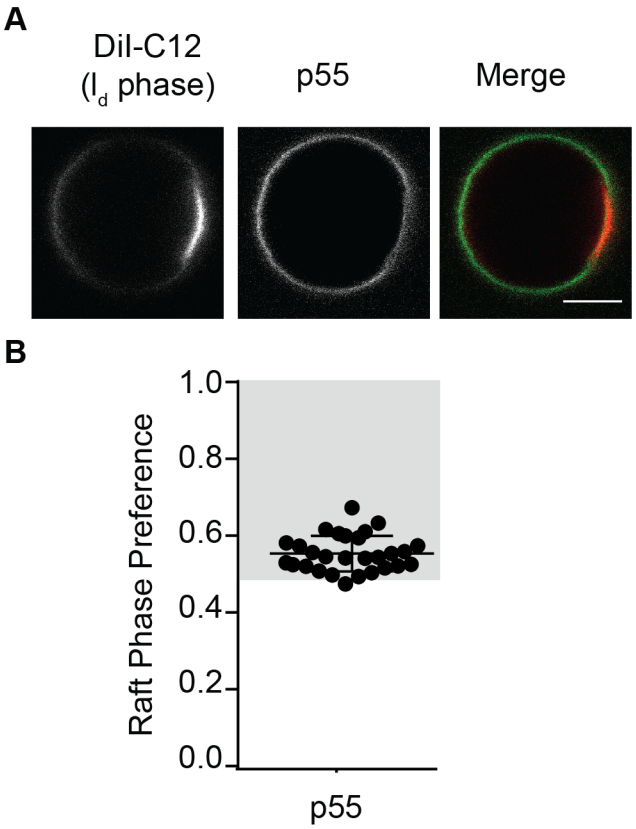

Figure 3.7 The p55 domain is sufficient for VacA partitioning into lipid rafts. (A) Representative images of GPMVs incubated with Alexa Fluor 488-VacA p55. Scale bar, 5 μm. l_d, liquid disordered phase. **(B)** Quantification of the phase preference of the VacA p55 domain. Each data point corresponds to a raft partitioning coefficient measured from a single GPMV. Bars and whiskers represent mean values ± SD. Gray-shaded area represents the liquid ordered phase. Nonshaded area represents the disordered phase.

DISCUSSION

Many bacterial protein toxins, including VacA, are thought to utilize lipid rafts as the first step in intoxication of host cells (187). To provide a direct measure of VacA's association with rafts, as well as to define features of the protein that mediate its affinity for raft versus nonraft domains, we analyzed VacA's phase preference using GPMVs. A major advantage of using GPMVs is that they contain the inherent compositional complexities of the plasma membrane and permit the direct visualization of lipid

organization by light microscopy (200). Thus, GPMVs minimize many of the artifacts that arise in other experimental systems and have proven to be a powerful tool for the study lipid rafts (203).

We show that VacA predominantly binds the ordered phase in GPMVs isolated from both HeLa and AGS cells, and we detect this phenomenon using two different approaches to isolate GPMVs. This finding is in agreement with previous studies that identified VacA as a raft-associated protein, using biochemical approaches (168, 174, 186, 194). Using GPMVs, we were also able to quantify the raft partitioning coefficient of VacA, and found that, on average, it ranged between 0.5 and 0.6 for essentially all the forms of VacA studied here. This is similar to the raft partitioning coefficient of the canonical lipid raft marker, cholera toxin B subunit, measured using the same approach (181). Thus, all forms of VacA analyzed partition primarily as raft-preferring proteins. Importantly, under the conditions of our experiments, GPMVs exhibit phase separation prior to the addition of VacA. Therefore, VacA binding is not responsible for driving raft formation in the GPMVs. We did, however, observe several behaviors that suggest that the extent to which VacA associates with rafts is a regulated process. First, in a small fraction of GPMVs, including those isolated from AGS cells, VacA partitioned into the disordered phase. Given that VacA is proposed to bind a wide range of receptors, it is possible that localization of VacA to nonraft domains in a subset of the GPMVs could be due to an interaction between VacA and a nonraft receptor (discussed in more detail below) (193). Second, the mean raft partitioning coefficients for VacA variants, while all within the raft-preferring range, were slightly lower than that of wild-type VacA (see Table 3.1). This suggests that wild-type VacA represents the most highly optimized form

of the toxin in terms of its raft partitioning activity.

To enhance VacA cell binding and activity *in vitro*, oligomeric VacA preparations are typically exposed to a low pH in order to acid activate the toxin (83, 86). It has previously been proposed that nonactivated VacA does not associate with lipid rafts, on the basis of studies of its association with DRMs. This led to the conclusion that acid activation not only enhances VacA cell binding but is also required for VacA to bind lipid rafts (186). In contrast, our data show that acid activation is not required for VacA to associate with lipid rafts, as both acid activated and nonactivated VacA bind the ordered phase of GPMVs.

Oligomerization has been shown to facilitate the raft association of several oligomeric bacterial toxins, including the classic AB5 toxins, cholera toxin B and Shiga toxin (181, 190, 224, 225). Additionally, it was shown that oligomerization of anthrax toxin is a prerequisite for its association with rafts and that artificial cross-linking of anthrax toxin monomers is sufficient to localize anthrax toxin and its receptor to lipid rafts (226). Our results indicate that oligomerization is not required for VacA to bind lipid rafts as the nonoligomerizing mutant, VacA Δ346-7, associates with the liquid ordered phase. Thus, we conclude that raft association of VacA is not an emergent behavior arising as a consequence of oligomerization but is due to the inherent affinity of monomeric VacA for lipid rafts.

Our results also provide insights into specific regions in the toxin that are responsible for raft association, including domains that contribute to pore formation. VacA has complex membrane interactions; both the p33 and p55 domains of VacA are thought to be involved in membrane binding (56, 161), while portions of the p33 domain

insert into membrane and are essential for pore formation (62, 63, 75). We utilized two mutants that do not form pores efficiently, VacA Δ6-27 and VacA s2m1, to probe whether the amino terminus of the toxin (a principal region involved in pore formation) is also involved in VacA's raft preference. Since both VacA Δ6-27 and VacA s2m1 associate with the liquid ordered phase, our results indicate that the lipid raft partitioning of VacA is not dependent on the amino-terminal hydrophobic region responsible for pore formation. Nevertheless, given that VacA associates with a raft-like environment, pore formation might preferentially occur in rafts. To further define the regions of VacA needed for raft partitioning, we utilized recombinant p55 containing the m1 region. Our results show that the p55 domain on its own is able to bind lipid rafts. Unfortunately, difficulties in purifying properly folded recombinant p33 make it challenging to determine whether the p33 domain alone is also able to bind lipid rafts. Therefore, although we conclude that the p55 domain is sufficient for VacA to bind lipid rafts, the role of p33 remains to be determined. A model summarizing all our results is shown in Figure 3.8.

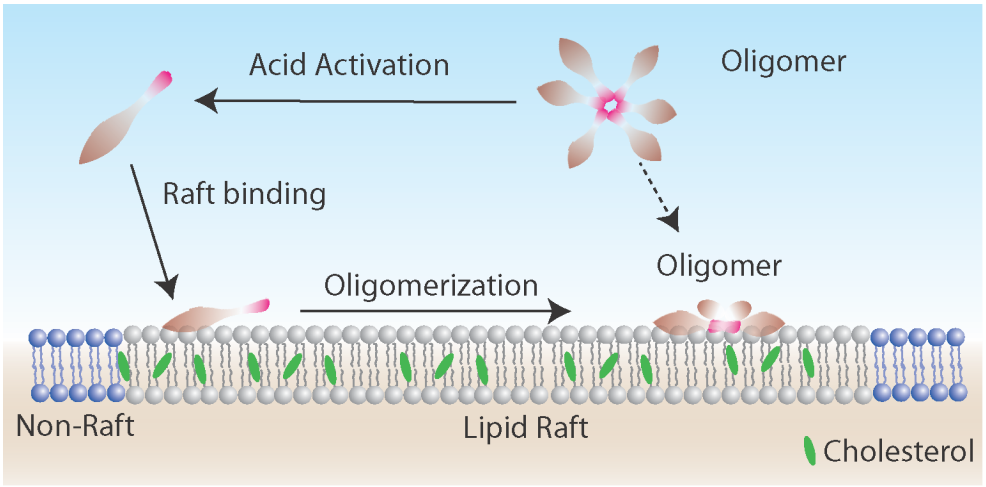

Figure 3.8 Working model of VacA partitioning into lipid rafts. Initially, acid activation promotes disassembly of VacA oligomers (1) into monomeric VacA (2).

Monomeric VacA primarily binds raft domains in cell membranes. Given that the p55 domain alone partitions into lipid rafts, we expect the p55 domain to play a large role in targeting VacA into the raft phase (3). VacA oligomerizes and potentially forms a pore in the raft phase. It is not known whether these two steps occur simultaneously or sequentially (4). In the absence of acid activation, VacA binds more weakly to cell membranes (in either an oligomeric or monomeric form) but is still targeted to lipid rafts.

The distinct preference of VacA for raft domains raises the question of whether specific receptors are involved in targeting VacA to lipid rafts or if the toxin instead recognizes lipid components of lipid rafts. To date, VacA has been proposed to bind a diverse list of receptors including epidermal growth factor receptor (EGFR), receptor-type tyrosine-protein phosphatase alpha (RPTPα), RPTPβ, low-density lipoprotein receptor-related protein 1 (LRP1), β2 integrin, and sphingomyelin (196). While some of these receptors are likely raft associated, suggesting that they could be directly responsible for bringing VacA to rafts, a subset of putative VacA receptors, such as RPTPβ and some forms of sphingomyelin, have been found to be associated with the nonraft phase (193, 227). Interestingly, the VacA-RPTPβ complex has been reported to translocate to rafts, suggesting that even nonraft receptors can potentially contribute to VacA's raft preference (193). It should also be noted that despite years of research, it is still unclear whether VacA binds to a single abundant-yet-low-affinity receptor or to multiple cell surface components (196). Indeed, previous studies have not agreed as to whether VacA displays saturable or nonsaturable binding to host cells (87, 159-163). Furthermore, VacA is known to bind artificial lipid membrane in the absence of any protein receptors (82, 103-105, 192). For example, although sphingomyelin localizes to lipid rafts and is proposed to be a receptor for VacA, one study showed that VacA bound large unilamellar vesicles equally well regardless of the presence or absence of

sphingomyelin (82). Thus, the interaction between VacA and lipid membrane is complex and thorough analysis of VacA-receptor interactions will be required to clarify the role VacA receptors play in VacA raft association and cellular intoxication.

VacA is but one of many toxins that appear to utilize lipid rafts for binding and entry into cells (191). However, VacA is different from many of these toxins in that its raft association appears to be independent of its oligomerization status and properties required for membrane pore formation (181, 191, 228). We anticipate that further studies of VacA and GPMVs will provide important insights into our understanding of the raft association of other, less-well-characterized pore-forming toxins.

CHAPTER IV

INTRACELLULAR DEGRADATION OF VACA AS A DETERMINANT OF GASTRIC EPITHELIAL CELL VIABILITY

A modified version was previously published as:

Foegeding NJ, Raghunathan K, Campbell AM, Kim SW, Lau KS, Kenworthy AK, Cover TL, Ohi MD. (2019) Intracellular Degradation of Helicobacter pylori VacA Toxin as a Determinant of Gastric Epithelial Cell Viability. *Infection and Immunity* 87:e00783-18

INTRODUCTION

One of the most extensively characterized VacA activities is its ability to induce the formation of large cytoplasmic vacuoles in cultured cells (46, 51). A current model for VacA-induced vacuolation (102, 229) proposes that VacA forms anion-selective channels in late endosomal/lysosomal membranes (62, 63, 101, 230), leading to an influx of chloride into endosomes, which stimulates increased proton pumping by the vacuolar ATPase and a subsequent decrease in intraluminal pH (104, 106, 107, 109). Membrane-permeant weak bases that diffuse into the endosome are protonated in the acidic environment and trapped, triggering osmotic swelling that manifests as cell vacuolation (108, 110).

Most cell types are relatively resistant to VacA-induced cell death, which requires exposure of cells to high concentrations of the toxin for long time periods (137-139, 141). One possible explanation is that cells might have mechanisms to protect from

VacA-induced toxicity. Indeed, there is growing evidence indicating that cells are able to respond and survive following exposure to several bacterial pore-forming toxins (PFTs), including *Staphylococcus aureus* alpha-toxin (231-233), *Vibrio cholera* cytolysin (234), *Aeromonas hydrophila* aerolysin (41), *Listeria monocytogenes* listeriolysin O (41), and *Streptococcus pyogenes* streptolysin O (235). Inhibiting cellular repair mechanism(s) enhances the toxicity of these PFTs (231, 233, 234).

Both the formation of VacA-induced vacuoles and VacA-induced cell death are enhanced in the presence of ammonium chloride (NH_4Cl), a weak base (51, 99, 108, 110, 138, 236). Consequently, in experimental studies in which cells are treated with purified VacA, the cell culture medium is often supplemented with NH_4Cl. The presence of weak bases in cell culture medium may mimic the conditions in the stomach during *H. pylori* infection, as *H. pylori* generates ammonia *in vivo* through the actions of urease and other enzymes, such as γ-glutamyl transpeptidase, asparaginase, and glutaminase (237-239). In this study, we investigated the mechanism(s) by which NH_4Cl influences the magnitude of VacA-induced cell death. We report that the presence of supplemental weak bases (such as NH_4Cl) inhibits intracellular VacA degradation, while having no detectable effect on VacA intracellular trafficking. Our results indicate that intracellular VacA degradation is independent of autophagy and proteasome activity, but dependent on lysosomal acidification. We propose that intracellular degradation of VacA in the lysosome enables host cells to resist VacA-induced vacuolation and cell death, and weak bases enhance VacA activity by inhibiting intracellular degradation of the toxin.

RESULTS

VacA-induced cell death is enhanced in the presence of supplemental NH_4Cl

As a first step in analyzing VacA-induced cell death, we performed experiments in which cells were treated with multiple successive doses of the toxin, potentially similar to conditions in the stomach where cells continually encounter newly synthesized VacA, in the absence or presence of NH_4Cl. Specifically, we treated AGS gastric epithelial cells once a day for five days with VacA (5 μg/mL) in the absence or presence of 5 mM NH_4Cl. Cell vacuolation was detected in the absence of NH_4Cl, but the cells continued to proliferate (Figure 4.1 A to C). In the presence of NH_4Cl, VacA-induced vacuolation was enhanced (Figure 4.1 D), and cell proliferation was inhibited (Figure 4.1 E and F). NH_4Cl alone did not induce significant vacuolation (Figure 4.1 G to L). After collecting transmitted light images, cellular ATP levels were determined to quantitatively assess cell viability. A small reduction in cell viability was observed in the presence of VacA alone or in the presence of NH_4Cl alone, but a large reduction in cell viability was only observed in the presence of both VacA and NH_4Cl (Figure 4.1 M). Thus, the reduction in cell viability in the presence of both VacA and NH_4Cl was synergistic, not additive. When the experiment was repeated with higher doses of VacA (20 μg/mL), once again the cells treated with VacA in the absence of NH_4Cl grew to confluency, whereas cells treated with VacA in the presence of NH_4Cl did not (Figure 4.1 N). Therefore, in the absence of NH_4Cl, repetitive treatment of cells with either low or high concentrations of VacA did not induce substantial cell death. Consistent with previous reports (138, 139), these data indicate that NH_4Cl enhances VacA-induced cell death.

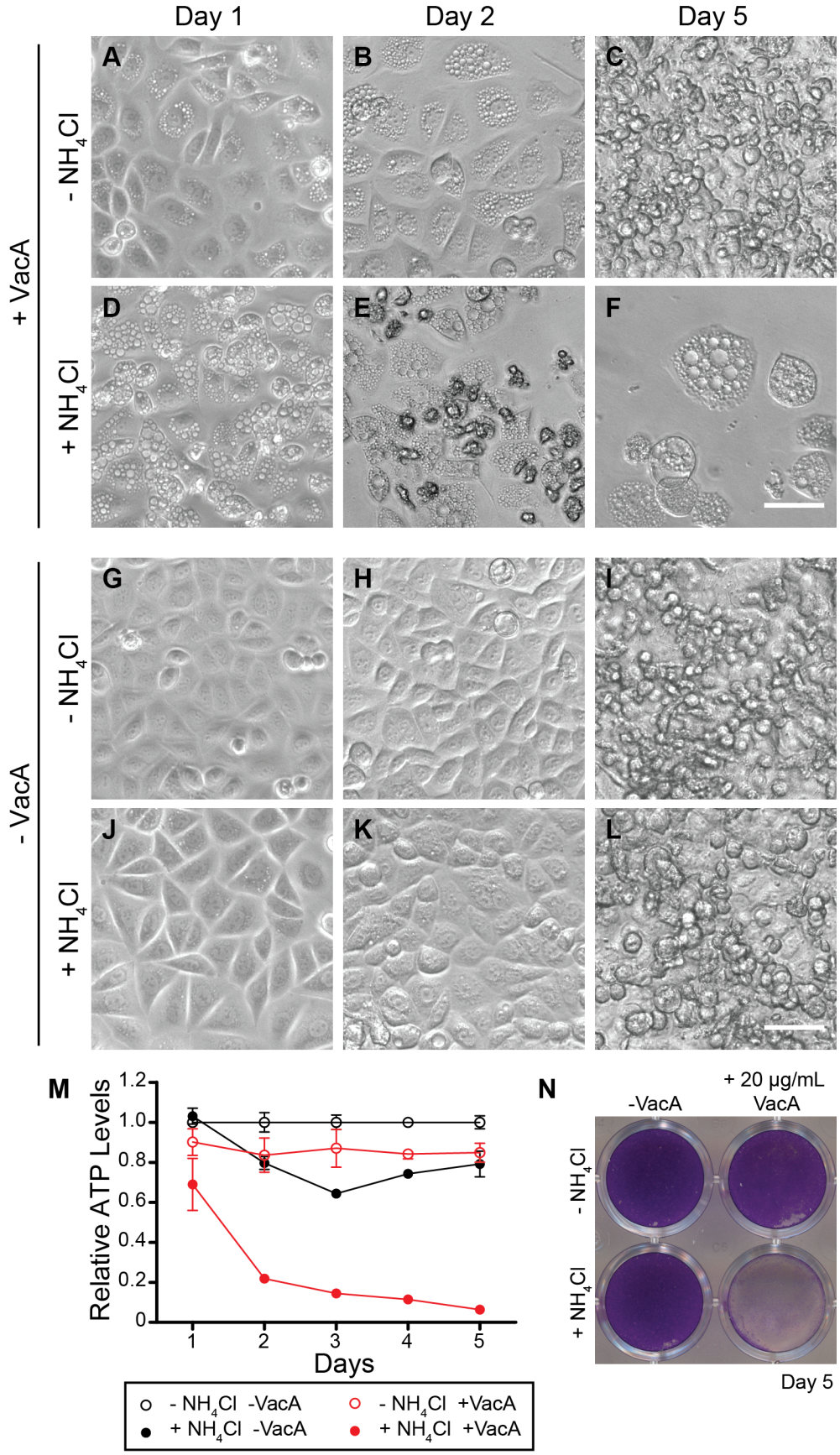
Day 1
Day 2
Day 5
+ VacA
- VacA
- NH4Cl
+ NH4Cl
A
B
C
D
E
F
G
H
I
J
K
L
M
Relative ATP Levels
1.2
1.0
0.8
0.6
0.4
0.2
0
1
2
3
4
5
Days
- NH4Cl -VacA
+ NH4Cl -VacA
- NH4Cl +VacA
+ NH4Cl +VacA
N
+ 20 µg/mL VacA
-VacA
- NH4Cl
+ NH4Cl
Day 5

Figure 4.1 Loss of cell viability requires treatment with both VacA and supplemental NH_4Cl. (A-L) AGS cells were treated once a day for five days with 5 μg/mL of VacA (A-F) or acidified buffer (G-L) in the absence (A-C, G-I) or presence (D-F, J-L) of 5 mM NH_4Cl. Transmitted light micrographs were collected after each successive day of VacA intoxication to assess for vacuolation. Scale bar, 50 μm. **(M)** Quantification of A-L using an ATPlite 1step Luminescence Assay to measure cellular ATP levels. Values represent luminescence signal normalized to control (- NH_4Cl - VacA) cells. **(N)** AGS cells were treated once a day for five days with 20 μg/mL of VacA in the absence or presence of 5 mM NH_4Cl. After five days, cells were fixed and stained with 0.5% crystal violet for 15 min to assess for the presence of cells.

NH_4Cl does not promote VacA trafficking to mitochondria

It has been suggested that VacA can induce cell death by directly trafficking to mitochondria and forming pores in mitochondrial membrane (115, 117, 119, 120, 141). Therefore, we tested whether NH_4Cl augments VacA-induced cell death by promoting VacA trafficking to mitochondria. To test this, we used Alexa Fluor 488-labeled VacA (488-VacA) to quantify VacA colocalization with mitochondria over time in the absence and presence of NH_4Cl. We observed that VacA was largely excluded from mitochondria (Figure 4.2 A) and we did not detect any consistent increase in VacA colocalization with mitochondria over time, regardless of whether cells were treated with VacA in the absence or presence of NH_4Cl (Figure 4.2 B and C and Table 4.1). Furthermore, there was no significant increase in VacA colocalization with mitochondria in the presence of NH_4Cl compared to VacA colocalization with mitochondria in the absence of NH_4Cl (Figure 4.2 D).

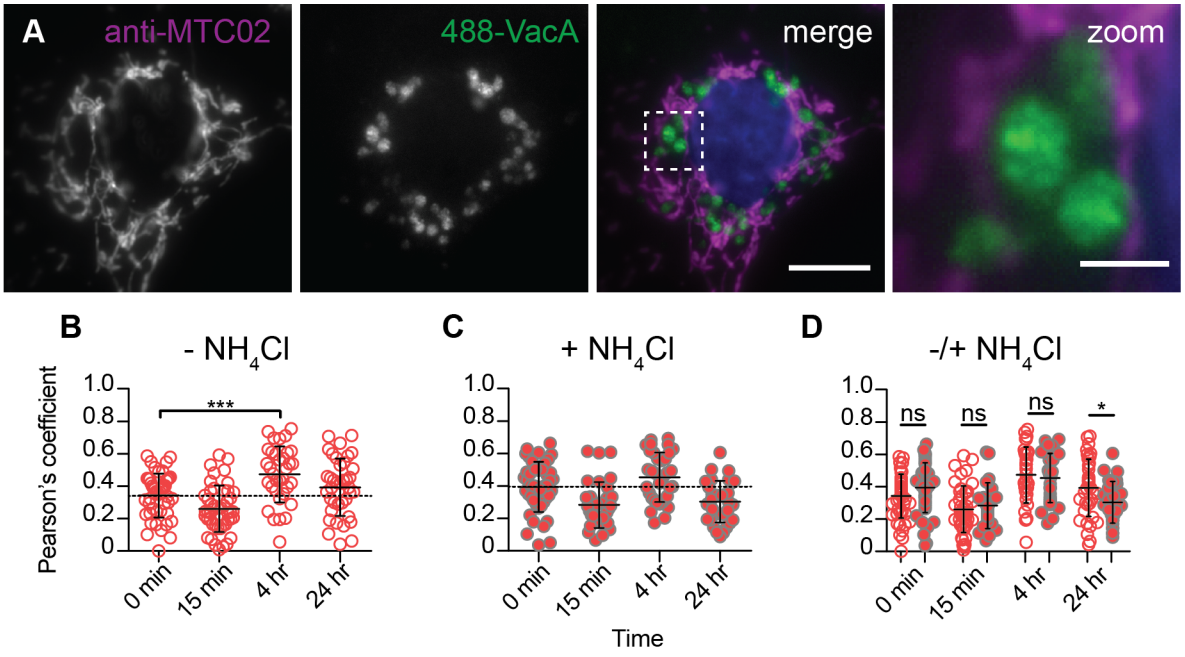

Figure 4.2 Treatment with NH_4Cl does not promote VacA trafficking to mitochondria. AGS cells were treated with a pulse of 488-VacA (1 hr at 4°C for the 0 min time point; 5 min at 37°C for all other time points), washed and incubated for various lengths of time in the absence or presence of 5 mM NH_4Cl, then fixed and stained with anti-MTC02 (mitochondria). **(A)** Representative image of a cell at the 24 hr time point in the presence of NH_4Cl. Image is a single, non-deconvolved z-slice. Scale bars, 10 μm in the full size image and 2 μm in the zoom. **(B-D)** The Pearson correlation coefficient was used to quantify colocalization of VacA with MTC02 in the (B) absence and (C) presence of NH_4Cl. Panel (D) represents the combined data. Open circles indicate absence of NH_4Cl and closed circles indicate presence of NH_4Cl. Each data point represents the Pearson's coefficient of an individual cell measured using ImageJ from a single, non-deconvolved z-slice. n ≥ 10 cells per condition per experiment from two independent experiments. (B,C) Error bars, ± SD. The means for each dataset are statistically different ($p \leq 0.0001$) as determined by an ANOVA. ***, $p \leq 0.001$ as determined by a Dunnett's Multiple Comparison Test. (D) Error bars, ± SD. ns, $p > 0.05$; *, $p = 0.0206$ as determined by an unpaired, two-tailed t test.

Table 4.1 Summary of the Pearson correlation coefficient for MTCO2, LAMP1, and LC3 with VacA[a]

	Condition	Time	PCC (mean ± SD)	Statistical Significance	Total number of cells measured for each condition
MTCO2	(-) NH4Cl	0 min	0.34 ± 0.14		47
		15 min	0.26 ± 0.14	*	46
		4 hr	0.47 ± 0.17	***	34
		24 hr	0.39 ± 0.18	ns	38
	(+) NH4Cl	0 min	0.39 ± 0.15		44
		15 min	0.28 ± 0.14	**	33
		4 hr	0.45 ± 0.15	ns	34
		24 hr	0.30 ± 0.13	*	32
LAMP1	(-) NH4Cl	0 min	0.27 ± 0.16		30
		15 min	0.36 ± 0.18	ns	36
		4 hr	0.71 ± 0.15	***	50
		24 hr	0.80 ± 0.15	***	50
	(+) NH4Cl	0 min	0.33 ± 0.18		41
		15 min	0.33 ± 0.14	ns	43
		4 hr	0.73 ± 0.11	***	26
		24 hr	0.82 ± 0.11	***	36
LC3	(-) NH4Cl	0 min	0.36 ± 0.14		51
		15 min	0.36 ± 0.14	ns	47
		4 hr	0.47 ± 0.17	**	48
		24 hr	0.47 ± 0.18	**	41
	(+) NH4Cl	0 min	0.47 ± 0.14		39
		15 min	0.38 ± 0.16	*	35
		4 hr	0.60 ± 0.13	***	47
		24 hr	0.70 ± 0.11	***	44

[a]The table is a summary of data from two independent experiments using Pearson's correlation coefficient (PCC) to assess VacA colocalization with mitochondria (MTCO2), lysosomes (LAMP1), and autophagosomes/autophagosomes (LC3). Statistical tests were done to determine whether the mean Pearson's coefficient at 15 min, 4 hr, or 24 hr was significantly different than the respective Pearson's coefficient at 0 min. The means for each dataset are statistically different ($p \leq 0.0001$) as determined by an ANOVA. ns, $p > 0.05$; *, $p \leq 0.05$; **, $p \leq 0.01$; ***, $p \leq 0.001$ as determined by a Dunnett's Multiple Comparison Test.

We also used live cell imaging to monitor VacA localization in relation to mitochondria. If VacA localizes to mitochondrial membrane, we expected to observe stable colocalization between VacA and mitochondria. However, we did not detect stable colocalization of VacA with mitochondria over time in either the presence (Figure 4.3) or absence of NH_4Cl (Figure 4.4). VacA-containing vesicles that appeared to be

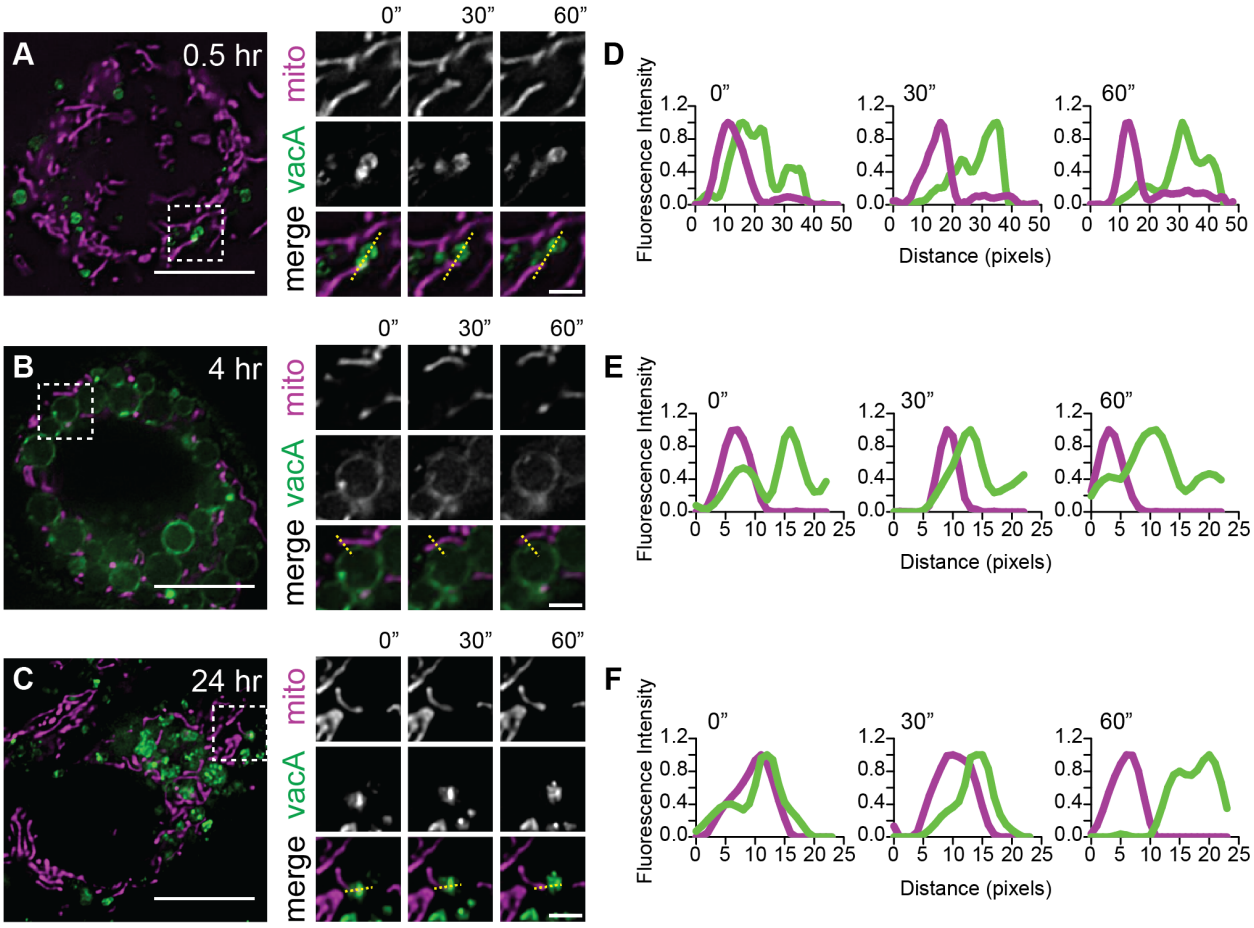

Figure 4.3 Analysis of VacA localization with mitochondria in living cells in the presence of NH_4Cl. (A-C) Live cell imaging of AGS cells transfected with Mito-RFP. Cells were treated with a pulse of 488-VacA for 5 min at 37°C, then washed and incubated at 37°C in medium supplemented with 5 mM NH_4Cl. Movies were collected at (A) 0.5 hr, (B) 4 hr, and (C) 24 hr post VacA treatment. Left, a single frame of the cell being imaged. Right, sequential images of the regions indicated in boxes. Time is indicated in seconds relative to the initial frame. Images are single z-slices. Scale bars, 10 μm in the full size images and 2 μm in the zooms. **(D-F)** Lines scans of the regions

indicated by yellow dashed lines in (A-C). Magenta line represents normalized Mito-RFP fluorescence intensity. Green line represents normalized 488-VacA fluorescence intensity. (D,F) The initial frame reveals VacA appearing near mitochondria, but subsequent frames reveal VacA moving away from mitochondria. (E) The frames reveal VacA initially appearing away from mitochondria, moving near mitochondria, then moving back away from mitochondria.

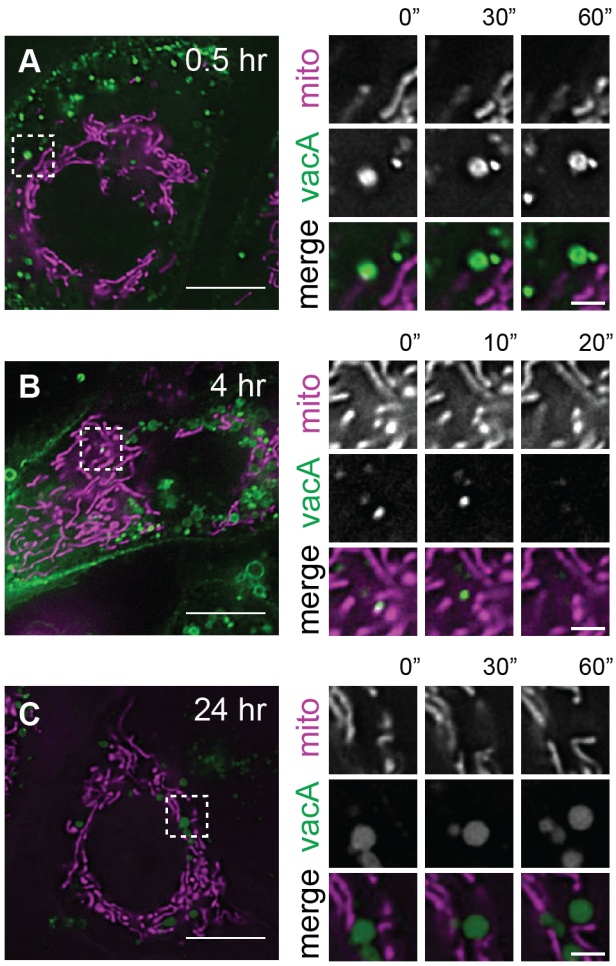

Figure 4.4 Analysis of VacA localization with mitochondria in living cells in the absence of NH_4Cl. (A-C) Live cell imaging of AGS cells transfected with Mito-RFP. Cells were treated with a pulse of 488-VacA for 5 min at 37°C, then washed and incubated at 37°C. Movies were collected at (A) 0.5 hr, (B) 4 hr, (C) 24 hr and post VacA treatment. Left, a single frame of the cell being imaged. Right, sequential images of the regions indicated in boxes. Time is indicated in seconds relative to initial frames. Images are single, z-slices. The initial frame reveals VacA appearing near mitochondria, but subsequent frames reveal VacA moving away from mitochondria. Scale bars, 10 μm in the full size images and 2 μm in the zooms.

near or colocalized with mitochondria moved away from mitochondria over time (Figure 4.3 D to F). In contrast, colocalized movement of VacA with early and late endosomes was routinely observed (Figure 4.5). These data indicate that NH_4Cl does not promote VacA trafficking to mitochondria. Additionally, this analysis suggests that either VacA is not targeted to mitochondria or that only a minor subpopulation of VacA traffics to mitochondria, making the interaction difficult to detect.

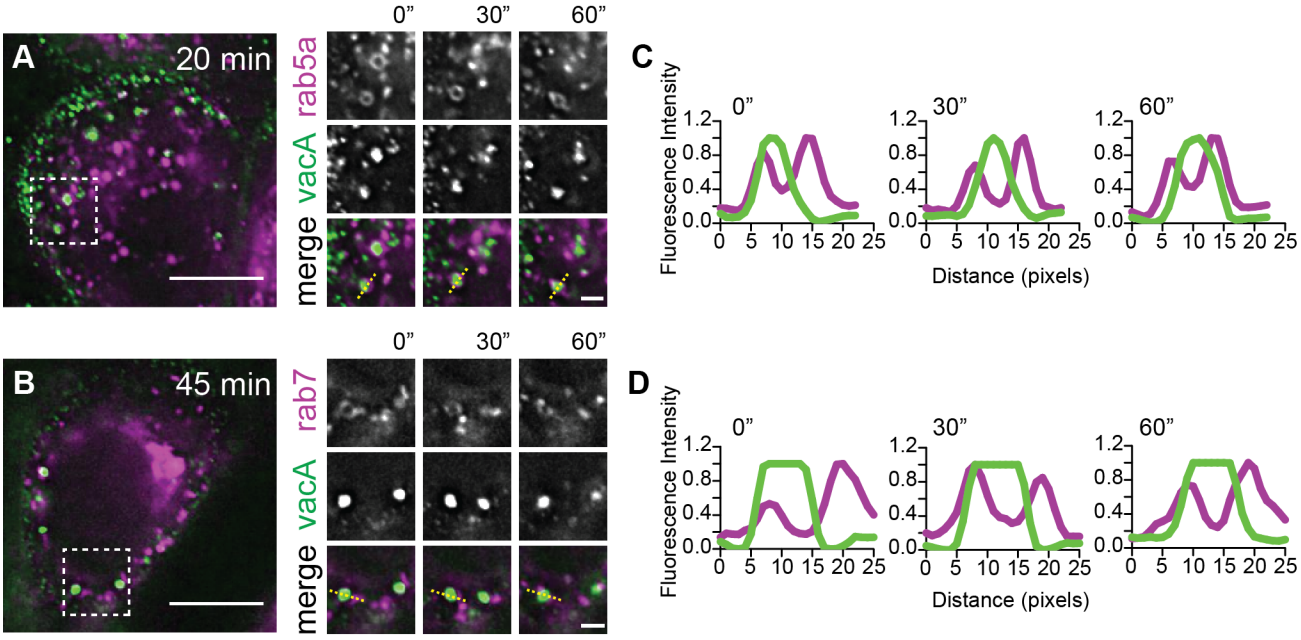

Figure 4.5 Analysis of VacA localization with early and late endosomes in living cells. (A,B) Live cell imaging of AGS cells transfected with (A) mCh-Rab5a or (B) mCh-Rab7 and treated with a pulse of 488-VacA for 1 hr at 4°C, then washed and incubated at 37°C. Movies were collected at (A) 20 min and (B) 45 min post treatment. Left, a single frame of the cell being imaged. Right, sequential images of regions indicated in boxes. Time is indicated in seconds relative to initial frames. Images are single z-slices. Scale bars, 10 μm in the full size images and 2 μm in the zooms. **(C,D)** Line scans of regions indicated by the yellow dashed lines in (A,B). Magenta line represents normalized (A) mCh-Rab5a or (B) mCh-Rab7 fluorescence intensity, appearing as two peaks due to their membrane localization. Green line represents normalized 488-VacA fluorescence intensity. Frames reveal a stable co-localization of VacA with early (Rab5a) and late (Rab7) endosomes.

NH_4Cl inhibits intracellular VacA degradation

While analyzing the fluorescence microscopy images from fixed cells, we noticed that at 24 hr, the intracellular level of VacA was significantly higher in cells treated with VacA in the presence of NH_4Cl compared to cells treated with VacA in the absence of NH_4Cl (Figure 4.6 A and B). This difference was not attributable to NH_4Cl-induced alterations in the amount of VacA that binds and is internalized into cells, because the levels of VacA associated with cells 0.5 hr after addition of the toxin were similar in the absence and presence of NH_4Cl (Figure 4.6 C and D). Ammonium ions accumulate within acidic intracellular organelles, resulting in increased intralysosomal pH, which in turn inhibits the activation of acid proteases required to break down cargo material (240-242). Therefore, we hypothesized that host cells degrade VacA and that NH_4Cl might augment VacA-induced cell death by inhibiting intracellular VacA degradation. To test this hypothesis, we monitored the stability of VacA in AGS cells using western blot analysis. In the absence of NH_4Cl, VacA was nearly undetectable 4 hr after addition of the toxin to cells (Figure 4.6 E), while in the presence of NH_4Cl, VacA levels remained stable throughout the 8 hr time course (Figure 4.6 F). At a 24 hr time point after the addition of VacA to cells, there was a significantly higher level of VacA in the presence of NH_4Cl compared to in the absence of NH_4Cl (Figure 4.6 G and H). VacA levels detected by Western blot analysis correlated with the presence of cellular vacuolation (Figure 4.6 I). Similar results were obtained with HeLa cells (Figure 4.7). Altogether, these data indicate that cells degrade VacA and that NH_4Cl inhibits VacA degradation.

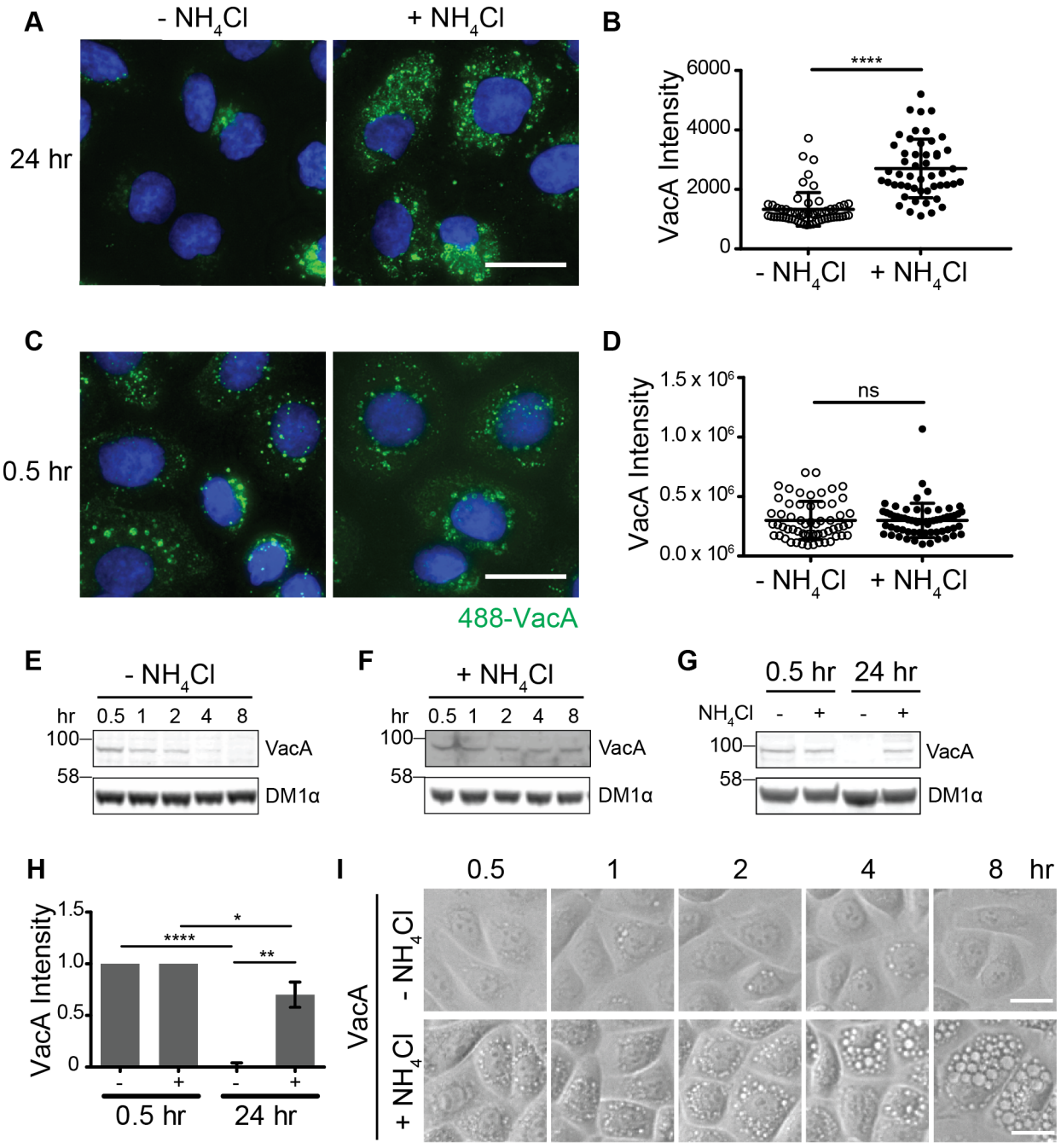

Figure 4.6 NH_4Cl inhibits intracellular VacA degradation. (A) Sum intensity z-projections of AGS cells treated with a pulse of 488-VacA for 5 min at 37°C, then washed and incubated for 24 hr in the absence or presence of 5 mM NH_4Cl. DNA, blue. Lookup Tables (LUTs) for the 488 channel are scaled identically. Scale bar, 20 μm. **(B)** Quantification of (A). n ≥ 50 cells per condition. Error bars, ± SD. ****, $p < 0.0001$ as determined by an unpaired, two-tailed t test. **(C)** Sum intensity z-projections of AGS cells treated with a pulse of 488-VacA for 5 min at 37°C, then washed and incubated for 0.5 hr in the absence or presence of 5 mM NH_4Cl. DNA, blue. LUTs for the 488 channel are scaled identically. Scale bar, 20 μm. **(D)** Quantification of C. n ≥ 59 cells per

condition. Error bars, ± SD. ns, p = 0.9784 as determined by an unpaired, two-tailed t test. **(E,F)** Western blots of whole cell lysates prepared from AGS cells treated for 5 min at 37°C with VacA, then washed and incubated for various lengths of time in the (E) absence or (F) presence of 25 mM NH_4Cl. Blot was probed with antibodies targeting VacA or tubulin (DM1α). 100 and 58 kDa references marked to the left. **(G)** Western blot of whole cell lysates prepared from AGS cells treated for 1 hr at 4°C with VacA, then washed and incubated for 0.5 or 24 hr in the absence or presence of 5 mM NH_4Cl. Blot was probed with antibodies targeting VacA and tubulin (DM1α). 100 and 58 kDa references marked to the left. **(H)** Quantification of (G), n=4. Error bars, ± SD. ****, p < 0.0001; *, p = 0.0163; **, p = 0.0016 as determined by a paired, two-tailed t test. **(I)** Transmitted light micrographs of cells used in (C,D) at each successive time point. Scale bars, 20 μm.

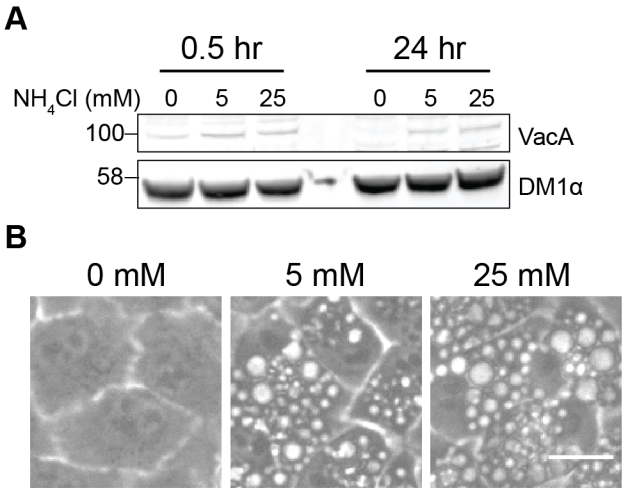

Figure 4.7 NH_4Cl inhibits VacA degradation in HeLa cells. (A) A Western blot of whole cell lysates prepared from HeLa cells treated for 1 hr at 4°C with VacA, then washed and incubated for 0.5 or 24 hr in the presence of increasing concentrations of NH_4Cl. Blot was probed with antibodies targeting VacA and tubulin (DM1α). 100 and 58 kDa references marked to the left. **(B)** Transmitted light micrographs of cells used in A) after 24 hr of VacA treatment. Scale bar, 20 μm.

VacA accumulates in lysosomes and autophagosomes/autolysosomes in both the absence and presence of NH_4Cl

To determine if NH_4Cl altered the intracellular trafficking of VacA to lysosomal or autophagosomal compartments, which are likely sites of intracellular VacA degradation, we evaluated VacA colocalization with lysosomal and autophagosomal markers

(LAMP1 and LC3, respectively). VacA colocalized with LAMP1 and LC3 in both the absence and presence of NH_4Cl (Figure 4.8). At 4 hr and 24 hr after addition of VacA, in both the absence and presence of NH_4Cl, there was a statistically significant increase in the colocalization of VacA with LAMP1 compared to what was observed in the 0 min control samples (Figure 4.8 B and C and Table 4.1). The same result was observed for VacA colocalization with LC3 (Figure 4.8 D and E and Table 4.1). These data indicate that VacA can localize to both lysosomes and autophagosomes/autolysosomes and that the presence of NH_4Cl does not disrupt VacA trafficking to these compartments.

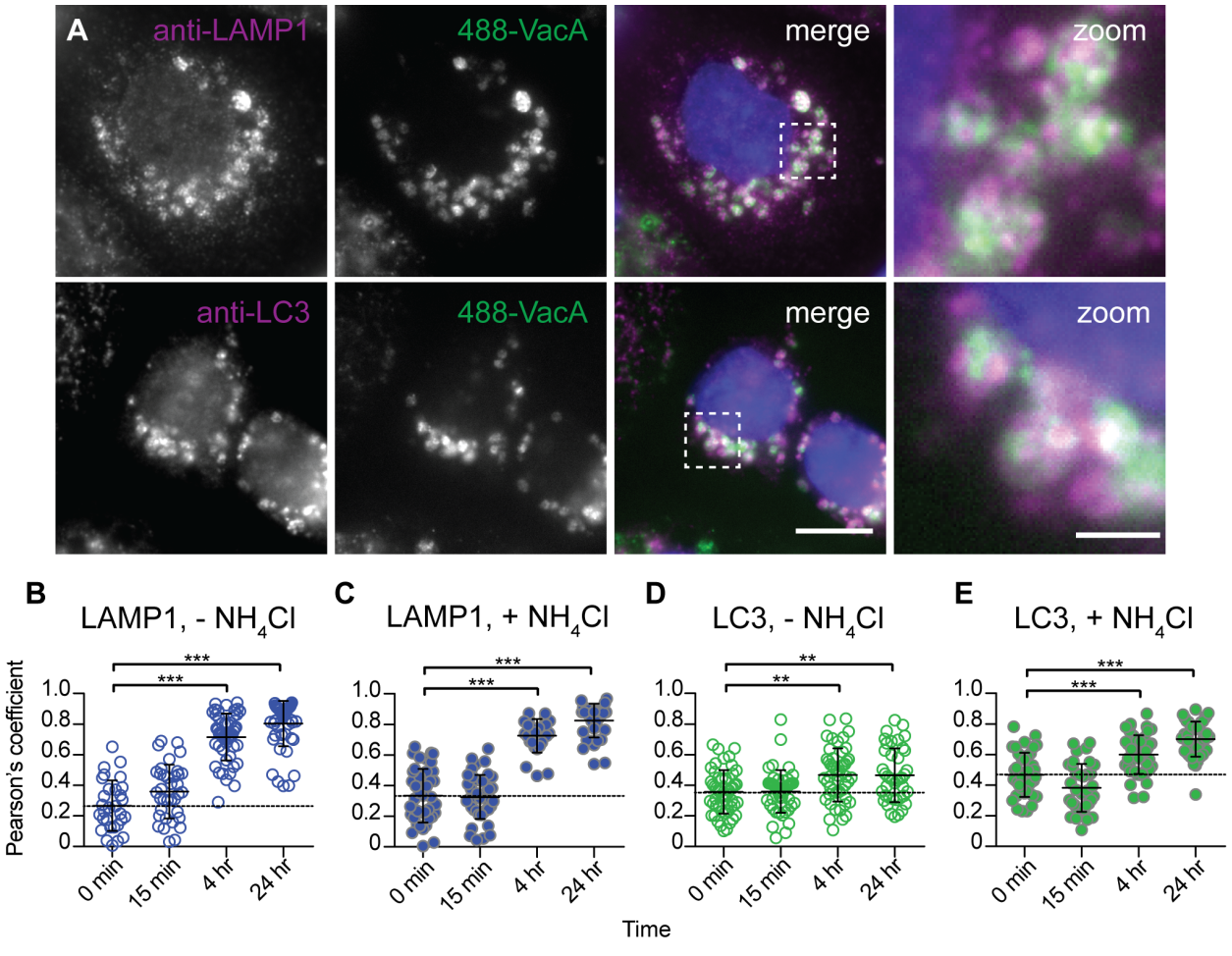

Figure 4.8 VacA accumulates in lysosomes and autophagosomes/autolysosomes in both the absence and presence of NH_4Cl. AGS cells were treated with a pulse of 488-VacA (1 hr at 4°C for the 0 min time point; 5 min at 37°C for all other time points), washed and incubated for various lengths of time in the absence or presence of 5 mM NH_4Cl, then fixed and stained with anti-LAMP1 (lysosomes) or anti-LC3 (autophagosomes/autolysosomes) antibody. **(A)** Representative images of cells at the 24 hr time point in the presence of NH_4Cl. Images are single, non-deconvolved z-slices. Scale bars, 10 μm in the full size image and 2 μm in the zoom. **(B-E)** The Pearson correlation coefficient was used to quantify colocalization of VacA with LAMP1 and LC3 in the (B,D) absence and (C,E) presence of NH_4Cl. Open circles indicate absence of NH_4Cl and closed circles indicate presence of NH_4Cl. Each data point represents the Pearson's coefficient of an individual cell measured using ImageJ from a single, non-deconvolved z-slice. n ≥ 10 cells per condition per experiment from two independent experiments. Error bars, ± SD. The means for each dataset are statistically different ($p \leq 0.0001$) as determined by an ANOVA. **, $p \leq 0.01$; ***, $p \leq 0.001$ as determined by a Dunnett's Multiple Comparison Test.

VacA degradation is independent of proteasome activity and autophagy, but dependent on lysosomal acidification

Next, we sought to determine the cellular pathway(s) involved in VacA degradation. To test the role of the proteasome, we used the proteasome inhibitor MG132. Treatment of cells with MG132 did not result in increased VacA levels or increased vacuolation compared to what was observed in control cells (Figure 4.9). To test the role of autophagy in VacA degradation, we used both chemical and genetic approaches to inhibit autophagy. First we treated cells with 3-methyladenine (3-MA), which inhibits type III phosphatidylinositol 3-kinases (PI3K) to block autophagosome formation (243, 244). While we noted that 3-MA alone induced a low level of vacuolation, treatment of cells with VacA in the presence of 3-MA did not result in increased cellular VacA levels or increased vacuolation compared to control cells (Figure 4.10 A to C). We then analyzed VacA degradation in two stable ATG5

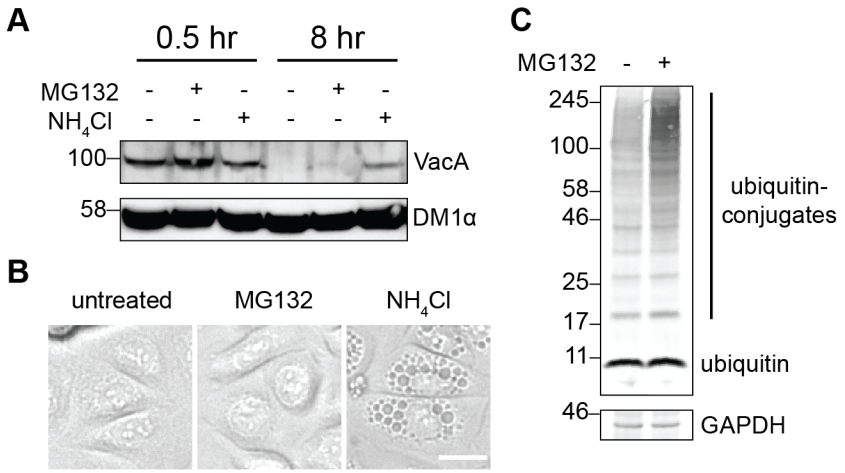

Figure 4.9 MG132 does not inhibit VacA degradation. (A) A Western blot of whole cell lysates prepared from AGS cells treated for 1 hr at 4°C with VacA, then washed and incubated for 0.5 or 8 hr in the presence of 5 μM MG132, or 5 mM NH_4Cl, or mock treated. Blot was probed with antibodies targeting VacA and tubulin (DM1α). 100 and 58 kDa references marked to the left. **(B)** Transmitted light micrographs of cells used in (A) at the 8 hr time point. Scale bar, 20 um. **(C)** To confirm that treatment of cells with 5 μM MG132 for 8 hr inhibits proteasome activity, cell lysate from the 8 hr time point in the absence or presence of MG132 was probed with antibodies targeting ubiquitin and GAPDH. A reduction in proteasome activity is indicated by an increase in ubiquitin-conjugated proteins in the presence of MG132 compared to in the absence of MG132.

knockdown (KD) cell lines generated using two different ATG5 shRNA clones. The ATG5 KD cell lines had knockdown efficiencies of 80% for ATG5 KD1 and 88% for ATG5 KD2 (Figure 4.10 D and E). Inhibition of autophagy by knocking down ATG5 did not result in increased VacA levels or increased vacuolation compared to control cells (Figure 4.10 F to H). We also analyzed VacA degradation in HeLa ATG16L1 KO cells generated using CRISPR/Cas9 (Figure 4.10 I). Inhibition of autophagy by knocking out ATG16L1 did not result in increased VacA levels or increased vacuolation compared to control cells (Figure 4.10 J to L).

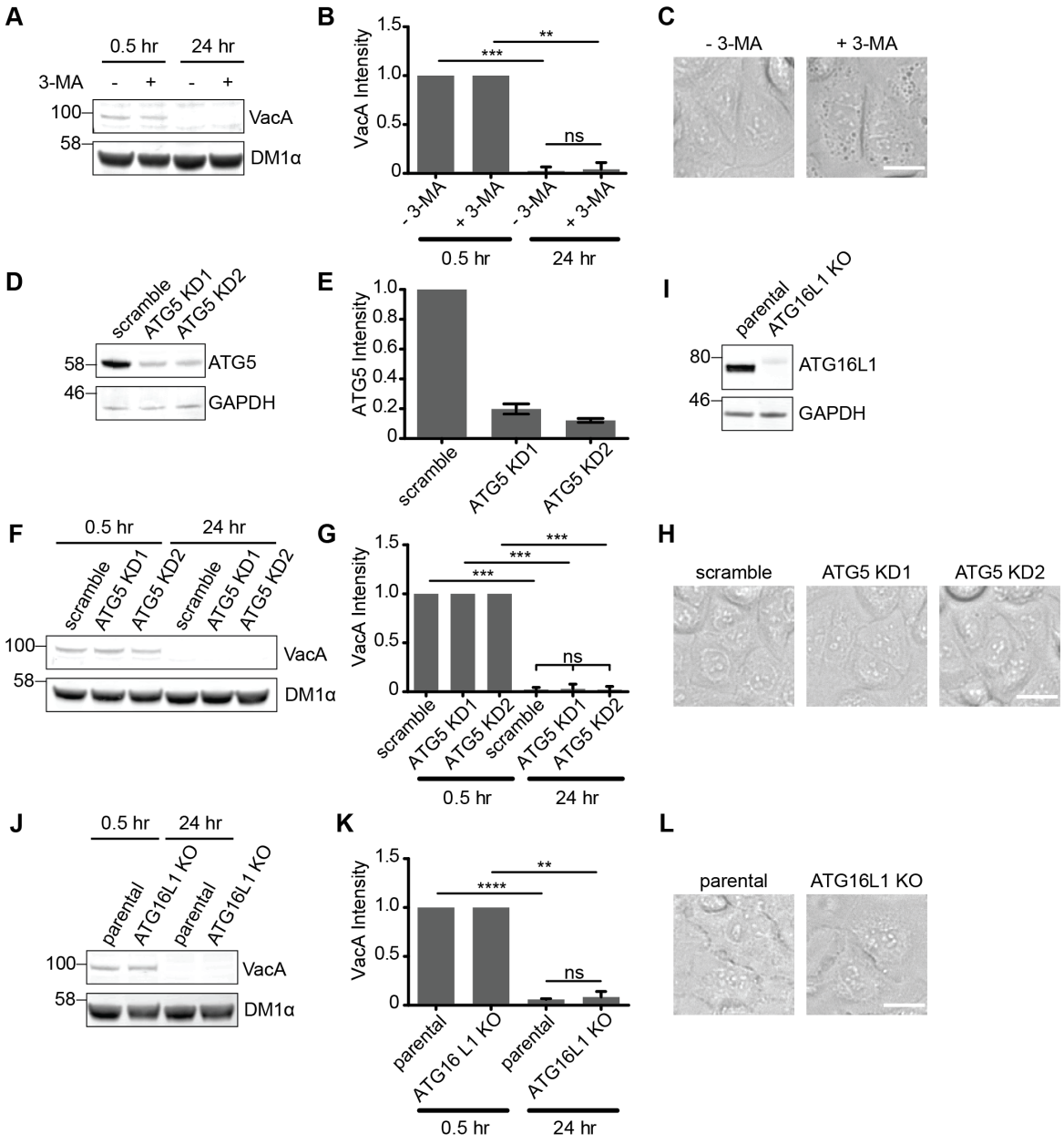

Figure 4.10 VacA degradation is independent of autophagy. (A) Representative Western blot of AGS cells treated for 1 hr at 4°C with VacA, then washed and incubated for 0.5 or 24 hr in the absence or presence of 10 mM 3-MA. Blot was probed with antibodies targeting VacA and tubulin (DM1α). **(B)** Quantification of (A), n=3. Error bars, ± SD. ***, p = 0.0006; **, p = 0.0018; ns, p = 0.4227; paired, two-tailed t test. **(C)** Transmitted light micrographs of cells used in (A) after 24 hr of VacA treatment. **(D)** Representative Western blot to validate ATG5 knockdown in AGS cells. Blot was probed with antibodies targeting ATG5 and GAPDH. **(E)** Quantification of (D), n=3. Error bars, ± SD. The knockdown (KD) was 80% efficient in cell line ATG5 KD1 (generated from shRNA clone TRCN0000151963) and 88% efficient in cell line ATG5 KD2 (generated from shRNA clone TRCN0000330392). **(F)** Representative Western blot of

whole cell lysates prepared from a scramble control cell line and two AGS ATG5 KD cell lines treated for 1 hr at 4°C with VacA, then washed and incubated for 0.5 or 24 hr. Blot was probed with antibodies targeting VacA and tubulin (DM1α). **(G)** Quantification of (F), n=3. Error bars, ± SD. ***, $p < 0.001$; paired, two-tailed t test. ns, $p = 0.9211$; ANOVA. **(H)** Transmitted light micrographs of cells used in (F) after 24 hr of VacA treatment. **(I)** Representative Western blot to validate ATG16L1 knockout in HeLa cells. Blot was probed with antibodies targeting ATG16L1 and GAPDH. **(J)** Representative Western blot of whole cell lysates prepared from parental HeLa and HeLa ATG16L1 KO cells treated for 1 hr at 4°C with VacA, then washed and incubated for 0.5 or 24 hr. Blot was probed with antibodies targeting VacA and tubulin (DM1α). **(K)** Quantification of (J), n=3. Error bars, ± SD. ****, $p < 0.0001$; **, $p = 0.0013$; ns, $p = 0.5992$; paired, two-tailed t test. **(L)** Transmitted light micrographs of cells used in (J) after 24 hr of VacA treatment. For all blots, molecular weight (kDa) references marked to the left. Scale bars, 20 μm.

To test the role of the lysosome in VacA degradation, we used chloroquine and bafilomycin A1 to inhibit lysosome acidification. Treatment of cells with chloroquine, a lysosomotrophic weak base which raises intralysosomal pH similarly to NH_4Cl, resulted in increased VacA levels and increased vacuolation compared to levels in control cells (Figure 4.11 A to C) (240). Furthermore, treatment of cells with bafilomycin A1, which raises intralysosomal pH by inhibiting the vacuolar H^+-ATPase, also resulted in increased VacA levels (Figure 4.11 D and F) (245). Since the vacuolar H^+-ATPase has previously been shown to be required for osmotic swelling of endosomes in response to VacA (246, 247), bafilomycin A1 inhibited VacA-induced vacuolation despite high intracellular levels of VacA (Figure 4.11 F). Altogether, these results provide evidence that cells degrade VacA through processes independent of proteasome activity and autophagy, but dependent on lysosomal acidification.

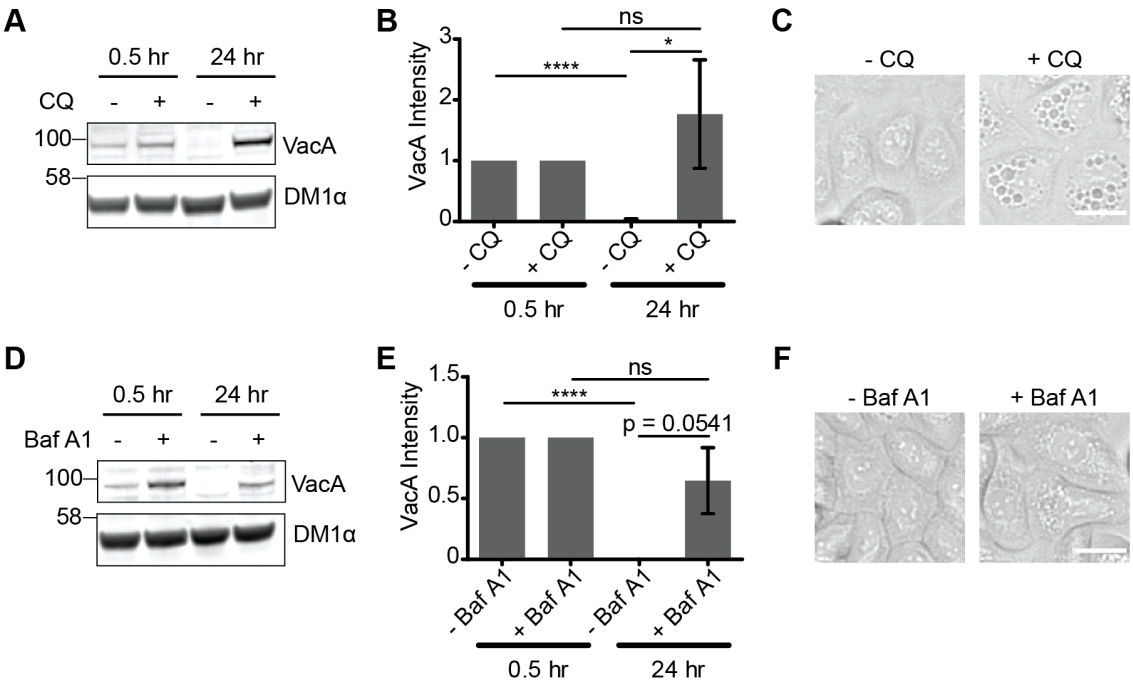

Figure 4.11 VacA degradation is dependent on lysosome acidification. (A) Representative Western blot of AGS cells treated for 1 hr at 4°C with VacA, then washed and incubated for 0.5 or 24 hr in the absence or presence of 100 μM chloroquine (CQ). **(B)** Quantification of (A), n=4. Error bars, ± SD. ****, $p < 0.0001$; ns, $p = 0.1839$; *, $p = 0.0275$; paired, two-tailed t test. **(C)** Transmitted light micrographs of cells used in (A) after 24 hr of VacA treatment. **(D)** Representative Western blot of AGS cells treated for 1 hr at 4°C with VacA, then washed and incubated for 0.5 or 24 hr in the absence or presence of 10 nM bafilomycin A1 (BafA1). **(E)** Quantification of (D), n=3. Error bars, ± SD. ****, $p < 0.0001$; ns, $p = 0.1532$; paired, two-tailed t test. **(F)** Transmitted light micrographs of cells used in (D) after 24 hr of VacA treatment. All blots were probed with antibodies targeting VacA and tubulin (DM1α). For all blots, molecular weight (kDa) references marked to the left. Scale bars, 20 μm.

DISCUSSION

In this study, we analyzed factors that influence the capacity of *H. pylori* VacA toxin to cause death of gastric epithelial cells. Consistent with previous reports, we show that the presence of supplemental NH_4Cl in cell culture medium enhances VacA-induced cell death (138). Conversely, we show that, in the absence of supplemental NH_4Cl, cells can resist VacA-induced vacuolation and cell death by degrading VacA.

Our results indicate that VacA degradation is inhibited when cells are treated with NH_4Cl or two other agents that interfere with lysosomal acidification, chloroquine and bafilomycin A1. NH_4Cl is known to enhance VacA-induced vacuolation, a phenomenon that has been attributed to the accumulation of NH_4Cl (a weak base) within endosomal compartments, leading to osmotic swelling (108, 110). In contrast, the role of NH_4Cl in enhancing VacA-induced cell death and mechanisms underlying this phenomenon has not been investigated in any detail. Our work suggests that VacA is degraded in the lysosome and that NH_4Cl enhances VacA-induced cellular damage by inhibiting VacA degradation within lysosomes.

Previous studies have shown that VacA can induce significant vacuolation and cell death in the absence of supplemental NH_4Cl if cells are co-cultured with VacA-producing *H. pylori* strains or treated with broth culture filtrate (BCF) from VacA-producing *H. pylori* strains (137-139, 248). In these experimental systems, ammonia is present at concentrations sufficiently high to influence VacA-induced vacuolation (238). In addition, ammonia-producing *H. pylori* enzymes, such as urease, γ-glutamyl transpeptidase, asparaginase, and glutaminase, are also present (50, 238, 239). Therefore, previous studies using *H. pylori* strains or BCF were not able to assess the effect of VacA on host cells in the absence of ammonia. Experiments in the current manuscript were performed using purified VacA, which allowed us to specifically evaluate the interactions of VacA with host cells in the presence of ammonia, as well as in the absence of ammonia and ammonia-producing *H. pylori* enzymes. This approach also permitted the concentration of VacA to be experimentally determined and carefully controlled.

Our work reveals that cells can degrade VacA within 4 hr after exposure to the toxin. In contrast, two earlier studies reported that VacA can persist inside cells for substantially longer time periods (87, 249). One study detected VacA by immunoblot analysis in lysates from MKN 28 cells that were treated with *H. pylori* BCF for 16 hr, then washed and incubated with medium for an additional 72 hr (249). BCF was dialyzed to remove ammonia prior to addition of the BCF to cells, but we presume that urease and/or γ-glutamyl transpeptidase in the BCF would subsequently generate additional ammonia from urea and glutamine, respectively, in the tissue culture medium. Another study reported that VacA persists inside cells for hours with no noticeable degradation (87), but the tissue culture medium was supplemented with 10 mM NH_4Cl in that study.

We propose that the influence of NH_4Cl on VacA degradation is due to the well-established ability of weak bases to raise intralysosomal pH (241). The activity of lysosomal enzymes is known to be dependent on lysosomal pH (242); therefore, it is not possible to discriminate whether the observed effects of NH_4Cl on intracellular VacA levels are specifically due to changes in lysosomal acidification, impaired protease activity, or a combination of these factors. We considered the possibility that NH_4Cl might alter intracellular VacA stability by preventing VacA trafficking to lysosomes. Indeed, weak bases can alter the pH of both endosomes and lysosomes, and regulated acidification is important for endosome maturation (250). However, we show that VacA localizes to both lysosomes and autophagosomes/autolysosomes in both the absence and presence of NH_4Cl. This suggests that NH_4Cl does not inhibit VacA degradation by disrupting the trafficking of VacA to the lysosome.

Recent studies have shown that upon exposure to pore-forming toxins (PFTs), cells can potentially respond, adapt, and survive (40, 41, 231, 251). Degradation of the toxin is one strategy that may be employed by cells to limit the extent of PFT-induced damage (234, 235, 252). Interestingly, a previous study suggested that the stability of intracellular VacA is modulated by autophagy (133). The authors reported that AGS cells treated with a pulse of BCF for 6 hr and chased for 24 hr degrade VacA over time, concomitant with the disappearance of cell vacuoles, while no degradation of VacA was observed in ATG12 KD cells and vacuoles remained present (133). In contrast, we show that neither knockdown of ATG5 nor knockout of ATG16L1 has an effect on VacA degradation. One possible explanation for why our results differ from the previous study is that cells may have a differing response to VacA following a short exposure to the purified toxin (1 hr pulse at 4°C in our study) versus an extended exposure to BCF from VacA-producing *H. pylori* strains (6 hr pulse at 37°C in a previous study) (133). Perhaps the toxin molecules internalized into cells following a short exposure are primarily degraded in the lysosome, whereas cells that internalize high doses of VacA following a long exposure might utilize both lysosomal-degradation and autophagy to degrade the toxin.

VacA has been reported to induce cell death via both apoptosis and necrosis (137-139); conversely, a recent study reported that VacA-induced cellular alterations do not induce apoptosis (253). Proposed mechanisms by which VacA induces cell death include direct pore formation in the mitochondrial membrane (117, 121, 122), or processes independent of mitochondrial targeting (116). In our analysis of VacA localization using live and fixed cell imaging, we did not detect a consistent increase in

VacA localization to mitochondria over time, and NH_4Cl had no detectable effect on VacA localization to mitochondria. Inability to observe VacA targeting to mitochondria in the current study is consistent with the results of one previous study (116), but differs from results of multiple other studies that used fluorescence microscopy to detect mitochondrial localization of VacA (115, 117, 119-121, 141). Other studies have detected interactions of VacA or VacA-containing vesicles with mitochondria using subcellular fractionation, *in vitro* experiments with isolated mitochondria, or immunogold labeling (117, 121, 122, 141, 254). The difference in results reported in the current study compared to previous studies may be attributable to the use of different methodology for detecting VacA localization. Specifically, this is the first time quantitative colocalization measurements have been combined with live-cell imaging to analyze the putative interaction between VacA and mitochondria. In a static fluorescence microscopy image, two objects that are in close proximity can appear colocalized due to resolution limitations. The benefit of live-cell imaging is that it permits the visualization of intracellular dynamics. The use of live-cell imaging allowed us to see that most VacA-containing vesicles that appear to be colocalized with mitochondria at a single time point did not remain colocalized with mitochondria over time. This implies that VacA is sometimes detected in the vicinity of mitochondria but is not stably localized to mitochondria. Consistent with our results, the only other study that used quantitative methods to assess VacA colocalization with mitochondria over time also found that most intracellular VacA is not associated with mitochondria (253). Therefore, the results in the current study suggest that VacA-induced cell death might occur through mechanisms that do not require direct targeting of mitochondria by the toxin. While we

cannot rule out the possibility that a minor, subpopulation of VacA localizes to mitochondria or that the conditions of our experiments did not permit the targeting of VacA to mitochondria, our results clearly indicate that, in the absence of exogenous NH_4Cl, cells are resistant to VacA-induced cell death.

VacA is known to maintain activity in low pH conditions and is relatively resistant to proteolytic digestion (83, 86). Therefore, it has been proposed that the toxin might resist degradation in lysosomes (249). The current study provides evidence that cells are capable of degrading intracellular VacA, and the data indicate that intracellular degradation of VacA allows cells to resist VacA-induced cell death. Conversely, if this process is impaired and intracellular levels of VacA accumulate, cells eventually undergo cell death (Figure 4.12). We speculate that VacA induces cell death by forming pores at the cell surface and in endosomes/lysosomes to disrupt cellular homeostasis.

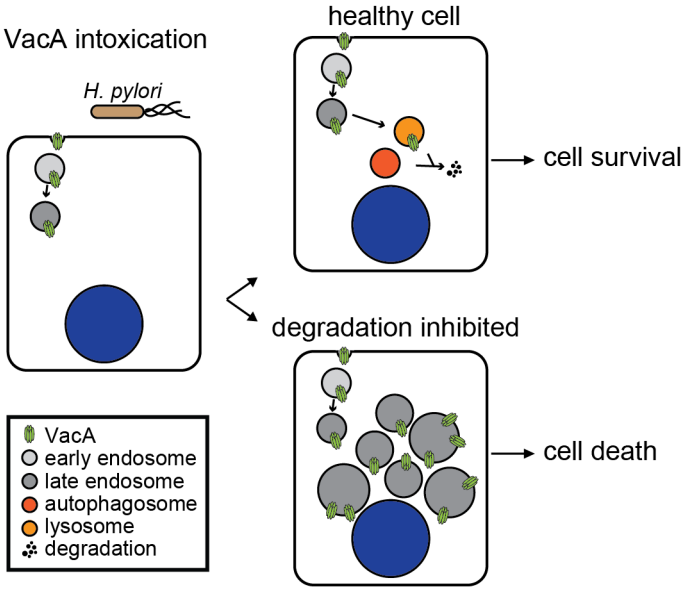

Figure 4.12 Proposed model for the cellular response to VacA. In a healthy cell, VacA is internalized, trafficked to the lysosome, and degraded. If lysosome activity is inhibited, VacA can accumulate in the lysosome, and cells exhibit vacuolation and eventually cell death.

More specifically, we propose that cells are able to tolerate a low level of VacA-induced homeostatic imbalances, but that when intracellular levels of VacA accumulate, these disruptions to cellular homeostasis reach a tipping point and trigger pro-cell death pathways. In support of this model, a recent study reported alterations in cellular amino acid homeostasis following treatment of cells with VacA (255).

In conclusion, this study shows that the ability of weak bases to enhance VacA activity is due at least in part to an ability of weak bases to inhibit VacA degradation. We presume that the effects of VacA on host cells are determined by the concentrations of toxin to which cells are exposed, as well as the rate at which intracellular VacA is degraded. Individuals infected with *H. pylori* are reported to have elevated levels of ammonia in their stomach due to the activity of *H. pylori* urease and other enzymes (256-258). Therefore, during infection, the concentration of ammonia or other weak bases in the mucus layer overlying gastric epithelial cells may influence the magnitude of VacA toxicity. Cells in the gastric mucosa directly in contact with *H. pylori*, exposed to high concentrations of VacA and high concentrations of ammonia, would be at the highest risk of undergoing cell death. Conversely, cells localized at a distance from *H. pylori,* exposed to lower concentrations of VacA and lower concentrations of ammonia, would be less likely to undergo VacA-induced cell death; subtle VacA-induced changes in these cells could potentially confer benefits to *H. pylori in vivo*. The manipulation of host cell lysosome activity to prevent toxin degradation is presumably not a unique property of *H. pylori*. Many intracellular pathogens are capable of subverting lysosomal function, which potentially alters the degradation of secreted bacterial proteins. In future studies it will be important to investigate whether the manipulation of host cell

degradation pathways is a strategy commonly utilized by extracellular bacteria to inhibit toxin degradation.

CHAPTER V

VACA INTOXICATION MODULATES MITOCHONDRIAL RESPIRATION

INTRODUCTION

VacA has been shown to modulate mitochondrial function, causing cytochrome *c* release (115, 117), dissipation of mitochondrial transmembrane potential (114, 115), and mitochondrial fragmentation (119). Properly functioning mitochondria are critical for the generation of ATP and for the maintenance of cellular metabolic processes (35, 259). A recent study suggested that mitochondrial dysfunction caused by VacA may modulate host cell metabolism (255). Specifically, the authors found that VacA intoxication caused a reduction in cellular amino acid levels, resulting in an inhibition of mammalian target of rapamycin complex 1 (mTORC1) (a key regulator of cellular metabolism), leading to autophagy (255). However, whether mitochondrial dysfunction caused by VacA modulates the respiratory capacity of mitochondria has not been closely investigated.

In this study, we tested whether cellular exposure to VacA has an effect on mitochondrial respiration. We report that VacA reduces the maximal rate of mitochondrial respiration while having no effect on basal respiration rates. VacA-induced disruption in mitochondrial respiration rates is associated with decreased

glutamine levels, but is not associated with changes in mitochondrial mass. Our results indicate that VacA intoxication can modulate mitochondrial respiration, potentially due to a depletion of glutamine and other sources of metabolic fuel, and we propose that this may reduce the capacity of VacA-treated cells to respond to added energy demands.

RESULTS

VacA causes changes to mitochondrial respiration

The ability of mitochondria to facilitate oxidative phosphorylation and generate ATP reflects the functional state of a cell. VacA has been shown to disrupt mitochondrial function and dynamics (114, 115, 117, 119), yet its ability to influence the respiratory capacity of mitochondria has not been investigated. To test whether VacA causes changes in mitochondrial respiration, we assessed oxygen consumption rates (OCR) from AGS and AZ521 cells treated with VacA for 4 hr. The OCRs were measured first under basal conditions and then after sequential additions of oligomycin (an ATP synthase inhibitor), FCCP (an uncoupling agent that disrupts mitochondrial transmembrane potential), and a mixture of rotenone and antimycin A (a complex I inhibitor and a complex III inhibitor, respectively) at the indicated times in order to measure different parameters of mitochondrial function. A reduction in OCRs was observed in both AGS and AZ521 cells following exposure to increasing concentrations of VacA for 4 hr (Figure 5.1 A and B). To confirm that the reduction in OCRs was not due to a loss in total cell number, which may occur as a result of VacA exposure, we quantified the total number of cells in each condition immediately after collecting OCR measurements. The reduction in OCRs did not correlate with a reduction in total cell

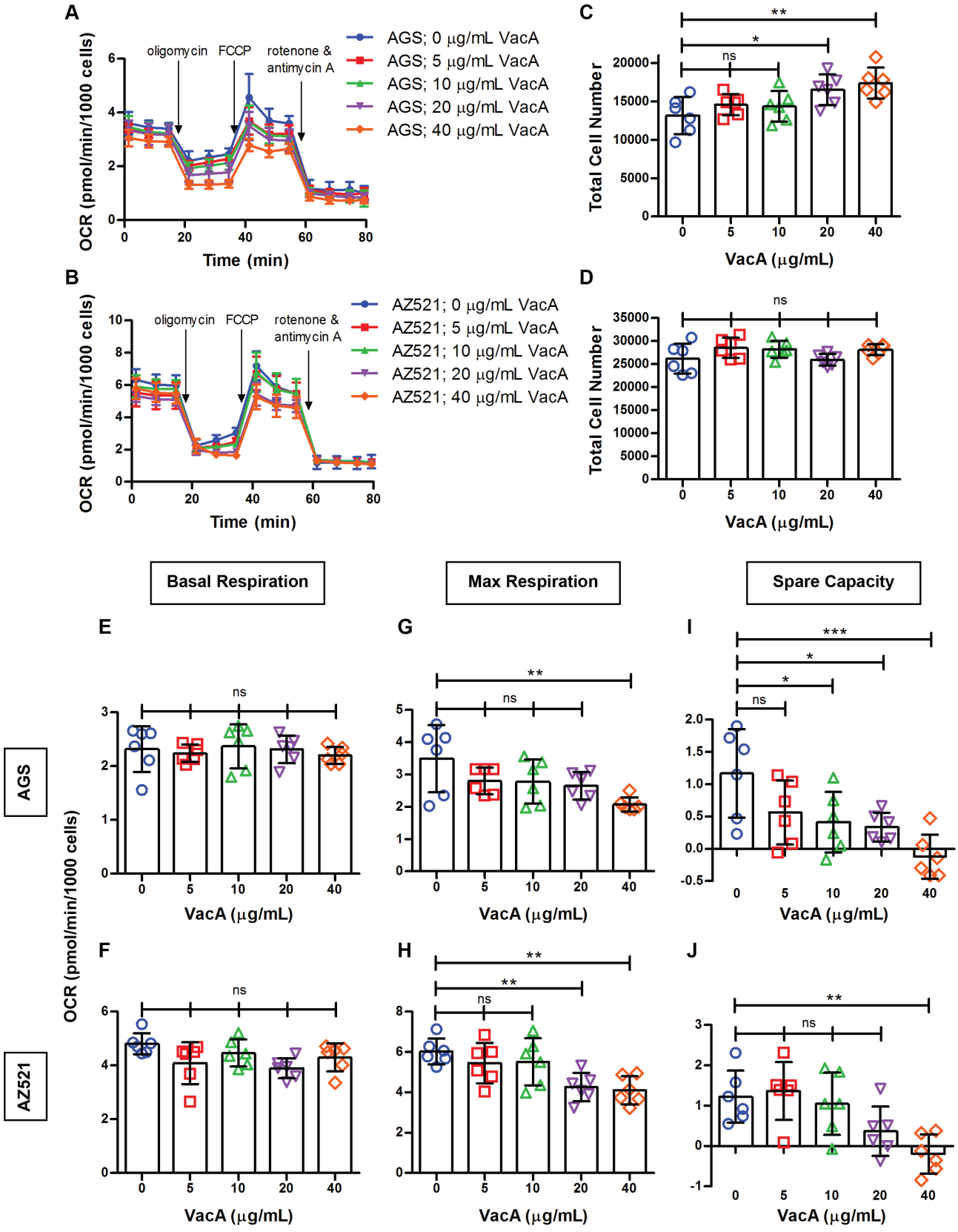
A
OCR (pmol/min/1000 cells)
oligomycin
FCCP
rotenone & antimycin A
Time (min)
AGS; 0 μg/mL VacA
AGS; 5 μg/mL VacA
AGS; 10 μg/mL VacA
AGS; 20 μg/mL VacA
AGS; 40 μg/mL VacA
B
AZ521; 0 μg/mL VacA
AZ521; 5 μg/mL VacA
AZ521; 10 μg/mL VacA
AZ521; 20 μg/mL VacA
AZ521; 40 μg/mL VacA
C
Total Cell Number
VacA (μg/mL)
D
Basal Respiration
Max Respiration
Spare Capacity
AGS
AZ521
E
F
G
H
I
J
ns
*
**
***

Figure 5.1 VacA causes changes to mitochondrial respiration in both AGS and AZ521 cells. (A, B) Oxygen consumption rates (OCRs) measured from A) AGS and B) AZ521 cells mock-treated or treated with the indicated concentration of VacA for 4 hr. The OCRs were measured first under basal conditions and then after sequential additions of oligomycin, FCCP, and a mixture of rotenone and antimycin A at the indicated times in order to measure different parameters of mitochondrial respiration. n = 6 wells per condition from a single experiment. Error bars, ± SD. **(C, D)** Total cell numbers for C) AGS and D) AZ521 cells quantified after OCRs were measured. Error bars, ± SD. **(E-J)** OCRs for basal respiration (E,F), maximal respiration (G,H), and spare capacity (I,J) in AGS (E, G, I) and AZ521 cells (F, H, J) derived from panels A and B. For each data set, differences between means were assessed by an ANOVA followed by the Dunnett's Multiple Comparison Test. ns, $p > 0.05$; *, $p \leq 0.05$; **, $p \leq 0.01$; ***, $p \leq 0.001$ as determined by a Dunnett's Multiple Comparison Test.

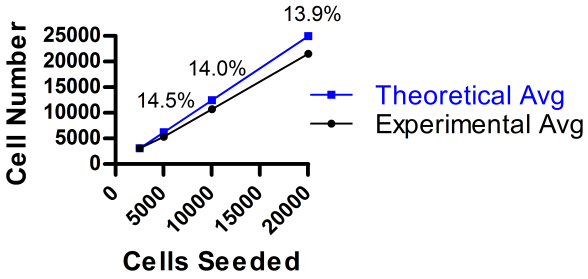

Figure 5.2 Assessment of total cell count accuracy. Cells were seeded, stained with Hoechst to label nuclei, and cell number was quantified. The experimental average is the average number of cells per condition as quantified using MetaXpress. The theoretical average was calculated from the lowest experimental average. Percent error, defined as $\left|\frac{avg_{exp} - avg_{theor}}{avg_{theor}}\right| \times 100$, is indicated above respective data points. n = 12-18 wells per condition from a single experiment.

number (Figure 5.1 C and D) and the method used to quantify total cell numbers was accurate, having a percent error of 13.9 – 14.5% (Figure 5.2). Therefore, VacA causes changes to mitochondrial respiration in a dose-dependent manner.

Further analysis of the data reveled that VacA treatment had no effect on basal respiration in either cell line tested (Figure 5.1 E and F). In contrast, maximal respiration

and spare respiratory capacity, two parameters of mitochondrial respiration, were reduced in both AGS and AZ521 cells following exposure to increasing concentrations of VacA (Figure 5.1 G to J).

Oligomerization and pore-formation are necessary for VacA to induce maximal changes to mitochondrial respiration

Many cellular effects elicited by VacA require the ability of VacA to oligomerize and form a membrane channel (75, 115, 222). Therefore, we next used VacA Δ346-7 and VacA s2m1 (a non-oligomerizing mutant and a VacA variant, respectively) to test whether oligomerization and pore formation were necessary for VacA induced changes to mitochondrial respiration. Details on the mutants used are provided in Table 3.2. VacA Δ346-7 lacks two amino acids in the p55 domain and does not oligomerize or induce cell vacuolation, but it is able to bind membrane (82, 179, 222). VacA s2m1 contains a 12-amino acid hydrophilic extension at the N-terminus that disrupts the capacity of VacA to form active membrane channels and inhibits the ability of VacA to induce cellular vacuolation (75, 223). A reduction in OCRs was observed in AGS cells following 4 hr of exposure to VacA s1m1 compared to VacA Δ346-7 and VacA s2m1 (Figure 5.3 A) and this reduction did not correlate with a reduction in total cell number (Figure 5.3 B). Further analysis of the data revealed that there was no significant difference in basal respiration between AGS cells treated with s1m1, s2m1, or Δ346-7 (Figure 5.3 C). AGS cells treated with s1m1 showed a trend toward reductions in maximal respiration and spare respiratory capacity compared to cells treated with either s2m1 or Δ346-7 (Figure 5.3 D and E), however the difference between the means is not

statistically significant. These data indicate that oligomerization and pore-formation are required for VacA to cause maximal changes to mitochondrial respiration.

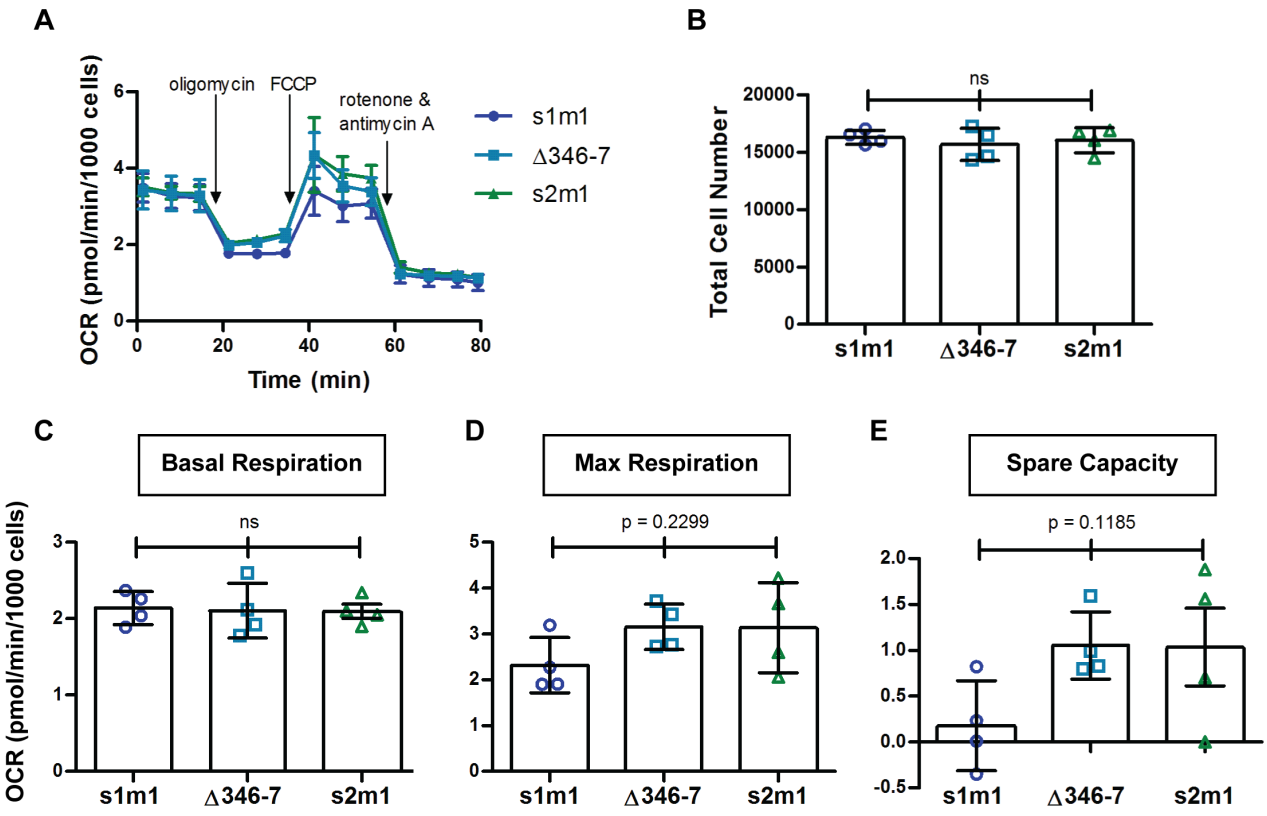

Figure 5.3 Oligomerization and pore-formation are necessary for VacA to induce maximal changes to mitochondrial respiration. (A) OCRs measured from AGS cells treated with 40 μg/mL of s1m1, s2m1, or Δ346-7 VacA for 4 hr. The OCRs were measured first under basal conditions and then after sequential additions of oligomycin, FCCP, and a mixture of rotenone and antimycin A at the indicated times in order to measure different parameters of mitochondrial function. n = 4 wells per condition from a single experiment. **(B)** Total cell numbers quantified after OCRs were measured. ns, p = 0.7258; ANOVA. **(C-E)** OCRs for basal respiration (C), maximal respiration (D), and spare capacity (E) in AGS cells, calculated from data in panel A. (C) ns, p = 0.9709; ANOVA. (D, E) Although both the mean maximal respiration rate and the mean spare respiratory capacity rate are lower for cells treated with s1m1 compared to cells treated with Δ346-7 or s2m1, the difference between the means is not statistically significant. (D) ns, p = 0.2299; ANOVA. (E) ns, p = 0.1185; ANOVA. All error bars, ± SD.

VacA does not cause changes to mitochondrial mass

We next asked whether the reduction in mitochondrial respiration detected in cells in response to VacA exposure was due to a decrease in total mitochondrial mass. To test this hypothesis, we used flow cytometry to assess mitochondrial mass in AGS cells following 4 hr of exposure to increasing concentrations of VacA. Mitochondria were labeled with MitoTracker Green (MTG), which localizes to mitochondrial membrane irrespective of membrane potential. We found that mitochondrial mass was not reduced following VacA treatment (Figure 5.4). This result suggests that VacA-induced changes in mitochondrial respiration are not due to a reduction in cellular mitochondrial mass.

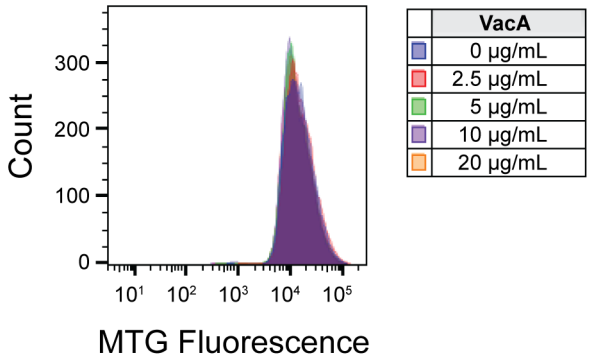

Figure 5.4 VacA does not cause changes to mitochondrial mass. AGS cells were mock treated or treated with the indicated concentration of VacA for 4 hr, then stained with MitoTracker Green (MTG) to assess mitochondrial mass by flow cytometry. MTG labels mitochondria independent of membrane potential.

VacA causes a reduction in glutamine and glutamic acid

We hypothesized that the reduction in mitochondrial respiration may be due to a decrease in available substrate(s) required for the tricarboxylic acid (TCA) cycle and oxidative phosphorylation. A key fuel for mitochondrial respiration is glutamine, which is

converted inside mitochondria into alpha-ketoglutarate, an intermediate in the TCA cycle (260). A previous study reported that treatment of HEK293T cells with VacA caused a reduction in cellular amino acid levels (255). Of the amino acids measured in this study, the level of cellular glutamine showed the largest reduction in response to VacA intoxication (255). Therefore, we tested whether VacA caused a similar reduction in cellular glutamine levels under our experimental conditions. To test this, we used targeted mass spectrometry to assess the level of a panel of metabolites in lysate from AGS cells treated in the presence or absence of VacA for 4 hr. Glutamine and 18 other amino acids were included in the panel. We detected a trend toward reduced levels of glutamine, as well as glutamic acid, in lysate from cells treated with VacA compared to lysate from mock treated cells (Figure 5.5 and Table 5.1). These data indicate that treatment of AGS cells with VacA causes a reduction in the level of cellular glutamine and glutamic acid.

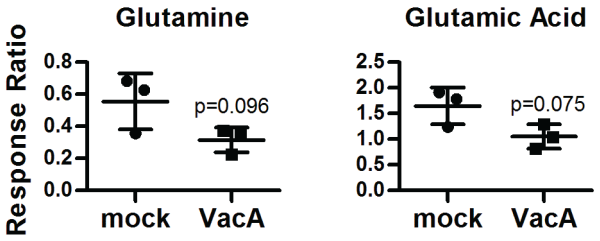

Figure 5.5 VacA causes a reduction in glutamine and glutamic acid. AGS cells were either mock-treated or treated with 20 μg/ml VacA for 4 hr, then cell lysate was collected and analyzed by targeted mass spectroscopy to detect changes in the levels of a panel of metabolites in VacA-treated cells compared to mock-treated cells. The "response ratio" is the ratio of the metabolite signal compared to the signal of an internal control. n = 3 replicates per condition from a single experiment. Error bars, ± SD. p values were calculated using an unpaired, two-tailed t test.

Table 5.1 List of the metabolites that were identified in cell lysate using targeted mass spectrometry to assess a panel of metabolites[a]

	Name	Ratio: VacA / mock	p value
1	Malic Acid	0.362	0.001
2	Choline	1.635	0.018
3	Taurine	0.415	0.031
4	Lactic Acid	0.482	0.041
5	Pantothenic Acid	0.356	0.069
6	Glutamic Acid[b]	0.638	0.075
7	Glutamine	0.569	0.096
8	Asparagine	0.562	0.127
9	Glutamic Acid[c]	0.668	0.127
10	Carnitine	0.762	0.134
11	Alanine	0.649	0.153
12	Hydroxyproline_aminolevul_1	0.765	0.175
13	Tyrosine	0.787	0.284
14	G-1-P_F-1-P	1.17	0.285
15	Reduced Glutathione	0.778	0.286
16	Inositol	0.764	0.339
17	Proline	0.815	0.34
18	Histidine	0.771	0.349
19	Leucine_Isoleucine	0.861	0.388
20	ATP[b]	0.918	0.428
21	Aspartic Acid	0.809	0.448
22	Oxidized Glutathione	1.141	0.49
23	Cystine	0.772	0.515
24	Phenylalanine	0.904	0.578
25	Arginine	0.853	0.609
26	Valine	0.916	0.649
27	Ornithine	0.914	0.679
28	ATP[c]	0.929	0.705
29	Lysine	1.056	0.737
30	ADP	1.086	0.738
31	Creatinine	0.966	0.882
32	Methionine	1.005	0.978

[a]The table is a list of the 32 metabolites detected in cell lysate from a targeted mass spectrometry analysis of a panel of 99 metabolites, ranked from smallest to largest p value. The middle column represents the ratio of metabolite signal intensity detected in lysate from VacA-treated cells compared to mock-treated cells. Red indicates the metabolite level is decreased in VacA-treated cells compared to control, green indicates the metabolite level is increased in VacA-treated cells compared to control. p values

were calculated using an unpaired, two-tailed t test. Grey shaded rows indicate a p value of > 0.05.
[b]Detected in the negative ionization mode of the mass spectrometer
[c]Detected in the positive ionization mode of the mass spectrometer

DISCUSSION

In this study, we analyzed the respiratory capacity of mitochondria following exposure of cells to VacA. We show that mitochondrial respiration is perturbed following VacA treatment, concomitant with a reduction in cellular glutamine, an important metabolic fuel for mitochondrial respiration. No reduction in mitochondrial mass was observed. Our results suggest that VacA treatment can impact cellular metabolism and the ability of cells to respond to energy demands.

We show that VacA treatment causes a reduction in the maximum rate of respiration achieved by mitochondria and depletes the spare respiratory capacity of cells. In contrast, no changes in baseline respiration rates occur following VacA treatment. Together, these results indicate that the baseline rates of mitochondrial respiration occurring in a VacA-treated cell are similar to those occurring in a mock-treated cell, as long as the cell is unperturbed. When challenged with increased energy demands, however, a VacA-treated cell will not be able to achieve the same maximal rate of respiration as an untreated cell, and may therefore have a reduced capacity to respond. Of note all experiments were completed in the absence of supplemental NH_4Cl. Therefore, the effect of VacA on mitochondrial respiration is not dependent on the presence of supplemental NH_4Cl, which we have previously shown enhances VacA activity by inhibiting its degradation.

The observed reduction in mitochondrial respiration could either be caused by

mitochondria dysfunction (i.e. mitochondria not working as well as they should) or by lack of available substrate necessary to drive mitochondrial respiration. We found that VacA treatment does not influence mitochondrial mass, indicating that the effect of VacA on mitochondrial respiration is not due to a loss in the total amount of cellular mitochondria. Although VacA has been proposed to induce mitochondrial fragmentation, further research is required to determine whether VacA-induced mitochondrial fragmentation is a cause of the reduced respiratory capacity of mitochondria in VacA-treated cells.

A key metabolic fuel for mitochondria is glutamine (260, 261). Glutamine is taken up into the cell from the extracellular environment by an amino acid transporter. Inside mitochondria, glutamine is converted into glutamate and then α-ketoglutarate, an intermediate in the TCA cycle. In this way, glutamine replenishes TCA cycle intermediates and helps fuel ATP production by mitochondria. We found that there were lower levels of glutamine and glutamic acid in VacA-treated cells compared to mock-treated cells. We speculate that glutamine reduction in cells treated with VacA may indicate that VacA exposure causes cells to increase glutamine catabolism in order to generate energy and respond to intoxication. This may deplete the available pool of glutamine, leading to a scenario in which VacA-treated cells have a reduced capacity to perform mitochondrial respiration and therefore respond to additional energy demands.

In conclusion, we speculate that the cellular response to VacA is energy demanding and depletes the available metabolites that drive energy generation, like glutamine. As a result, following VacA exposure, an intoxicated cell does not function efficiently and may be more susceptible to further cellular stress or cytotoxic agents.

CHAPTER VI

CONCLUDING REMARKS

VacA is associated with an increased risk of *H. pylori*-mediated peptic ulcer disease and gastric cancer, yet the precise role of VacA as a virulence factor is not clear. Progress made toward addressing this question will contribute to our understanding of host-pathogen interactions and our understanding of this unique pore-forming toxin. Work detailed in Chapter III showed that VacA has an inherently strong preference to bind lipid rafts within host cell membrane. The characterization of VacA intracellular trafficking and stability reported in Chapter IV revealed that toxin concentration and the extracellular environment influence the cellular response to VacA and are therefore important factors of VacA activity. And finally, Chapter V documented the ability of VacA to modulate mitochondrial respiration and the level of cellular metabolites. These insights expand our understanding of VacA toxicity, yet many questions remain, particularly about the mechanistic function of VacA pore-formation and about how to accurately define the role(s) VacA plays during disease. In this chapter, I discuss these questions and the experimental approaches that can begin to address them.

VacA cell surface binding and receptors

The biophysical work presented in Chapter III revealed that VacA has an inherently strong preference to bind lipid rafts. These findings can be expanded upon to determine which specific amino acids within the p55 domain target VacA to lipid rafts. Also, GPMVs provide an excellent system with which to study the interaction between VacA and putative protein receptors. VacA is proposed to bind several protein receptors in epithelial cells, including epidermal growth factor receptor (EGFR), heparan sulphate, low-density lipoprotein receptor-related protein 1 (LRP1), and receptor protein tyrosine phosphatases (RPTP) α and β (84, 94, 134, 164-166). A detailed analysis of VacA-receptor interactions using GPMVs could be used to test whether a particular receptor contributes to the association of VacA with lipid rafts or with non-rafts (as non-raft targeting of VacA was observed in a subpopulation of GPMVs). One way to approach this would be to silence the expression of putative receptor genes, generate GPMVs, and test whether VacA shows a reduced ability bind the GPMVs or a reduced preference for lipid rafts. Alternatively, cells can be transfected with genes encoding fluorescently-labeled putative receptors of VacA, and then the derived GPMVs and can be used to test whether the over-expression of a particular receptor sways the phase preference of VacA.

The target and function of the VacA pore

Inside the cell, VacA shows distinct localization to endosomal and lysosomal compartments. Work presented in Chapter IV suggests that, in contrast to the canonical model for VacA trafficking, mitochondria may not be a primary target of VacA, and

although it has been proposed that VacA may localize to Golgi and ER, VacA targeting of these organelles has not been heavily investigated (176). If endosomes and lysosomes are the primary target of VacA inside host cells, what does VacA pore-formation in these organelles lead to? A few studies report that VacA intoxication results in the inhibition of epidermal growth factor degradation (111), the inhibition of procathepsin D maturation (111), perturbation of transferrin recycling (112), and the inhibition of antigen presentation in immune cells (113). These finding suggest that the presence of VacA in endosomal and lysosomal compartments may perturb intracellular trafficking. Disruptions to orchestrated intracellular trafficking processes may inhibit the ability of cells to target proteins to the right place, at the right time. The ability of VacA to interfere with intracellular trafficking may have wide ranging downstream effects, which might help explain why VacA can cause such disparate effects on target cells. As one example, it would be interesting to investigate whether VacA-induced perturbation of endosomal/lysosomal function is associated with changes in metabolite levels and mitochondrial respiration rates reported in Chapter V.

An unexplored idea is whether VacA can target and kill other bacterial cells. Colicins are a family of pore-forming toxins produced by *Escherichia coli* which kill other bacteria by forming pores in bacterial membrane (30). In addition to *H. pylori,* an assortment of bacterial species colonizes the human stomach. The predominant phyla in the human stomach include *Proteobacteria, Firmicutes, Actinobacteria, Bacteroidetes,* and *Fusobacteria* (262). It has been shown that VacA can bind to the surface of *E. coli* cells, suggesting VacA has the capacity to bind bacterial membrane (263). However, to the best of our knowledge, the ability of VacA to kill other bacteria

has never been investigated. This would be an interesting future direction for VacA research, for if VacA can kill other bacteria, VacA may influence the composition of the gastric microbiota and play a role in microbial competition for resources.

Determining the structure of VacA in a pore-forming state

A clear understanding of the molecules that can and cannot pass through a VacA channel would provide mechanistic insight into the downstream consequences of VacA channel formation, which is critical for a comprehensive understanding of VacA toxicity. By comparing the structure of soluble VacA and membrane-inserted VacA, we can gain an understanding of the conformational changes that facilitate VacA channel formation and thereby the molecules that can potentially translocate through that channel. Therefore, future efforts to determine the structure of VacA in a pore-forming conformation will contribute greatly to our understanding of VacA activity.

The physiological concentration of VacA

Our ability to understand the role of PFTs, like VacA, in bacterial infection is limited by the difficultly in determining the physiological concentrations of PFTs during infection. The PFT concentration cells are exposed to *in vivo* likely differs according to site of infection, stage of infection, the composition of the extracellular environment, and many other variables. The physiological concentration of VacA to which cells are exposed to *in vivo* is not known. We conducted most experiments using a concentration of VacA (5 μg/mL or ~55 nM) that is sufficiently high to cause detectable cellular alterations, but not substantially higher, corresponding to one of the lowest

concentrations commonly used for *in vitro* experiments (115, 119, 120, 218, 255). Future studies directed at establishing a physiologically relevant VacA concentration range would help in the design and interpretation of *in vitro* experiments, particularly in light of the findings discussed in Chapter IV, that VacA concentration influences the cellular response to intoxication.

VacA is well known to elicit maximal activity in cell culture experiments after exposure to acidic pH (83, 87). This is due to the fact that VacA assembles into inactive VacA oligomers at neutral pH, and acidic pH causes the dissociation of these oligomers into monomers that can then re-oligomerize on target membrane. In addition to promoting monomer formation, exposure to acidic pH may also induce conformational changes that enhance VacA binding and/or activity (61). Disruptions to the neutral mucus layer residing above epithelial cells may influence the local pH. Therefore, we wanted to test whether lowering the pH of the solution surrounding cells increases the amount of VacA that associates with cells. To test this, we treated cells exposed to acidic buffer (pH 3.5 to 5.5) or to regular culture medium with VacA for 1 hr at 4°C and assessed VacA levels by Western blot. We detected higher levels of VacA associated with cells when cells were exposed to acidic buffer compared to when cells were exposed to regular cell culture medium (Figure 6.1). On a technical level, these results indicate that, during *in vitro* experiments, the concentration of VacA that associates with cells is lower than the concentration of VacA that is added to the cell culture medium. More broadly, these results indicate that the concentration of VacA that associates with cells varies depending on the extracellular pH. This suggests that disruptions to the neutral mucus layer residing above epithelial cells may influence that amount of VacA

that associates with cells and thereby VacA toxicity. In support of this idea, a previous study showed that the amount of VacA internalized into target cells is enhanced when cells are exposed to acidic buffer compared to neutral buffer (87).

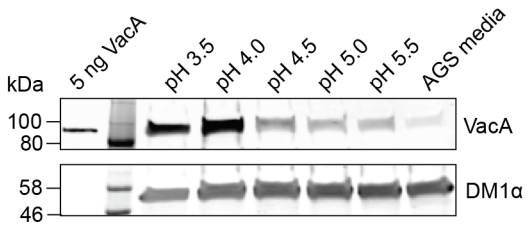

Figure 6.1 The ability of VacA to associate with cells is influenced by the extracellular pH. Western blot analysis of cell lysate from AGS cells exposed to acidic buffer (50 mM citrate-buffered saline, 1 mM calcium chloride, 1 mM magnesium chloride, pH 3.5 – 5.5) or regular culture medium and treated with 5 μg/mL acid-activated VacA for 1 hr at 4°C.

Cell fate following VacA intoxication

Research within the past decade has revealed that cells have mechanisms to respond and recover following exposure to PFTs (30, 40) and that cell death following PFT exposure depends on toxin dose and cell type. The findings presented in Chapter IV reveal that the ability of VacA to induce cell death in gastric epithelial cells depends on toxin dose and the extracellular environment. Therefore, although the most extreme cellular response to VacA is cell death, VacA may also elicit non-lethal effects on target cells that modulate cellular behavior and promote bacterial growth and dissemination. It will be important to design future studies to monitor for subtle, non-lethal effects of VacA and how they may influence the host environment. Towards this end, we have shown in Chapter V that VacA causes a reduction in the level of glutamine and glutamic acid, which is associated with a reduction in mitochondrial respiration. In addition to

glutamine, the level of several other metabolites are reduced or elevated in VacA-treated cells compared to mock-treated cells. For example, malic acid, taurine, and lactic acid levels are reduced in VacA-treated cells compared to control cells, while choline levels are increased in VacA-treated cells compared to control cells (Table 5.1). A thorough characterization of metabolic changes in response to VacA treatment, and how these changes influence cellular function and/or the extracellular environment, may yield new insights into the potential role non-lethal effects of VacA play in *H. pylori* colonization and disease.

A remaining question about VacA toxicity during infection is whether there is interplay between VacA and other *H. pylori* factors. For example, a previous study suggested that CagA can inhibit VacA-induced apoptosis (120). We have shown that ammonia, proposed to be at high levels during infection due to the activity of *H. pylori* enzymes, inhibits VacA degradation thereby enhancing VacA toxicity. The work presented here involved treatment of cultured cells with purified toxin, which was advantageous as it enabled us to establish an understanding of the cellular response to VacA in the absence of additional factors that may be present during infection. With this foundational information, we can begin to study VacA within more complex environments that may better mimic *in vivo* conditions. One strategy would be to co-culture cells with live *H. pylori,* and various *H. pylori* mutants, to test whether other *H. pylori* factors influence VacA toxicity, and vice versa. Co-culture studies could also be used to further test the hypothesis that *H. pylori*-generated ammonia influences intracellular VacA degradation.

REFERENCES

1. **Marshall B**. 2006. Helicobacter connections.ChemMedChem. John Wiley & Sons, Ltd.

2. **Warren JR**, **Marshall B**. 1983. Unidentified curved bacilli on gastric epithelium in active chronic gastritis. Lancet **1**:1273–1275.

3. **Marshall BJ**, **Warren JR**. 1984. Unidentified curved bacilli in the stomach of patients with gastritis and peptic ulceration. Lancet **1**:1311–1315.

4. **Yang I**, **Nell S**, **Suerbaum S**. 2013. Survival in hostile territory: the microbiota of the stomach. FEMS Microbiol Rev **37**:736–761.

5. **Marshall BJ**, **Armstrong JA**, **McGechie DB**, **Clancy RJ**. 1985. Attempt to fulfil Koch's postulates for pyloric Campylobacter. Medical Journal of Australia **142**:436–439.

6. **Kusters JG**, **van Vliet AHM**, **Kuipers EJ**. 2006. Pathogenesis of Helicobacter pylori Infection. Clinical Microbiology Reviews **19**:449–490.

7. **Ferlay J**, **Soerjomataram I**, **Dikshit R**, **Eser S**, **Mathers C**, **Rebelo M**, **Parkin DM**, **Forman D**, **Bray F**. 2015. Cancer incidence and mortality worldwide: Sources, methods and major patterns in GLOBOCAN 2012. International Journal of Cancer **136**:E359–E386.

8. **Plummer M**, **de Martel C**, **Vignat J**, **Ferlay J**, **Bray F**, **Franceschi S**. 2016. Global burden of cancers attributable to infections in 2012: a synthetic analysis. Lancet Glob Health **4**:e609–16.

9. 2014. Helicobacter pylori Eradication as a Strategy for Preventing Gastric Cancer 1–190.

10. **Hooi JKY**, **Lai WY**, **Ng WK**, **Suen MMY**, **Underwood FE**, **Tanyingoh D**, **Malfertheiner P**, **Graham DY**, **Wong VWS**, **Wu JCY**, **Chan FKL**, **Sung JJY**, **Kaplan GG**, **Ng SC**. 2017. Global Prevalence of Helicobacter pylori Infection: Systematic Review and Meta-Analysis. Gastroenterology **153**:420–429.

11. **Peek RM**, **Blaser MJ**. 2002. Helicobacter pylori and gastrointestinal tract adenocarcinomas. Nat Rev Cancer **2**:28–37.

12. **Cover TL**, **Blaser MJ**. 2009. Helicobacter pylori in Health and Disease. Gastroenterology **136**:1863–1873.

13. **Van Doorn LJ**, **Figueiredo C**, **Mégraud F**, **Pena S**, **Midolo P**, **Queiroz DM**, **Carneiro F**, **Vanderborght B**, **Pegado MD**, **Sanna R**, **De Boer W**, **Schneeberger PM**, **Correa P**, **Ng EK**, **Atherton J**, **Blaser MJ**, **Quint WG**. 1999. Geographic distribution of vacA allelic types of Helicobacter pylori.

Gastroenterology **116**:823–830.

14. **Gerhard M**, **Lehn N**, **Neumayer N**, **Borén T**, **Rad R**, **Schepp W**, **Miehlke S**, **Classen M**, **Prinz C**. 1999. Clinical relevance of the Helicobacter pylori gene for blood-group antigen-binding adhesin. Proc Natl Acad Sci USA **96**:12778–12783.

15. **Omar El EM**, **Carrington M**, **Chow WH**, **McColl KE**, **Bream JH**, **Young HA**, **Herrera J**, **Lissowska J**, **Yuan CC**, **Rothman N**, **Lanyon G**, **Martin M**, **Fraumeni JF**, **Rabkin CS**. 2000. Interleukin-1 polymorphisms associated with increased risk of gastric cancer. Nature **404**:398–402.

16. **Beckett AC**, **Piazuelo MB**, **Noto JM**, **Peek RM**, **Washington MK**, **Algood HMS**, **Cover TL**. 2016. Dietary Composition Influences Incidence of Helicobacter pylori-Induced Iron Deficiency Anemia and Gastric Ulceration. Infect Immun **84**:3338–3349.

17. **Gaddy JA**, **Radin JN**, **Loh JT**, **Zhang F**, **Washington MK**, **Peek RM Jr**, **Algood HMS**, **Cover TL**. 2013. High Dietary Salt Intake Exacerbates Helicobacter pylori-Induced Gastric Carcinogenesis. Infect Immun **81**:2258–2267.

18. **Noto JM**, **Gaddy JA**, **Lee JY**, **Piazuelo MB**, **Friedman DB**, **Colvin DC**, **Romero-Gallo J**, **Suarez G**, **Loh J**, **Slaughter JC**, **Tan S**, **Morgan DR**, **Wilson KT**, **Bravo LE**, **Correa P**, **Cover TL**, **Amieva MR**, **Peek RM**. 2013. Iron deficiency accelerates Helicobacter pylori-induced carcinogenesis in rodents and humans. J Clin Invest **123**:479–492.

19. **Correa P**. 1992. Human gastric carcinogenesis: a multistep and multifactorial process--First American Cancer Society Award Lecture on Cancer Epidemiology and Prevention. Cancer Res **52**:6735–6740.

20. **Suerbaum S**, **Michetti P**. 2002. Helicobacter pylori infection. N Engl J Med **347**:1175–1186.

21. **Parsonnet J**, **Hansen S**, **Rodriguez L**, **Gelb AB**, **Warnke RA**, **Jellum E**, **Orentreich N**, **Vogelman JH**, **Friedman GD**. 1994. Helicobacter pylori infection and gastric lymphoma. N Engl J Med **330**:1267–1271.

22. **Martinsen TC**, **Bergh K**, **Waldum HL**. 2005. Gastric juice: a barrier against infectious diseases. Basic Clin Pharmacol Toxicol **96**:94–102.

23. **Kauffman GL**. 1981. Gastric mucus and bicarbonate secretion in relation to mucosal protection. J Clin Gastroenterol **3**:45–50.

24. **Josenhans C**, **Suerbaum S**. 2002. The role of motility as a virulence factor in bacteria. Int J Med Microbiol **291**:605–614.

25. **Schreiber S**, **Konradt M**, **Groll C**, **Scheid P**, **Hanauer G**, **Werling H-O**,

Josenhans C, **Suerbaum S**. 2004. The spatial orientation of Helicobacter pylori in the gastric mucus. Proc Natl Acad Sci USA **101**:5024–5029.

26. **Huang JY**, **Sweeney EG**, **Sigal M**, **Zhang HC**, **Remington SJ**, **Cantrell MA**, **Kuo CJ**, **Guillemin K**, **Amieva MR**. 2015. Chemodetection and Destruction of Host Urea Allows Helicobacter pylori to Locate the Epithelium. Cell Host Microbe **18**:147–156.

27. **Marshall BJ**, **Barrett LJ**, **Prakash C**, **McCallum RW**, **Guerrant RL**. 1990. Urea protects Helicobacter (Campylobacter) pylori from the bactericidal effect of acid. Gastroenterology **99**:697–702.

28. **Hatakeyama M**. 2014. Helicobacter pylori CagA and gastric cancer: a paradigm for hit-and-run carcinogenesis. Cell Host Microbe **15**:306–316.

29. **Styer CM**, **Hansen LM**, **Cooke CL**, **Gundersen AM**, **Choi SS**, **Berg DE**, **Benghezal M**, **Marshall BJ**, **Peek RM**, **Borén T**, **Solnick JV**. 2010. Expression of the BabA adhesin during experimental infection with Helicobacter pylori. Infect Immun **78**:1593–1600.

30. **Los FCO**, **Randis TM**, **Aroian RV**, **Ratner AJ**. 2013. Role of pore-forming toxins in bacterial infectious diseases. Microbiol Mol Biol Rev **77**:173–207.

31. **Lakey JH**, **Gisou van der Goot F**, **Pattus F**. 1994. All in the family: the toxic activity of pore-forming colicins. Toxicology **87**:85–108.

32. **Collier RJ**. 2009. Membrane translocation by anthrax toxin. Mol Aspects Med **30**:413–422.

33. **Geny B**, **Popoff MR**. 2006. Bacterial protein toxins and lipids: pore formation or toxin entry into cells. Biol Cell **98**:667–678.

34. **Schnupf P**, **Portnoy DA**. 2007. Listeriolysin O: a phagosome-specific lysin. Microbes Infect **9**:1176–1187.

35. **Alberts B**, **Johnson A**, **Lewis J**, **Raff M**, **Roberts K**, **Walter P**. 2007. Molecular Biology of the Cell, 5 ed. Garland Science.

36. **Parker MW**, **Buckley JT**, **Postma JP**, **Tucker AD**, **Leonard K**, **Pattus F**, **Tsernoglou D**. 1994. Structure of the Aeromonas toxin proaerolysin in its water-soluble and membrane-channel states. Nature **367**:292–295.

37. **Peraro MD**, **van der Goot FG**. 2015. Pore-forming toxins: ancient, but never really out of fashion. Nat Rev Microbiol.

38. **Hotze EM**, **Tweten RK**. 2012. Membrane assembly of the cholesterol-dependent cytolysin pore complex. Biochim Biophys Acta **1818**:1028–1038.

39. **Bischofberger M**, **Iacovache I**, **van der Goot FG**. 2012. Pathogenic pore-forming proteins: function and host response. Cell Host Microbe **12**:266–275.

40. **Aroian R**, **van der Goot FG**. 2007. Pore-forming toxins and cellular non-immune defenses (CNIDs). Curr Opin Microbiol **10**:57–61.

41. **Gonzalez MR**, **Bischofberger M**, **Frêche B**, **Ho S**, **Parton RG**, **van der Goot FG**. 2011. Pore-forming toxins induce multiple cellular responses promoting survival. Cell Microbiol **13**:1026–1043.

42. **Bhakdi S**, **Tranum-Jensen J**. 1991. Alpha-toxin of Staphylococcus aureus. Microbiol Rev **55**:733–751.

43. **Berube BJ**, **Wardenburg JB**. 2013. Staphylococcus aureus α-Toxin: Nearly a Century of Intrigue. Toxins (Basel) **5**:1140–1166.

44. **Hamon MA**, **Ribet D**, **Stavru F**, **Cossart P**. 2012. Listeriolysin O: the Swiss army knife of Listeria. Trends Microbiol **20**:360–368.

45. **Leunk RD**, **Johnson PT**, **David BC**, **Kraft WG**, **Morgan DR**. 1988. Cytotoxic activity in broth-culture filtrates of Campylobacter pylori. J Med Microbiol **26**:93–99.

46. **Cover TL**, **Blanke SR**. 2005. Helicobacter pylori VacA, a paradigm for toxin multifunctionality. Nat Rev Microbiol **3**:320–332.

47. **Cover TL**, **Tummuru MK**, **Cao P**, **Thompson SA**, **Blaser MJ**. 1994. Divergence of genetic sequences for the vacuolating cytotoxin among Helicobacter pylori strains. J Biol Chem **269**:10566–10573.

48. **Telford JL**, **Ghiara P**, **Dell'Orco M**, **Comanducci M**, **Burroni D**, **Bugnoli M**, **Tecce MF**, **Censini S**, **Covacci A**, **Xiang Z**. 1994. Gene structure of the Helicobacter pylori cytotoxin and evidence of its key role in gastric disease. J Exp Med **179**:1653–1658.

49. **Nguyen VQ**, **Caprioli RM**, **Cover TL**. 2001. Carboxy-Terminal Proteolytic Processing ofHelicobacter pylori Vacuolating Toxin. Infect Immun **69**:543–546.

50. **Bumann D**, **Aksu S**, **Wendland M**, **Janek K**, **Zimny-Arndt U**, **Sabarth N**, **Meyer TF**, **Jungblut PR**. 2002. Proteome analysis of secreted proteins of the gastric pathogen Helicobacter pylori. Infect Immun **70**:3396–3403.

51. **Cover TL**, **Blaser MJ**. 1992. Purification and characterization of the vacuolating toxin from Helicobacter pylori. J Biol Chem **267**:10570–10575.

52. **Schmitt W**, **Haas R**. 1994. Genetic analysis of the Helicobacter pylori vacuoiating cytotoxin: structural similarities with the IgA protease type of exported protein. Mol Microbiol, 2nd ed. **12**:307–319.

53. **Bumann D**, **Aksu S**, **Wendland M**, **Janek K**, **Zimny-Arndt U**, **Sabarth N**, **Meyer TF**, **Jungblut PR**. 2002. Proteome Analysis of Secreted Proteins of the Gastric Pathogen Helicobacter pylori. Infect Immun **70**:3396–3403.

54. **Fischer W**, **Buhrdorf R**, **Gerland E**, **Haas R**. 2001. Outer Membrane Targeting of Passenger Proteins by the Vacuolating Cytotoxin Autotransporter of Helicobacter pylori. Infect Immun **69**:6769–6775.

55. **Torres VJ**, **McClain MS**, **Cover TL**. 2004. Interactions between p-33 and p-55 domains of the Helicobacter pylori vacuolating cytotoxin (VacA). J Biol Chem **279**:2324–2331.

56. **Torres VJ**, **Ivie SE**, **McClain MS**, **Cover TL**. 2005. Functional properties of the p33 and p55 domains of the Helicobacter pylori vacuolating cytotoxin. J Biol Chem **280**:21107–21114.

57. **González-Rivera C**, **Gangwer KA**, **McClain MS**, **Eli IM**, **Chambers MG**, **Ohi MD**, **Lacy DB**, **Cover TL**. 2010. Reconstitution of Helicobacter pylori VacA Toxin from Purified Components. Biochemistry **49**:5743–5752.

58. **Gangwer KA**, **Mushrush DJ**, **Stauff DL**, **Spiller B**, **McClain MS**, **Cover TL**, **Lacy DB**. 2007. Crystal structure of the Helicobacter pylori vacuolating toxin p55 domain. Proc Natl Acad Sci USA **104**:16293–16298.

59. **Junker M**, **Schuster CC**, **McDonnell AV**, **Sorg KA**, **Finn MC**, **Berger B**, **Clark PL**. 2006. Pertactin beta-helix folding mechanism suggests common themes for the secretion and folding of autotransporter proteins. Proc Natl Acad Sci USA **103**:4918–4923.

60. **Su M**, **Erwin AL**, **Campbell AM**, **Pyburn TM**, **Salay LE**, **Hanks JL**, **Lacy DB**, **Akey DL**, **Cover TL**, **Ohi MD**. 2019. Cryo-EM Analysis Reveals Structural Basis of Helicobacter pylori VacA Toxin Oligomerization. J Mol Biol.

61. **Zhang K**, **Zhang H**, **Li S**, **Pintilie GD**, **Mou T-C**, **Gao Y**, **Zhang Q**, **van den Bedem H**, **Schmid MF**, **Au SWN**, **Chiu W**. 2019. Cryo-EM structures of Helicobacter pylori vacuolating cytotoxin A oligomeric assemblies at near-atomic resolution. Proc Natl Acad Sci USA **116**:6800–6805.

62. **Vinion-Dubiel AD**, **McClain MS**, **Czajkowsky DM**, **Iwamoto H**, **Ye D**, **Cao P**, **Schraw W**, **Szabo G**, **Blanke SR**, **Shao Z**, **Cover TL**. 1999. A dominant negative mutant of Helicobacter pylori vacuolating toxin (VacA) inhibits VacA-induced cell vacuolation. J Biol Chem **274**:37736–37742.

63. **McClain MS**, **Iwamoto H**, **Cao P**, **Vinion-Dubiel AD**, **Li Y**, **Szabo G**, **Shao Z**, **Cover TL**. 2003. Essential role of a GXXXG motif for membrane channel formation by Helicobacter pylori vacuolating toxin. J Biol Chem **278**:12101–12108.

64. **de Bernard M**, **Arico B**, **Papini E**, **Rizzuto R**, **Grandi G**, **Rappuoli R**, **Montecucco C**. 1997. Helicobacter pylori toxin VacA induces vacuole formation by acting in the cell cytosol. Mol Microbiol **26**:665–674.

65. **de Bernard M**, **Burroni D**, **Papini E**, **Rappuoli R**, **Telford J**, **Montecucco C**. 1998. Identification of the Helicobacter pylori VacA toxin domain active in the cell cytosol. Infect Immun **66**:6014–6016.

66. **Ye D**, **Willhite DC**, **Blanke SR**. 1999. Identification of the minimal intracellular vacuolating domain of the Helicobacter pylori vacuolating toxin. J Biol Chem **274**:9277–9282.

67. **Kim S**, **Chamberlain AK**, **Bowie JU**. 2004. Membrane channel structure of Helicobacter pylori vacuolating toxin: Role of multiple GXXXG motifs in cylindrical channels. Proc Natl Acad Sci USA **101**:5988–5991.

68. **McClain MS**, **Cao P**, **Cover TL**. 2001. Amino-Terminal Hydrophobic Region ofHelicobacter pylori Vacuolating Cytotoxin (VacA) Mediates Transmembrane Protein Dimerization. Infect Immun **69**:1181–1184.

69. **Ye D**, **Blanke SR**. 2000. Mutational analysis of the Helicobacter pylori vacuolating toxin amino terminus: identification of amino acids essential for cellular vacuolation. Infect Immun **68**:4354–4357.

70. **McClain MS**, **Czajkowsky DM**, **Torres VJ**, **Szabo G**, **Shao Z**, **Cover TL**. 2006. Random mutagenesis of Helicobacter pylori vacA to identify amino acids essential for vacuolating cytotoxic activity. Infect Immun **74**:6188–6195.

71. **Cover TL**, **Cao P**, **Lind CD**, **Tham KT**, **Blaser MJ**. 1993. Correlation between vacuolating cytotoxin production by Helicobacter pylori isolates in vitro and in vivo. Infect Immun **61**:5008–5012.

72. **Forsyth MH**, **Atherton JC**, **Blaser MJ**, **Cover TL**. 1998. Heterogeneity in levels of vacuolating cytotoxin gene (vacA) transcription among Helicobacter pylori strains. Infect Immun **66**:3088–3094.

73. **Atherton JC**, **Cao P**, **Peek RM**, **Tummuru MK**, **Blaser MJ**, **Cover TL**. 1995. Mosaicism in vacuolating cytotoxin alleles of Helicobacter pylori. Association of specific vacA types with cytotoxin production and peptic ulceration. J Biol Chem **270**:17771–17777.

74. **Rhead JL**, **Letley DP**, **Mohammadi M**, **Hussein N**, **Mohagheghi MA**, **Eshagh Hosseini M**, **Atherton JC**. 2007. A new Helicobacter pylori vacuolating cytotoxin determinant, the intermediate region, is associated with gastric cancer. Gastroenterology **133**:926–936.

75. **McClain MS**, **Cao P**, **Iwamoto H**, **Vinion-Dubiel AD**, **Szabo G**, **Shao Z**, **Cover TL**. 2001. A 12-amino-acid segment, present in type s2 but not type s1

Helicobacter pylori VacA proteins, abolishes cytotoxin activity and alters membrane channel formation. J Bacteriol **183**:6499–6508.

76. **González-Rivera C**, **Algood HMS**, **Radin JN**, **McClain MS**, **Cover TL**. 2012. The intermediate region of Helicobacter pylori VacA is a determinant of toxin potency in a Jurkat T cell assay. Infect Immun **80**:2578–2588.

77. **Pagliaccia C**, **de Bernard M**, **Pietro Lupetti**, **Ji X**, **Burroni D**, **Cover TL**, **Papini E**, **Rappuoli R**, **Telford JL**, **Reyrat J-M**. 1998. The m2 form of the Helicobacter pylori cytotoxin has cell type-specific vacuolating activity. Proc Natl Acad Sci USA **95**:10212–10217.

78. **Pagliaccia C**, **de Bernard M**, **Lupetti P**, **Ji X**, **Burroni D**, **Cover TL**, **Papini E**, **Rappuoli R**, **Telford JL**, **Reyrat JM**. 1998. The m2 form of the Helicobacter pylori cytotoxin has cell type-specific vacuolating activity. Proc Natl Acad Sci USA **95**:10212–10217.

79. **Tombola F**, **Pagliaccia C**, **Campello S**, **Telford JL**, **Montecucco C**, **Papini E**, **Zoratti M**. 2001. How the Loop and Middle Regions Influence the Properties of Helicobacter pylori VacA Channels. Biophys J **81**:3204–3215.

80. **Chambers MG**, **Pyburn TM**, **González-Rivera C**, **Collier SE**, **Eli I**, **Yip CK**, **Takizawa Y**, **Lacy DB**, **Cover TL**, **Ohi MD**. 2013. Structural analysis of the oligomeric states of Helicobacter pylori VacA toxin. J Mol Biol **425**:524–535.

81. **Ivie SE**, **McClain MS**, **Torres VJ**, **Algood HMS**, **Lacy DB**, **Yang R**, **Blanke SR**, **Cover TL**. 2008. Helicobacter pylori VacA subdomain required for intracellular toxin activity and assembly of functional oligomeric complexes. Infect Immun **76**:2843–2851.

82. **Pyburn TM**, **Foegeding NJ**, **González-Rivera C**, **McDonald NA**, **Gould KL**, **Cover TL**, **Ohi MD**. 2016. Structural organization of membrane-inserted hexamers formed by Helicobacter pylori VacA toxin. Mol Microbiol **102**:22–36.

83. **Cover TL**, **Hanson PI**, **Heuser JE**. 1997. Acid-induced dissociation of VacA, the Helicobacter pylori vacuolating cytotoxin, reveals its pattern of assembly. J Cell Biol **138**:759–769.

84. **Yahiro K**, **Niidome T**, **Kimura M**, **Hatakeyama T**, **Aoyagi H**, **Kurazono H**, **Imagawa KI**, **Wada A**, **Moss J**, **Hirayama T**. 1999. Activation of Helicobacter pylori VacA toxin by alkaline or acid conditions increases its binding to a 250-kDa receptor protein-tyrosine phosphatase beta. J Biol Chem **274**:36693–36699.

85. **Gangwer KA**, **Mushrush DJ**, **Stauff DL**, **Spiller B**, **McClain MS**, **Cover TL**, **Lacy DB**. 2007. Crystal structure of the Helicobacter pylori vacuolating toxin p55 domain. Proc Natl Acad Sci USA **104**:16293–16298.

86. **de Bernard M**, **Papini E**, **de Filippis V**, **Gottardi E**, **Telford J**, **Manetti R**, **Fontana A**, **Rappuoli R**, **Montecucco C**. 1995. Low pH activates the vacuolating toxin of Helicobacter pylori, which becomes acid and pepsin resistant. J Biol Chem **270**:23937–23940.

87. **McClain MS**, **Schraw W**, **Ricci V**, **Boquet P**, **Cover TL**. 2000. Acid activation of Helicobacter pylori vacuolating cytotoxin (VacA) results in toxin internalization by eukaryotic cells. Mol Microbiol **37**:433–442.

88. **Oertli M**, **Noben M**, **Engler DB**, **Semper RP**, **Reuter S**, **Maxeiner J**, **Gerhard M**, **Taube C**, **Müller A**. 2013. Helicobacter pylori γ-glutamyl transpeptidase and vacuolating cytotoxin promote gastric persistence and immune tolerance. Proc Natl Acad Sci USA **110**:3047–3052.

89. **Salama NR**, **Otto G**, **Tompkins L**, **Falkow S**. 2001. Vacuolating Cytotoxin of Helicobacter pylori Plays a Role during Colonization in a Mouse Model of Infection. Infect Immun **69**:730–736.

90. **Winter JA**, **Letley DP**, **Cook KW**, **Rhead JL**, **Zaitoun AAM**, **Ingram RJM**, **Amilon KR**, **Croxall NJ**, **Kaye PV**, **Robinson K**, **Atherton JC**. 2014. A Role for the Vacuolating Cytotoxin, VacA, in Colonization and Helicobacter pylori–Induced Metaplasia in the Stomach. J Infect Dis **210**:jiu154–963.

91. **Eaton KA**, **Cover TL**, **Tummuru MK**, **Blaser MJ**, **Krakowka S**. 1997. Role of vacuolating cytotoxin in gastritis due to Helicobacter pylori in gnotobiotic piglets. Infect Immun **65**:3462–3464.

92. **Wirth HP**, **Beins MH**, **Yang M**, **Tham KT**, **Blaser MJ**. 1998. Experimental infection of Mongolian gerbils with wild-type and mutant Helicobacter pylori strains. Infect Immun **66**:4856–4866.

93. **Ogura K**, **Maeda S**, **Nakao M**, **Watanabe T**, **Tada M**, **Kyutoku T**, **Yoshida H**, **Shiratori Y**, **Omata M**. 2000. Virulence Factors of Helicobacter pylori Responsible for Gastric Diseases in Mongolian Gerbil. J Exp Med **192**:1601–1610.

94. **Fujikawa A**, **Shirasaka D**, **Yamamoto S**, **Ota H**, **Yahiro K**, **Fukada M**, **Shintani T**, **Wada A**, **Aoyama N**, **Hirayama T**, **Fukamachi H**, **Noda M**. 2003. Mice deficient in protein tyrosine phosphatase receptor type Z are resistant to gastric ulcer induction by VacA of Helicobacter pylori. Nat Genet **33**:375–381.

95. **Supajatura V**, **Ushio H**, **Wada A**, **Yahiro K**, **Okumura K**, **Ogawa H**, **Hirayama T**, **Ra C**. 2002. Cutting Edge: VacA, a Vacuolating Cytotoxin of Helicobacter pylori, Directly Activates Mast Cells for Migration and Production of Proinflammatory Cytokines. J Immunol **168**:2603–2607.

96. **Ghiara P**, **Marchetti M**, **Blaser MJ**, **Tummuru MK**, **Cover TL**, **Segal ED**, **Tompkins LS**, **Rappuoli R**. 1995. Role of the Helicobacter pylori virulence

factors vacuolating cytotoxin, CagA, and urease in a mouse model of disease. Infect Immun **63**:4154–4160.

97. **Winter JA**, **Letley DP**, **Cook KW**, **Rhead JL**, **Zaitoun AAM**, **Ingram RJM**, **Amilon KR**, **Croxall NJ**, **Kaye PV**, **Robinson K**, **Atherton JC**. 2014. A Role for the Vacuolating Cytotoxin, VacA, in Colonization and Helicobacter pylori–Induced Metaplasia in the Stomach. J Infect Dis **210**:954–963.

98. **Engler DB**, **Reuter S**, **van Wijck Y**, **Urban S**, **Kyburz A**, **Maxeiner J**, **Martin H**, **Yogev N**, **Waisman A**, **Gerhard M**, **Cover TL**, **Taube C**, **Müller A**. 2014. Effective treatment of allergic airway inflammation with Helicobacter pylori immunomodulators requires BATF3-dependent dendritic cells and IL-10. PNAS **111**:11810–11815.

99. **Cover TL**, **Vaughn SG**, **Cao P**, **Blaser MJ**. 1992. Potentiation of Helicobacter pylori vacuolating toxin activity by nicotine and other weak bases. J Infect Dis **166**:1073–1078.

100. **Papini E**, **de Bernard M**, **Milia E**, **Bugnoli M**, **Zerial M**, **Rappuoli R**, **Montecucco C**. 1994. Cellular vacuoles induced by Helicobacter pylori originate from late endosomal compartments. Proc Natl Acad Sci USA **91**:9720–9724.

101. **Molinari M**, **Galli C**, **Norais N**, **Telford JL**, **Rappuoli R**, **Luzio JP**, **Montecucco C**. 1997. Vacuoles induced by Helicobacter pylori toxin contain both late endosomal and lysosomal markers. J Biol Chem **272**:25339–25344.

102. **Montecucco C**, **Rappuoli R**. 2001. Living dangerously: how Helicobacter pylori survives in the human stomach. Nat Rev Mol Cell Biol **2**:457–466.

103. **Czajkowsky DM**, **Iwamoto H**, **Cover TL**, **Shao Z**. 1999. The vacuolating toxin from Helicobacter pylori forms hexameric pores in lipid bilayers at low pH. Proc Natl Acad Sci USA **96**:2001–2006.

104. **Tombola F**, **Carlesso C**, **Szabò I**, **de Bernard M**, **Reyrat JM**, **Telford JL**, **Rappuoli R**, **Montecucco C**, **Papini E**, **Zoratti M**. 1999. Helicobacter pylori vacuolating toxin forms anion-selective channels in planar lipid bilayers: possible implications for the mechanism of cellular vacuolation. Biophys J **76**:1401–1409.

105. **Iwamoto H**, **Czajkowsky DM**, **Cover TL**, **Szabo G**, **Shao Z**. 1999. VacA from Helicobacter pylori: a hexameric chloride channel. FEBS Lett **450**:101–104.

106. **Tombola F**, **Oregna F**, **Brutsche S**, **Szabò I**, **Del Giudice G**, **Rappuoli R**, **Montecucco C**, **Papini E**, **Zoratti M**. 1999. Inhibition of the vacuolating and anion channel activities of the VacA toxin of Helicobacter pylori. FEBS Lett **460**:221–225.

107. **Szabò I**, **Brutsche S**, **Tombola F**, **Moschioni M**, **Satin B**, **Telford JL**, **Rappuoli R**, **Montecucco C**, **Papini E**, **Zoratti M**. 1999. Formation of anion-

selective channels in the cell plasma membrane by the toxin VacA of Helicobacter pylori is required for its biological activity. EMBO J **18**:5517–5527.

108. **Morbiato L**, **Tombola F**, **Campello S**, **Del Giudice G**, **Rappuoli R**, **Zoratti M**, **Papini E**. 2001. Vacuolation induced by VacA toxin of Helicobacter pylori requires the intracellular accumulation of membrane permeant bases, Cl− and water. FEBS Lett **508**:479–483.

109. **Genisset C**, **Puhar A**, **Calore F**, **de Bernard M**, **Dell'Antone P**, **Montecucco C**. 2007. The concerted action of the Helicobacter pylori cytotoxin VacA and of the v-ATPase proton pump induces swelling of isolated endosomes. Cell Microbiol **9**:1481–1490.

110. **Ricci V**, **Sommi P**, **Fiocca R**, **Romano M**, **Solcia E**, **Ventura U**. 1997. Helicobacter pylori vacuolating toxin accumulates within the endosomal-vacuolar compartment of cultured gastric cells and potentiates the vacuolating activity of ammonia. The Journal of Pathology **183**:453–459.

111. **Satin B**, **Norais N**, **Telford J**, **Rappuoli R**, **Murgia M**, **Montecucco C**, **Papini E**. 1997. Effect of helicobacter pylori vacuolating toxin on maturation and extracellular release of procathepsin D and on epidermal growth factor degradation. J Biol Chem **272**:25022–25028.

112. **Tan S**, **Noto JM**, **Romero-Gallo J**, **Peek RM Jr**, **Amieva MR**. 2011. Helicobacter pylori Perturbs Iron Trafficking in the Epithelium to Grow on the Cell Surface. PLoS Pathog **7**:e1002050.

113. **Molinari M**, **Salio M**, **Galli C**, **Norais N**, **Rappuoli R**, **Lanzavecchia A**, **Montecucco C**. 1998. Selective inhibition of Ii-dependent antigen presentation by Helicobacter pylori toxin VacA. J Exp Med **187**:135–140.

114. **Kimura M**, **Goto S**, **Wada A**, **Yahiro K**, **Niidome T**, **Hatakeyama T**, **Aoyagi H**, **Hirayama T**, **Kondo T**. 1999. Vacuolating cytotoxin purified from Helicobacter pylori causes mitochondrial damage in human gastric cells. Microb Pathog **26**:45–52.

115. **Willhite DC**, **Blanke SR**. 2004. Helicobacter pylori vacuolating cytotoxin enters cells, localizes to the mitochondria, and induces mitochondrial membrane permeability changes correlated to toxin channel activity. Cell Microbiol **6**:143–154.

116. **Yamasaki E**, **Wada A**, **Kumatori A**, **Nakagawa I**, **Funao J**, **Nakayama M**, **Hisatsune J**, **Kimura M**, **Moss J**, **Hirayama T**. 2006. Helicobacter pylori vacuolating cytotoxin induces activation of the proapoptotic proteins Bax and Bak, leading to cytochrome c release and cell death, independent of vacuolation. J Biol Chem **281**:11250–11259.

117. **Galmiche A**, **Rassow J**, **Doye A**, **Cagnol S**, **Chambard JC**, **Contamin S**, **de**

Thillot V, **Just I**, **Ricci V**, **Solcia E**, **Van Obberghen E**, **Boquet P**. 2000. The N-terminal 34 kDa fragment of Helicobacter pylori vacuolating cytotoxin targets mitochondria and induces cytochrome c release. EMBO J **19**:6361–6370.

118. **Willhite DC**, **Cover TL**, **Blanke SR**. 2003. Cellular vacuolation and mitochondrial cytochrome c release are independent outcomes of Helicobacter pylori vacuolating cytotoxin activity that are each dependent on membrane channel formation. J Biol Chem **278**:48204–48209.

119. **Jain P**, **Luo Z-Q**, **Blanke SR**. 2011. Helicobacter pylori vacuolating cytotoxin A (VacA) engages the mitochondrial fission machinery to induce host cell death. Proc Natl Acad Sci USA **108**:16032–16037.

120. **Oldani A**, **Cormont M**, **Hofman V**, **Chiozzi V**, **Oregioni O**, **Canonici A**, **Sciullo A**, **Sommi P**, **Fabbri A**, **Ricci V**, **Boquet P**. 2009. Helicobacter pylori counteracts the apoptotic action of its VacA toxin by injecting the CagA protein into gastric epithelial cells. PLoS Pathog **5**:e1000603.

121. **Domańska G**, **Motz C**, **Meinecke M**, **Harsman A**, **Papatheodorou P**, **Reljic B**, **Dian-Lothrop EA**, **Galmiche A**, **Kepp O**, **Becker L**, **Günnewig K**, **Wagner R**, **Rassow J**. 2010. Helicobacter pylori VacA toxin/subunit p34: targeting of an anion channel to the inner mitochondrial membrane. PLoS Pathog **6**:e1000878.

122. **Foo JH**, **Culvenor JG**, **Ferrero RL**, **Kwok T**, **Lithgow T**, **Gabriel K**. 2010. Both the p33 and p55 subunits of the Helicobacter pylori VacA toxin are targeted to mammalian mitochondria. J Mol Biol **401**:792–798.

123. **Tombola F**, **Morbiato L**, **Del Giudice G**, **Rappuoli R**, **Zoratti M**, **Papini E**. 2001. The Helicobacter pylori VacA toxin is a urea permease that promotes urea diffusion across epithelia. J Clin Invest **108**:929–937.

124. **Debellis L**, **Papini E**, **Caroppo R**, **Montecucco C**, **Curci S**. 2001. Helicobacter pylori cytotoxin VacA increases alkaline secretion in gastric epithelial cells. American Journal of Physiology - Gastrointestinal and Liver Physiology **281**:G1440–G1448.

125. **Papini E**, **Satin B**, **Norais N**, **de Bernard M**, **Telford JL**, **Rappuoli R**, **Montecucco C**. 1998. Selective increase of the permeability of polarized epithelial cell monolayers by Helicobacter pylori vacuolating toxin. J Clin Invest **102**:813–820.

126. **Amieva MR**, **Vogelmann R**, **Covacci A**, **Tompkins LS**, **Nelson WJ**, **Falkow S**. 2003. Disruption of the Epithelial Apical-Junctional Complex by Helicobacter pylori CagA. Science **300**:1430–1434.

127. **Pelicic V**, **Reyrat J-M**, **Sartori L**, **Pagliaccia C**, **Rappuoli R**, **Telford JL**, **Montecucco C**, **Papini E**. 1999. Helicobacter pylori VacA cytotoxin associated with the bacteria increases epithelial permeability independently of its

vacuolating activity. Microbiology **145**:2043–2050.

128. **Nakayama M**, **Kimura M**, **Wada A**, **Yahiro K**, **Ogushi K-I**, **Niidome T**, **Fujikawa A**, **Shirasaka D**, **Aoyama N**, **Kurazono H**, **Noda M**, **Moss J**, **Hirayama T**. 2004. Helicobacter pylori VacA activates the p38/activating transcription factor 2-mediated signal pathway in AZ-521 cells. J Biol Chem **279**:7024–7028.

129. **Hisatsune J**, **Yamasaki E**, **Nakayama M**, **Shirasaka D**, **Kurazono H**, **Katagata Y**, **Inoue H**, **Han J**, **Sap J**, **Yahiro K**, **Moss J**, **Hirayama T**. 2007. Helicobacter pylori VacA enhances prostaglandin E2 production through induction of cyclooxygenase 2 expression via a p38 mitogen-activated protein kinase/activating transcription factor 2 cascade in AZ-521 cells. Infect Immun **75**:4472–4481.

130. **Boncristiano M**, **Paccani SR**, **Barone S**, **Ulivieri C**, **Patrussi L**, **Ilver D**, **Amedei A**, **D'Elios MM**, **Telford JL**, **Baldari CT**. 2003. The Helicobacter pylori vacuolating toxin inhibits T cell activation by two independent mechanisms. J Exp Med **198**:1887–1897.

131. **Caputo R**, **Tuccillo C**, **Manzo BA**, **Zarrilli R**, **Tortora G**, **Blanco CDV**, **Ricci V**, **Ciardiello F**, **Romano M**. 2003. Helicobacter pylori VacA toxin up-regulates vascular endothelial growth factor expression in MKN 28 gastric cells through an epidermal growth factor receptor-, cyclooxygenase-2-dependent mechanism. Clin Cancer Res **9**:2015–2021.

132. **Nakayama M**, **Hisatsune J**, **Yamasaki E**, **Isomoto H**, **Kurazono H**, **Hatakeyama M**, **Azuma T**, **Yamaoka Y**, **Yahiro K**, **Moss J**, **Hirayama T**. 2009. Helicobacter pylori VacA-induced inhibition of GSK3 through the PI3K/Akt signaling pathway. J Biol Chem **284**:1612–1619.

133. **Terebiznik MR**, **Raju D**, **Vázquez CL**, **Torbricki K**, **Kulkarni R**, **Blanke SR**, **Yoshimori T**, **Colombo MI**, **Jones NL**. 2009. Effect of Helicobacter pylori's vacuolating cytotoxin on the autophagy pathway in gastric epithelial cells. Autophagy **5**:370–379.

134. **Yahiro K**, **Satoh M**, **Nakano M**, **Hisatsune J**, **Isomoto H**, **Sap J**, **Suzuki H**, **Nomura F**, **Noda M**, **Moss J**, **Hirayama T**. 2012. Low-density lipoprotein receptor-related protein-1 (LRP1) mediates autophagy and apoptosis caused by Helicobacter pylori VacA. J Biol Chem **287**:31104–31115.

135. **Raju D**, **Hussey S**, **Ang M**, **Terebiznik MR**, **Sibony M**, **Galindo-Mata E**, **Gupta V**, **Blanke SR**, **Delgado A**, **Romero-Gallo J**, **Ramjeet MS**, **Mascarenhas H**, **Peek RM**, **Correa P**, **Streutker C**, **Hold G**, **Kunstmann E**, **Yoshimori T**, **Silverberg MS**, **Girardin SE**, **Philpott DJ**, **Omar El E**, **Jones NL**. 2012. Vacuolating cytotoxin and variants in Atg16L1 that disrupt autophagy promote Helicobacter pylori infection in humans. Gastroenterology **142**:1160–1171.

136. **Greenfield LK**, **Jones NL**. 2013. Modulation of autophagy by Helicobacter pylori and its role in gastric carcinogenesis. Trends Microbiol **21**:602–612.

137. **Kuck D**, **Kolmerer B**, **Iking-Konert C**, **Krammer PH**, **Stremmel W**, **Rudi J**. 2001. Vacuolating Cytotoxin of Helicobacter pylori Induces Apoptosis in the Human Gastric Epithelial Cell Line AGS. Infect Immun **69**:5080–5087.

138. **Cover TL**, **Krishna US**, **Israel DA**, **Peek RM**. 2003. Induction of gastric epithelial cell apoptosis by Helicobacter pylori vacuolating cytotoxin. Cancer Res **63**:951–957.

139. **Radin JN**, **González-Rivera C**, **Ivie SE**, **McClain MS**, **Cover TL**. 2011. Helicobacter pylori VacA induces programmed necrosis in gastric epithelial cells. Infect Immun **79**:2535–2543.

140. **Radin JN**, **González-Rivera C**, **Frick-Cheng AE**, **Sheng J**, **Gaddy JA**, **Rubin DH**, **Algood HMS**, **McClain MS**, **Cover TL**. 2014. Role of connexin 43 in Helicobacter pylori VacA-induced cell death. Infect Immun **82**:423–432.

141. **Calore F**, **Genisset C**, **Casellato A**, **Rossato M**, **Codolo G**, **Esposti MD**, **Scorrano L**, **de Bernard M**. 2010. Endosome-mitochondria juxtaposition during apoptosis induced by H. pylori VacA. Cell Death Differ **17**:1707–1716.

142. **Matsumoto A**, **Isomoto H**, **Nakayama M**, **Hisatsune J**, **Nishi Y**, **Nakashima Y**, **Matsushima K**, **Kurazono H**, **Nakao K**, **Hirayama T**, **Kohno S**. 2011. Helicobacter pylori VacA Reduces the Cellular Expression of STAT3 and Pro-survival Bcl-2 Family Proteins, Bcl-2 and Bcl-XL, Leading to Apoptosis in Gastric Epithelial Cells. Dig Dis Sci **4**:999–1006.

143. **Akazawa Y**, **Isomoto H**, **Matsushima K**, **Kanda T**, **Minami H**, **Yamaghchi N**, **Taura N**, **Shiozawa K**, **Ohnita K**, **Takeshima F**, **Nakano M**, **Moss J**, **Hirayama T**, **Nakao K**. 2013. Endoplasmic Reticulum Stress Contributes to Helicobacter Pylori VacA-Induced Apoptosis. PLOS ONE **8**:e82322.

144. **Kim JM**, **Kim JS**, **Lee JY**, **Kim Y-J**, **Youn H-J**, **Kim IY**, **Chee YJ**, **Oh Y-K**, **Kim N**, **Jung HC**, **Song IS**. 2007. Vacuolating cytotoxin in Helicobacter pylori water-soluble proteins upregulates chemokine expression in human eosinophils via Ca2+ influx, mitochondrial reactive oxygen intermediates, and NF-kappaB activation. Infect Immun **75**:3373–3381.

145. **Kim JM**, **Kim JS**, **Lee JY**, **Sim Y-S**, **Kim Y-J**, **Oh Y-K**, **Yoon HJ**, **Kang JS**, **Youn J**, **Kim N**, **Jung HC**, **Kim S**. 2010. Dual effects of Helicobacter pylori vacuolating cytotoxin on human eosinophil apoptosis in early and late periods of stimulation. Eur J Immunol **40**:1651–1662.

146. **Supajatura V**, **Ushio H**, **Wada A**, **Yahiro K**, **Okumura K**, **Ogawa H**, **Hirayama T**, **Ra C**. 2002. Cutting edge: VacA, a vacuolating cytotoxin of Helicobacter pylori, directly activates mast cells for migration and production of

proinflammatory cytokines. J Immunol **168**:2603–2607.

147. **de Bernard M**, **Cappon A**, **Pancotto L**, **Ruggiero P**, **Rivera J**, **Del Giudice G**, **Montecucco C**. 2005. The Helicobacter pylori VacA cytotoxin activates RBL-2H3 cells by inducing cytosolic calcium oscillations. Cell Microbiol **7**:191–198.

148. **Kim JM**, **Kim JS**, **Yoo DY**, **Ko SH**, **Kim N**, **Kim H**, **Kim YJ**. 2011. Stimulation of dendritic cells with Helicobacter pylori vacuolating cytotoxin negatively regulates their maturation via the restoration of E2F1. Clinical & Experimental Immunology **166**:34–45.

149. **Gebert B**, **Fischer W**, **Weiss E**, **Hoffmann R**, **Haas R**. 2003. Helicobacter pylori vacuolating cytotoxin inhibits T lymphocyte activation. Science **301**:1099–1102.

150. **Sundrud MS**, **Torres VJ**, **Unutmaz D**, **Cover TL**. 2004. Inhibition of primary human T cell proliferation by Helicobacter pylori vacuolating toxin (VacA) is independent of VacA effects on IL-2 secretion. Proc Natl Acad Sci USA **101**:7727–7732.

151. **Torres VJ**, **VanCompernolle SE**, **Sundrud MS**, **Unutmaz D**, **Cover TL**. 2007. Helicobacter pylori vacuolating cytotoxin inhibits activation-induced proliferation of human T and B lymphocyte subsets. J Immunol **179**:5433–5440.

152. **Allen LA**, **Schlesinger LS**, **Kang B**. 2000. Virulent strains of Helicobacter pylori demonstrate delayed phagocytosis and stimulate homotypic phagosome fusion in macrophages. J Exp Med **191**:115–128.

153. **Zheng PY**, **Jones NL**. 2003. Helicobacter pylori strains expressing the vacuolating cytotoxin interrupt phagosome maturation in macrophages by recruiting and retaining TACO (coronin 1) protein. Cell Microbiol **5**:25–40.

154. **Weiss G**, **Forster S**, **Irving A**, **Tate M**, **Ferrero RL**, **Hertzog P**, **Frøkiær H**, **Kaparakis-Liaskos M**. 2013. Helicobacter pylori VacA suppresses Lactobacillus acidophilus-induced interferon beta signaling in macrophages via alterations in the endocytic pathway. MBio **4**:e00609–12.

155. **Hisatsune J**, **Nakayama M**, **Isomoto H**, **Kurazono H**, **Mukaida N**, **Mukhopadhyay AK**, **Azuma T**, **Yamaoka Y**, **Sap J**, **Yamasaki E**, **Yahiro K**, **Moss J**, **Hirayama T**. 2008. Molecular characterization of Helicobacter pylori VacA induction of IL-8 in U937 cells reveals a prominent role for p38MAPK in activating transcription factor-2, cAMP response element binding protein, and NF-kappaB activation. J Immunol **180**:5017–5027.

156. **Menaker RJ**, **Ceponis PJM**, **Jones NL**. 2004. Helicobacter pylori induces apoptosis of macrophages in association with alterations in the mitochondrial pathway. Infect Immun **72**:2889–2898.

157. **Kobayashi H**, **Kamiya S**, **Suzuki T**, **Kohda K**, **Muramatsu S**, **Kurumada T**, **Ohta U**, **Miyazawa M**, **Kimura N**, **Mutoh N**, **Shirai T**, **Takagi A**, **Harasawa S**, **Tani N**, **Miwa T**. 1996. The effect of Helicobacter pylori on gastric acid secretion by isolated parietal cells from a guinea pig. Association with production of vacuolating toxin by H. pylori. Scand J Gastroenterol **31**:428–433.

158. **Wang F**, **Xia P**, **Wu F**, **Wang D**, **Wang W**, **Ward T**, **Liu Y**, **Aikhionbare F**, **Guo Z**, **Powell M**, **Liu B**, **Bi F**, **Shaw A**, **Zhu Z**, **Elmoselhi A**, **Fan D**, **Cover TL**, **Ding X**, **Yao X**. 2008. Helicobacter pylori VacA disrupts apical membrane-cytoskeletal interactions in gastric parietal cells. J Biol Chem **283**:26714–26725.

159. **Massari P**, **Manetti R**, **Burroni D**, **Nuti S**, **Norais N**, **Rappuoli R**, **Telford JL**. 1998. Binding of the Helicobacter pylori vacuolating cytotoxin to target cells. Infect Immun **66**:3981–3984.

160. **Wang HJ**, **Wang WC**. 2000. Expression and binding analysis of GST-VacA fusions reveals that the C-terminal approximately 100-residue segment of exotoxin is crucial for binding in HeLa cells. Biochem Biophys Res Commun **278**:449–454.

161. **Wang WC**, **Wang HJ**, **Kuo CH**. 2001. Two distinctive cell binding patterns by vacuolating toxin fused with glutathione S-transferase: one high-affinity m1-specific binding and the other lower-affinity binding for variant m forms. Biochemistry **40**:11887–11896.

162. **Ricci V**, **Galmiche A**, **Doye A**, **Necchi V**, **Solcia E**, **Boquet P**. 2000. High cell sensitivity to Helicobacter pylori VacA toxin depends on a GPI-anchored protein and is not blocked by inhibition of the clathrin-mediated pathway of endocytosis. Mol Biol Cell **11**:3897–3909.

163. **Patel HK**, **Willhite DC**, **Patel RM**, **Ye D**, **Williams CL**, **Torres EM**, **Marty KB**, **MacDonald RA**, **Blanke SR**. 2002. Plasma membrane cholesterol modulates cellular vacuolation induced by the Helicobacter pylori vacuolating cytotoxin. Infect Immun **70**:4112–4123.

164. **Yahiro K**, **Wada A**, **Nakayama M**, **Kimura T**, **Ogushi K-I**, **Niidome T**, **Aoyagi H**, **Yoshino K-I**, **Yonezawa K**, **Moss J**, **Hirayama T**. 2003. Protein-tyrosine phosphatase alpha, RPTP alpha, is a Helicobacter pylori VacA receptor. J Biol Chem **278**:19183–19189.

165. **Yahiro K**, **Wada A**, **Yamasaki E**, **Nakayama M**, **Nishi Y**, **Hisatsune J**, **Morinaga N**, **Sap J**, **Noda M**, **Moss J**, **Hirayama T**. 2004. Essential domain of receptor tyrosine phosphatase beta (RPTPbeta) for interaction with Helicobacter pylori vacuolating cytotoxin. J Biol Chem **279**:51013–51021.

166. **Seto K**, **Hayashi-Kuwabara Y**, **Yoneta T**, **Suda H**, **Tamaki H**. 1998. Vacuolation induced by cytotoxin from Helicobacter pylori is mediated by the EGF receptor in HeLa cells. FEBS Lett **431**:347–350.

167. **Utt M**, **Danielsson B**, **Wadström T**. 2001. Helicobacter pylori vacuolating cytotoxin binding to a putative cell surface receptor, heparan sulfate, studied by surface plasmon resonance. FEMS Immunol Med Microbiol **30**:109–113.

168. **Gupta VR**, **Patel HK**, **Kostolansky SS**, **Ballivian RA**, **Eichberg J**, **Blanke SR**. 2008. Sphingomyelin functions as a novel receptor for Helicobacter pylori VacA. PLoS Pathog **4**:e1000073.

169. **Gupta VR**, **Wilson BA**, **Blanke SR**. 2010. Sphingomyelin is important for the cellular entry and intracellular localization of Helicobacter pylori VacA. Cell Microbiol **12**:1517–1533.

170. **Roche N**, **Ilver D**, **Angström J**, **Barone S**, **Telford JL**, **Teneberg S**. 2007. Human gastric glycosphingolipids recognized by Helicobacter pylori vacuolating cytotoxin VacA. Microbes Infect **9**:605–614.

171. **Molinari M**, **Galli C**, **de Bernard M**, **Norais N**, **Ruysschaert JM**, **Rappuoli R**, **Montecucco C**. 1998. The acid activation of Helicobacter pylori toxin VacA: structural and membrane binding studies. Biochem Biophys Res Commun **248**:334–340.

172. **Sewald X**, **Gebert-Vogl B**, **Prassl S**, **Barwig I**, **Weiss E**, **Fabbri M**, **Osicka R**, **Schiemann M**, **Busch DH**, **Semmrich M**, **Holzmann B**, **Sebo P**, **Haas R**. 2008. Integrin subunit CD18 Is the T-lymphocyte receptor for the Helicobacter pylori vacuolating cytotoxin. Cell Host Microbe **3**:20–29.

173. **Gauthier NC**, **Ricci V**, **Gounon P**, **Doye A**, **Tauc M**, **Poujeol P**, **Boquet P**. 2004. Glycosylphosphatidylinositol-anchored proteins and actin cytoskeleton modulate chloride transport by channels formed by the Helicobacter pylori vacuolating cytotoxin VacA in HeLa cells. J Biol Chem **279**:9481–9489.

174. **Gauthier NC**, **Monzo P**, **Kaddai V**, **Doye A**, **Ricci V**, **Boquet P**. 2005. Helicobacter pylori VacA cytotoxin: a probe for a clathrin-independent and Cdc42-dependent pinocytic pathway routed to late endosomes. Mol Biol Cell **16**:4852–4866.

175. **Gauthier NC**, **Monzo P**, **Gonzalez T**, **Doye A**, **Oldani A**, **Gounon P**, **Ricci V**, **Cormont M**, **Boquet P**. 2007. Early endosomes associated with dynamic F-actin structures are required for late trafficking of H. pylori VacA toxin. J Cell Biol **177**:343–354.

176. **Kern B**, **Jain U**, **Utsch C**, **Otto A**, **Busch B**, **Jiménez-Soto L**, **Becher D**, **Haas R**. 2015. Characterization of Helicobacter pylori VacA-containing vacuoles (VCVs), VacA intracellular trafficking and interference with calcium signalling in T lymphocytes. Cell Microbiol **17**:1811–1832.

177. **Suzuki H**, **Yanaka A**, **Shibahara T**, **Matsui H**, **Nakahara A**, **Tanaka N**, **Muto H**, **Momoi T**, **Uchiyama Y**. 2002. Ammonia-induced apoptosis is accelerated at

higher pH in gastric surface mucous cells. American Journal of Physiology - Gastrointestinal and Liver Physiology **283**:G986–95.

178. **Nakamura E**, **Hagen SJ**. 2002. Role of glutamine and arginase in protection against ammonia-induced cell death in gastric epithelial cells. American Journal of Physiology - Gastrointestinal and Liver Physiology **283**:G1264–75.

179. **González-Rivera C**, **Campbell AM**, **Rutherford SA**, **Pyburn TM**, **Foegeding NJ**, **Barke TL**, **Spiller BW**, **McClain MS**, **Ohi MD**, **Lacy DB**, **Cover TL**. 2016. A Nonoligomerizing Mutant Form of Helicobacter pylori VacA Allows Structural Analysis of the p33 Domain. Infect Immun **84**:2662–2670.

180. **Levental I**, **Lingwood D**, **Grzybek M**, **Coskun U**, **Simons K**. 2010. Palmitoylation regulates raft affinity for the majority of integral raft proteins. Proc Natl Acad Sci USA **107**:22050–22054.

181. **Raghunathan K**, **Wong TH**, **Chinnapen DJ**, **Lencer WI**, **Jobling MG**, **Kenworthy AK**. 2016. Glycolipid Crosslinking Is Required for Cholera Toxin to Partition Into and Stabilize Ordered Domains. Biophys J **111**:2547–2550.

182. **Raghunathan K**, **Ahsan A**, **Ray D**, **Nyati MK**, **Veatch SL**. 2015. Membrane Transition Temperature Determines Cisplatin Response. PLOS ONE **10**:e0140925.

183. **Säälik P**, **Niinep A**, **Pae J**, **Hansen M**, **Lubenets D**, **Langel Ü**, **Pooga M**. 2011. Penetration without cells: Membrane translocation of cell-penetrating peptides in the model giant plasma membrane vesicles. Journal of Controlled Release **153**:117–125.

184. **Crawley SW**, **Shifrin DA**, **Grega-Larson NE**, **McConnell RE**, **Benesh AE**, **Mao S**, **Zheng Y**, **Zheng QY**, **Nam KT**, **Millis BA**, **Kachar B**, **Tyska MJ**. 2014. Intestinal brush border assembly driven by protocadherin-based intermicrovillar adhesion. Cell **157**:433–446.

185. **Li Q**, **Lau A**, **Morris TJ**, **Guo L**, **Fordyce CB**, **Stanley EF**. 2004. A syntaxin 1, Galpha(o), and N-type calcium channel complex at a presynaptic nerve terminal: analysis by quantitative immunocolocalization. J Neurosci **24**:4070–4081.

186. **Schraw W**, **Li Y**, **McClain MS**, **van der Goot FG**, **Cover TL**. 2002. Association of Helicobacter pylori vacuolating toxin (VacA) with lipid rafts. J Biol Chem **277**:34642–34650.

187. **Toledo A**, **Benach JL**. 2015. Hijacking and Use of Host Lipids by Intracellular Pathogens. Microbiology spectrum **3**:637–666.

188. **Lingwood D**, **Kaiser H-J**, **Levental I**, **Simons K**. 2009. Lipid rafts as functional heterogeneity in cell membranes. Biochem Soc Trans **37**:955–960.

189. **Simons K**, **Gerl MJ**. 2010. Revitalizing membrane rafts: new tools and insights. Nat Rev Mol Cell Biol **11**:688–699.

190. **Sandvig K**, **Bergan J**, **Kavaliauskiene S**, **Skotland T**. 2014. Lipid requirements for entry of protein toxins into cells. Progress in Lipid Research **54**:1–13.

191. **Aigal S**, **Claudinon J**, **Römer W**. 2015. Plasma membrane reorganization: A glycolipid gateway for microbes. Biochimica et Biophysica Acta (BBA) - Molecular Cell Research **1853**:858–871.

192. **Geisse NA**, **Cover TL**, **Henderson RM**, **Edwardson JM**. 2004. Targeting of Helicobacter pylori vacuolating toxin to lipid raft membrane domains analysed by atomic force microscopy. Biochemical Journal **381**:911–917.

193. **Nakayama M**, **Hisatsune J**, **Yamasaki E**, **Nishi Y**, **Wada A**, **Kurazono H**, **Sap J**, **Yahiro K**, **Moss J**, **Hirayama T**. 2006. Clustering of Helicobacter pylori VacA in lipid rafts, mediated by its receptor, receptor-like protein tyrosine phosphatase beta, is required for intoxication in AZ-521 Cells. Infect Immun **74**:6571–6580.

194. **Kuo C-H**, **Wang W-C**. 2003. Binding and internalization of Helicobacter pylori VacA via cellular lipid rafts in epithelial cells. Biochem Biophys Res Commun **303**:640–644.

195. **Boquet P**, **Ricci V**. 2012. Intoxication strategy of Helicobacter pylori VacA toxin. Trends Microbiol **20**:165–174.

196. **Yahiro K**, **Hirayama T**, **Moss J**, **Noda M**. 2016. New Insights into VacA Intoxication Mediated through Its Cell Surface Receptors. Toxins (Basel) **8**:152.

197. **Sezgin E**, **Levental I**, **Mayor S**, **Eggeling C**. 2017. The mystery of membrane organization: composition, regulation and roles of lipid rafts. Nat Rev Mol Cell Biol **18**:361–374.

198. **Baumgart T**, **Hammond AT**, **Sengupta P**, **Hess ST**, **Holowka DA**, **Baird BA**, **Webb WW**. 2007. Large-scale fluid/fluid phase separation of proteins and lipids in giant plasma membrane vesicles. Proc Natl Acad Sci USA **104**:3165–3170.

199. **Veatch SL**, **Cicuta P**, **Sengupta P**, **Honerkamp-Smith A**, **Holowka D**, **Baird B**. 2008. Critical fluctuations in plasma membrane vesicles. ACS Chem Biol **3**:287–293.

200. **Sezgin E**, **Kaiser H-J**, **Baumgart T**, **Schwille P**, **Simons K**, **Levental I**. 2012. Elucidating membrane structure and protein behavior using giant plasma membrane vesicles. Nature Protocols 2012 7:6 **7**:1042–1051.

201. **Levental KR**, **Levental I**. 2015. Isolation of Giant Plasma Membrane Vesicles for Evaluation of Plasma Membrane Structure and Protein Partitioning, pp. 65–

77. *In* Methods in Membrane Lipids. Humana Press, New York, NY, New York, NY.

202. **Levental I**, **Veatch S**. 2016. The Continuing Mystery of Lipid Rafts. J Mol Biol **428**:4749–4764.

203. **Levental KR**, **Levental I**. 2015. Giant Plasma Membrane Vesicles: Models for Understanding Membrane Organization. Current Topics in Membranes **75**:25–57.

204. **Levental KR**, **Lorent JH**, **Lin X**, **Skinkle AD**, **Surma MA**, **Stockenbojer EA**, **Gorfe AA**, **Levental I**. 2016. Polyunsaturated Lipids Regulate Membrane Domain Stability by Tuning Membrane Order. Biophys J **110**:1800–1810.

205. **Sezgin E**, **Schwille P**. 2012. Model membrane platforms to study protein-membrane interactions. Molecular Membrane Biology **29**:144–154.

206. **Howitt MR**, **Garrett WS**. 2012. A complex microworld in the gut: Gut microbiota and cardiovascular disease connectivity. Nat Med **18**:1188–1189.

207. **Sengupta P**, **Hammond A**, **Holowka D**, **Baird B**. 2008. Structural determinants for partitioning of lipids and proteins between coexisting fluid phases in giant plasma membrane vesicles. Biochimica et Biophysica Acta (BBA) - Biomembranes **1778**:20–32.

208. **Zhou Y**, **Maxwell KN**, **Sezgin E**, **Lu M**, **Liang H**, **Hancock JF**, **Dial EJ**, **Lichtenberger LM**, **Levental I**. 2013. Bile acids modulate signaling by functional perturbation of plasma membrane domains. J Biol Chem **288**:35660–35670.

209. **Levental I**, **Byfield FJ**, **Chowdhury P**, **Gai F**, **Baumgart T**, **Janmey PA**. 2009. Cholesterol-dependent phase separation in cell-derived giant plasma-membrane vesicles. Biochemical Journal **424**:163–167.

210. **Gray EM**, **Díaz-Vázquez G**, **Veatch SL**. 2015. Growth Conditions and Cell Cycle Phase Modulate Phase Transition Temperatures in RBL-2H3 Derived Plasma Membrane Vesicles. PLOS ONE **10**:e0137741.

211. **Nikolaus J**, **Scolari S**, **Bayraktarov E**, **Jungnick N**, **Engel S**, **Plazzo AP**, **Stöckl M**, **Volkmer R**, **Veit M**, **Herrmann A**. 2010. Hemagglutinin of Influenza Virus Partitions into the Nonraft Domain of Model Membranes. Biophys J **99**:489–498.

212. **Burns M**, **Wisser K**, **Wu J**, **Levental I**, **Veatch SL**. 2017. Miscibility Transition Temperature Scales with Growth Temperature in a Zebrafish Cell Line. Biophys J **113**:1212–1222.

213. **Tisza MJ**, **Zhao W**, **Fuentes JSR**, **Prijic S**, **Chen X**, **Levental I**, **Chang JT**.

2016. Motility and stem cell properties induced by the epithelial-mesenchymal transition require destabilization of lipid rafts. Oncotarget **7**:51553–51568.

214. **Beck-García K**, **Beck-García E**, **Bohler S**, **Zorzin C**, **Sezgin E**, **Levental I**, **Alarcón B**, **Schamel WWA**. 2015. Nanoclusters of the resting T cell antigen receptor (TCR) localize to non-raft domains. Biochimica et Biophysica Acta (BBA) - Molecular Cell Research **1853**:802–809.

215. **Diaz-Rohrer BB**, **Levental KR**, **Simons K**, **Levental I**. 2014. Membrane raft association is a determinant of plasma membrane localization. Proc Natl Acad Sci USA **111**:8500–8505.

216. **Lorent JH**, **Levental I**. 2015. Structural determinants of protein partitioning into ordered membrane domains and lipid rafts. Chem Phys Lipids **192**:23–32.

217. **Yang S-T**, **Kreutzberger AJB**, **Kiessling V**, **Ganser-Pornillos BK**, **White JM**, **Tamm LK**. 2017. HIV virions sense plasma membrane heterogeneity for cell entry. Science Advances **3**:e1700338.

218. **Li Y**, **Wandinger-Ness A**, **Goldenring JR**, **Cover TL**. 2004. Clustering and redistribution of late endocytic compartments in response to Helicobacter pylori vacuolating toxin. Mol Biol Cell **15**:1946–1959.

219. **Johnson SA**, **Stinson BM**, **Go MS**, **Carmona LM**, **Reminick JI**, **Fang X**, **Baumgart T**. 2010. Temperature-dependent phase behavior and protein partitioning in giant plasma membrane vesicles. Biochimica et Biophysica Acta (BBA) - Biomembranes **1798**:1427–1435.

220. **Levental I**, **Grzybek M**, **Simons K**. 2011. Raft domains of variable properties and compositions in plasma membrane vesicles. Proc Natl Acad Sci USA **108**:11411–11416.

221. **Windschiegl B**, **Orth A**, **Römer W**, **Berland L**, **Stechmann B**, **Bassereau P**, **Johannes L**, **Steinem C**. 2009. Lipid Reorganization Induced by Shiga Toxin Clustering on Planar Membranes. PLOS ONE **4**:e6238.

222. **Ivie SE**, **McClain MS**, **Torres VJ**, **Algood HMS**, **Lacy DB**, **Yang R**, **Blanke SR**, **Cover TL**. 2008. Helicobacter pylori VacA Subdomain Required for Intracellular Toxin Activity and Assembly of Functional Oligomeric Complexes. Infect Immun **76**:2843–2851.

223. **Letley DP**, **Atherton JC**. 2000. Natural diversity in the N terminus of the mature vacuolating cytotoxin of Helicobacter pylori determines cytotoxin activity. J Bacteriol **182**:3278–3280.

224. **Hammond AT**, **Heberle FA**, **Baumgart T**, **Holowka D**, **Baird B**, **Feigenson GW**. 2005. Crosslinking a lipid raft component triggers liquid ordered-liquid disordered phase separation in model plasma membranes. PNAS **102**:6320–

6325.

225. **Solovyeva V**, **Johannes L**, **Simonsen AC**. 2015. Shiga toxin induces membrane reorganization and formation of long range lipid order. Soft Matter **11**:186–192.

226. **Abrami L**, **Liu S**, **Cosson P**, **Leppla SH**, **van der Goot FG**. 2003. Anthrax toxin triggers endocytosis of its receptor via a lipid raft–mediated clathrin-dependent process. J Cell Biol **160**:321–328.

227. **Epand RM**, **Epand RF**. 2004. Non-raft forming sphingomyelin–cholesterol mixtures. Chem Phys Lipids **132**:37–46.

228. **Skočaj M**, **Bakrač B**, **Križaj I**, **Maček P**, **Anderluh G**, **Sepčić K**. 2013. The sensing of membrane microdomains based on pore-forming toxins. Curr Med Chem **20**:491–501.

229. **Reyrat JM**, **Pelicic V**, **Papini E**, **Montecucco C**, **Rappuoli R**, **Telford JL**. 1999. Towards deciphering the Helicobacter pylori cytotoxin. Mol Microbiol **34**:197–204.

230. **Papini E**, **de Bernard M**, **Milia E**, **Bugnoli M**, **Zerial M**, **Rappuoli R**, **Montecucco C**. 1994. Cellular vacuoles induced by Helicobacter pylori originate from late endosomal compartments. Proc Natl Acad Sci USA **91**:9720–9724.

231. **Maurer K**, **Reyes-Robles T**, **Alonzo F**, **Durbin J**, **Torres VJ**, **Cadwell K**. 2015. Autophagy mediates tolerance to Staphylococcus aureus alpha-toxin. Cell Host Microbe **17**:429–440.

232. **Walev I**, **Palmer M**, **Martin E**, **Jonas D**, **Weller U**, **Höhn-Bentz H**, **Husmann M**, **Bhakdi S**. 1994. Recovery of human fibroblasts from attack by the pore-forming alpha-toxin of Staphylococcus aureus. Microb Pathog **17**:187–201.

233. **Husmann M**, **Beckmann E**, **Boller K**, **Kloft N**, **Tenzer S**, **Bobkiewicz W**, **Neukirch C**, **Bayley H**, **Bhakdi S**. 2009. Elimination of a bacterial pore-forming toxin by sequential endocytosis and exocytosis. FEBS Lett **583**:337–344.

234. **Gutierrez MG**, **Saka HA**, **Chinen I**, **Zoppino FCM**, **Yoshimori T**, **Bocco JL**, **Colombo MI**. 2007. Protective role of autophagy against Vibrio cholerae cytolysin, a pore-forming toxin from V. cholerae. Proc Natl Acad Sci USA **104**:1829–1834.

235. **Corrotte M**, **Fernandes MC**, **Tam C**, **Andrews NW**. 2012. Toxin pores endocytosed during plasma membrane repair traffic into the lumen of MVBs for degradation. Traffic **13**:483–494.

236. **Cover TL**, **Halter SA**, **Blaser MJ**. 1992. Characterization of HeLa cell vacuoles induced by Helicobacter pylori broth culture supernatant. Hum Pathol **23**:1004–

1010.

237. **Sachs G**, **Weeks DL**, **Melchers K**, **Scott DR**. 2003. The gastric biology of Helicobacter pylori. Annu Rev Physiol **65**:349–369.

238. **Cover TL**, **Puryear W**, **Perez-Perez GI**, **Blaser MJ**. 1991. Effect of urease on HeLa cell vacuolation induced by Helicobacter pylori cytotoxin. Infect Immun **59**:1264–1270.

239. **Ling SSM**, **Khoo LHB**, **Hwang L-A**, **Yeoh KG**, **Ho B**. 2015. Instrumental Role of Helicobacter pylori γ-Glutamyl Transpeptidase in VacA-Dependent Vacuolation in Gastric Epithelial Cells. PLOS ONE **10**:e0131460.

240. **Ohkuma S**, **Poole B**. 1978. Fluorescence probe measurement of the intralysosomal pH in living cells and the perturbation of pH by various agents. Proc Natl Acad Sci USA **75**:3327–3331.

241. **De Duve C**, **De Barsy T**, **Poole B**, **Trouet A**, **Tulkens P**, **Van Hoof FO**. 1974. Lysosomotropic agents. Biochemical Pharmacology **23**:2495–2531.

242. **Bond JS**, **Butler PE**. 1987. Intracellular proteases. Annu Rev Biochem **56**:333–364.

243. **Seglen PO**, **Gordon PB**. 1982. 3-Methyladenine: specific inhibitor of autophagic/lysosomal protein degradation in isolated rat hepatocytes. Proc Natl Acad Sci USA **79**:1889–1892.

244. **Wu Y-T**, **Tan H-L**, **Shui G**, **Bauvy C**, **Huang Q**, **Wenk MR**, **Ong C-N**, **Codogno P**, **Shen H-M**. 2010. Dual role of 3-methyladenine in modulation of autophagy via different temporal patterns of inhibition on class I and III phosphoinositide 3-kinase. J Biol Chem **285**:10850–10861.

245. **Yoshimori T**, **Yamamoto A**, **Moriyama Y**, **Futai M**, **Tashiro Y**. 1991. Bafilomycin A1, a specific inhibitor of vacuolar-type H(+)-ATPase, inhibits acidification and protein degradation in lysosomes of cultured cells. J Biol Chem **266**:17707–17712.

246. **Cover TL**, **Reddy LY**, **Blaser MJ**. 1993. Effects of ATPase inhibitors on the response of HeLa cells to Helicobacter pylori vacuolating toxin. Infect Immun **61**:1427–1431.

247. **Papini E**, **Bugnoli M**, **de Bernard M**, **Figura N**, **Rappuoli R**, **Montecucco C**. 1993. Bafilomycin A1 inhibits Helicobacter pylori-induced vacuolization of HeLa cells. Mol Microbiol **7**:323–327.

248. **Cover TL**, **Dooley CP**, **Blaser MJ**. 1990. Characterization of and human serologic response to proteins in Helicobacter pylori broth culture supernatants with vacuolizing cytotoxin activity. Infect Immun **58**:603–610.

249. **Sommi P**, **Ricci V**, **Fiocca R**, **Necchi V**, **Romano M**, **Telford JL**, **Solcia E**, **Ventura U**. 1998. Persistence of Helicobacter pylori VacA toxin and vacuolating potential in cultured gastric epithelial cells. Am J Physiol **275**:G681–8.

250. **Huotari J**, **Helenius A**. 2011. Endosome maturation. EMBO J **30**:3481–3500.

251. **Bischofberger M**, **Gonzalez MR**, **van der Goot FG**. 2009. Membrane injury by pore-forming proteins. Curr Opin Cell Biol **21**:589–595.

252. **Saka HA**, **Gutiérrez MG**, **Bocco JL**, **Colombo MI**. 2007. The autophagic pathway: a cell survival strategy against the bacterial pore-forming toxin Vibrio cholerae cytolysin. Autophagy **3**:363–365.

253. **Chatre L**, **Fernandes J**, **Michel V**, **Fiette L**, **Avé P**, **Arena G**, **Jain U**, **Haas R**, **Wang TC**, **Ricchetti M**, **Touati E**. 2017. Helicobacter pylori targets mitochondrial import and components of mitochondrial DNA replication machinery through an alternative VacA-dependent and a VacA-independent mechanisms. Scientific Reports **7**:15901.

254. **Necchi V**, **Sommi P**, **Vanoli A**, **Fiocca R**, **Ricci V**, **Solcia E**. 2017. Natural history of Helicobacter pylori VacA toxin in human gastric epithelium in vivo: vacuoles and beyond. Scientific Reports **7**:14526.

255. **Kim I-J**, **Lee J**, **Oh SJ**, **Yoon M-S**, **Jang S-S**, **Holland RL**, **Reno ML**, **Hamad MN**, **Maeda T**, **Chung HJ**, **Chen J**, **Blanke SR**. 2018. Helicobacter pylori Infection Modulates Host Cell Metabolism through VacA-Dependent Inhibition of mTORC1. Cell Host Microbe **23**:583–593.e8.

256. **Marshall BJ**, **Langton SR**. 1986. Urea hydrolysis in patients with Campylobacter pyloridis infection. Lancet **1**:965–966.

257. **Kim H**, **Park C**, **Jang WI**, **Lee KH**, **Kwon SO**, **Robey-Cafferty SS**, **Ro JY**, **Lee YB**. 1990. The gastric juice urea and ammonia levels in patients with Campylobacter pylori. Am J Clin Pathol **94**:187–191.

258. **Graham DY**, **Go MF**, **Evans DJ Jr**. 1992. Review article: urease, gastric ammonium/ammonia, and Helicobacter pylori - the past, the present, and recommendations for future research. Alimentary Pharmacology & Therapeutics **6**:659–669.

259. **Detmer SA**, **Chan DC**. 2007. Functions and dysfunctions of mitochondrial dynamics. Nat Rev Mol Cell Biol **8**:870–879.

260. **Cantor JR**, **Sabatini DM**. 2012. Cancer cell metabolism: one hallmark, many faces. Cancer Discov **2**:881–898.

261. **DeBerardinis RJ**, **Cheng T**. 2010. Q's next: the diverse functions of glutamine in metabolism, cell biology and cancer. Oncogene **29**:313–324.

262. **Bik EM**, **Eckburg PB**, **Gill SR**, **Nelson KE**, **Purdom EA**, **Francois F**, **Perez-Perez G**, **Blaser MJ**, **Relman DA**. 2006. Molecular analysis of the bacterial microbiota in the human stomach. PNAS **103**:732–737.

263. **Fitchen N**, **Letley DP**, **O'Shea P**, **Atherton JC**, **Williams P**, **Hardie KR**. 2005. All subtypes of the cytotoxin VacA adsorb to the surface of Helicobacter pylori post-secretion. J Med Microbiol **54**:621–630.